



Christina Wappl, Dipl.-Ing. BSc

Avenues for Improvement of State of the Art Chemical Anchors

DISSERTATION

zur Erlangung des akademischen Grades

Doktorin der technischen Wissenschaften

eingereicht an der

Technischen Universität Graz

Betreuer

Assoc.Prof. Dipl.-Ing. Dr.techn. Christian Slugovc

Institut für Chemische Technologie von Materialien

EIDESSTATTLICHE ERKLÄRUNG

Ich erkläre an Eides statt, dass ich die vorliegende Arbeit selbstständig verfasst, andere als die angegebenen Quellen/Hilfsmittel nicht benutzt, und die den benutzten Quellen wörtlich und inhaltlich entnommenen Stellen als solche kenntlich gemacht habe. Das in TUGRAZonline hochgeladene Textdokument ist mit der vorliegenden Dissertation identisch.

Datum

Unterschrift

Für meine Familie

DANKSAGUNG

An dieser Stelle möchte ich mich ganz herzlich bei all jenen bedanken, die mich während der Doktorarbeit und darüber hinaus stets unterstützt und somit die nun vorliegende Arbeit maßgeblich geprägt haben.

Mein besonderer Dank gilt meinem Betreuer Christian Slugovc für die großartige Unterstützung, die unzähligen, hilfreichen Tipps und fast ebenso vielen humorvollen Kommentare. Ich bin dankbar für die Möglichkeit, nicht nur in diesem hoch spannenden, industrienahen Projekt zu arbeiten sondern auch an internationalen Konferenzen teilzunehmen.

Ich möchte mich sehr herzlich bei Armin Pfeil von der Hilti Entwicklungsgesellschafts mbH für die erstklassige Betreuung, das Teilen des großen Wissensschatzes rund um chemische Dübel und die vielen, interessanten Gespräche bedanken. Für die tatkräftige Unterstützung im Labor und im Testfeld möchte ich Aude-Héloïse Bonardi, Monika Dinauer, Josie Ender, Klaus Gebauer, Wolfgang Lieberth, Stefanie Prefahl, Monika Rajnai und Fabian Schubert danken. Außerdem bedanke ich mich bei Jens Bunzen, Thomas Bürgel, Anna Khalyavina, Emin Kumru, Martin Lang, Juliane Marauska und Katja Student für die anregenden Diskussionen am aber auch abseits des Besprechungstisches.

Bei meinem Exkurs in die Welt der Sauerstoffinhibierung am Anfang meiner Dissertation wurde ich herzlich am Institut für Theoretische und Physikalische Chemie aufgenommen. Allen voran möchte ich mich bei Georg Gescheidt-Demner für die hervorragende Betreuung bedanken. Für die grandiose Zusammenarbeit möchte ich besonders Hilde Freißmuth, Anna Eibel, Roman Geier, Marion Hofmeister, Herbert Lang und Dmytro Neshchadin danken.

Bei meinen Kollegen vom Institut für Chemische Technologie von Materialien möchte ich mich für die wunderbare Zeit, die lustigen Feiern zu diversen Anlässen und das angenehme Arbeitsumfeld bedanken. Ein besonderer Dank für den unermüdlichen Einsatz im Labor geht an Birgit Ehmman und Anja Baumer. Ich danke Petra Kaschnitz für spezielle NMR-Messungen, Josefine Hobisch für diverse Analysen sowie Renate Trebizan und Liane Hochgatterer für die Hilfe in organisatorischen Fragen. Meiner Arbeitsgruppe rund um Petra Hofstadler, Christian Leybold, Nika Mahne, Aleksej Samojlov und Lukas Schafzahl danke ich für die amüsanten Gespräche bei gemeinsamen (Mittags-)Pausen, die den Arbeitsalltag versüßen. Besonders möchte ich Anita Peters und Bettina Schafzahl für ihre umsichtige Art und großartige Unterstützung in allen Belangen danken. Mein spezieller Dank geht an Simone Strasser für ihre Freundschaft, die wertvollen Ratschläge für alle Lebenslagen und das Teilen von Freud und Mittagessen.

Meine Dankbarkeit möchte ich auch meinen Freunden abseits der Arbeit zum Ausdruck bringen, die mich auch in stressigen Zeiten immer unterstützt haben. Für die Fähigkeit, mich mit den richtigen Worten schnell wieder aufzubauen und mit den typischen Sprüchen für gute Laune zu sorgen, möchte ich Marko danken. Besonderen Dank möchte ich an meine beste Freundin Angi richten, die eine wichtige Säule in meinem Leben ist und es auf einzigartige Weise schafft, noch mehr aus mir herauszuholen. Von ganzem Herzen möchte ich meinen Eltern, Josefa und Heinrich, sowie meinem Bruder Michi und seiner Frau Berni Danke sagen. Durch Eure Unterstützung und Liebe, Euer Verständnis und das Vertrauen in mich ist das alles erst möglich geworden. Dafür bin ich unendlich dankbar.

ABSTRACT

This work discusses the formulation of a chemical anchoring system based on new functional monomers. We aimed at a fast curing system with high reactivity also at curing temperature below 0 °C, low polymerisation shrinkage and high network density characterised by a high glass transition temperature.

Various polymerisation techniques were examined in terms of gel time and curing efficiency at curing temperatures varying from -20 °C to room temperature. Increased reactivity combined with low polymerisation shrinkage was obtained by tuning the monomer structure and initiation systems. The mechanical and thermal properties of the respective polymers were analysed extensively. The newly designed formulations were adjusted to fulfil the requirements for the intended application. Both the potential and drawbacks of the developed chemical anchor systems were pointed out in various experiments.

KURZFASSUNG

Diese Arbeit behandelt die Formulierung eines chemischen Dübelsystems, welches auf neuen funktionellen Monomeren basiert. Ziel der Arbeit war die Entwicklung eines schnell härtenden Systems mit hoher Reaktivität auch bei Aushärtetemperaturen unter 0 °C, geringem Polymerisationsschrumpf und hoher Netzwerkdicke gekennzeichnet durch eine hohe Glasübergangstemperatur.

Verschiedene Polymerisationstechniken wurden hinsichtlich der Gelzeit und der Aushärtungseffizienz in einem Temperaturbereich von -20 °C bis Raumtemperatur untersucht. Eine erhöhte Reaktivität kombiniert mit geringem Polymerisationsschrumpf wurde durch das Abstimmen der Monomerstruktur und der Initiierungssysteme erhalten. Die mechanischen und thermischen Eigenschaften der erhaltenen Polymere wurden ausführlich analysiert. Die neu entwickelten Formulierungen wurden an die Anwendungsanforderungen angepasst. Sowohl das Potenzial als auch die Nachteile des neuen chemischen Dübelsystems wurden in verschiedenen Experimenten aufgezeigt.

TABLE OF CONTENT

1 OBJECTIVE AND MOTIVATION.....	11
2 STATE OF THE ART.....	12
2.1 Chemical Anchors.....	12
2.2 Combining ROMP with Controlled Radical Polymerisation.....	15
2.2.1 ROMP.....	15
2.2.2 CRP.....	15
2.2.3 Compatibility of ROMP and CRP Reactants.....	16
The Role of Norbornene in Radical Polymerisation.....	16
The Role of (Meth)Acrylates in Olefin Metathesis.....	18
The Role of Ruthenium Complexes in Radical Polymerisation.....	19
2.2.4 ROMP-CRP Copolymers.....	20
3 ROMP FOR CHEMICAL ANCHORS.....	28
3.1 Developing a Dual Cure Chemical Anchor System.....	28
3.1.1 Preliminary Curing Tests.....	31
Single Cure SET System.....	32
Single Cure ATRA System.....	33
Dual Cure ATRA-ROMP System.....	35
Single Cure RadP System.....	36
Comparative Study.....	37
3.1.2 Stability of the ROMP Initiator.....	38
Standard Benchmark ROMP Reaction.....	38
UV/Vis Spectroscopy.....	40
¹ H- and ³¹ P-NMR Spectroscopy.....	41
3.1.3 Interaction of the ROMP Initiator and Methacrylate.....	43
3.1.4 Composition of a Dual Cure System.....	44

3.1.5 Investigation on the Reactivity of ROMP-Monomers.....	45
Preliminary Curing Tests.....	46
Kinetic NMR Study.....	47
3.1.6 Comparative Studies on Unfilled Formulations.....	49
Rheokinetics.....	49
Shrinkage Test.....	53
Dynamic Mechanical Analysis.....	55
3.2 Filled Dual Cure Formulations for Chemical Anchors.....	57
3.2.1 Developing Filled Dual Cure Formulations.....	57
Curing Tests.....	57
Geltimer Measurements.....	60
Pull Off Tests.....	61
3.2.2 Application of Filled Dual Cure Formulations as Chemical Anchors.....	63
Pull Out Tests.....	63
Geltimer and Yokogawa Measurements.....	68
Pull Off Tests.....	69
Thermal Analysis.....	70
3.2.3 Mon13 and Mon14 in HY 200-A Formulations.....	73
3.3 Synthesis of Monomers.....	74
4 CONCLUSION.....	77
5 EXPERIMENTAL.....	78
5.1 Syntheses.....	78
5.1.1 Monomer Synthesis.....	78
Standard Operating Procedure for Diels-Alder Reactions.....	78
Standard Operating Procedure for Esterification Reactions.....	79
5.1.2 Polymerisation in Bulk.....	82
Single Cure SET, ATRA and RadP and Dual Cure ATRA-ROMP - Preliminary Curing Tests.....	82
Single Cure RadP and Dual Cure RadP-ROMP - Rheokinetics.....	86
Single Cure RadP and Dual Cure RadP-ROMP - Shrinkage Tests.....	87

Single Cure RadP and ROMP and Dual Cure RadP-ROMP - Dynamic Mechanical Analysis.....	88
Dual Cure RadP-ROMP - Curing Tests.....	88
Dual Cure RadP-ROMP - Geltimer Measurements and Pull Off Tests.....	90
Dual Cure RadP-ROMP and Single Cure RadP - 2K 10+1 Formulations - Pull Out and Pull Off Tests, Geltimer and Yokogawa Measurements and Thermal Analysis	91
5.1.3 Polymerisation in Solution.....	94
Standard Benchmark ROMP Reaction.....	94
Kinetic Studies - NMR Spectroscopy.....	97
5.2 Degradation Studies.....	98
UV/Vis Spectroscopy.....	98
NMR Spectroscopy.....	98
6 APPENDIX.....	99
6.1. Chemicals and Instruments.....	99
6.2. Abbreviations.....	102
6.3. Further Contribution.....	104
6.4. References.....	110

1 OBJECTIVE AND MOTIVATION

The synthesis and characterisation of duroplastic thermosets via ring opening metathesis polymerisation (ROMP) of dicyclopentadiene and multifunctional norbornene monomers (Single Cure) was investigated in the course of the preceding master thesis. In a feasibility study the potential of ROMP in the field of chemical anchors was demonstrated. Appropriate mechanical, thermal and chemical properties were achieved albeit only at too high curing temperatures for the intended application.

In this contribution, a chemical anchor system combining ROMP of norbornenes with radical polymerisation of methacrylates (Dual Cure) was investigated. This new approach takes advantage of the fast curing process and excellent reactivity also at low curing temperature of radically initiated, methacrylate based systems. The combination with ROMP leads to covalently cross-linked, duroplastic materials with high network density but reduced polymerisation shrinkage.

For this purpose, two bifunctional monomers bearing both a norbornene and a methacrylate moiety were synthesised. In combination with mono-functional norbornenes and a methacrylate various radical initiation systems were tested. Besides the benzoyl peroxide initiated radical polymerisation (RadP), curing with peroxide-free controlled radical polymerisation based on single electron transfer (SET) and atom transfer radical addition (ATRA) was evaluated. The increased reactivity of the Dual Cure system as well as of a Single Cure RadP system, compared to the Single Cure ROMP system, was demonstrated by polymerisation in bulk at lower temperature (-20 °C). Compatibility tests revealed the influence of the single compounds of the radical systems on the performance of the ROMP initiator. Further tests showed significant impact of the monomeric structure on the ROMP kinetics. Based on these results, two component formulations were developed. The curing behaviour and polymerisation shrinkage of these formulations and the thermal properties of the obtained polymers were examined.

Finally, the filled two component formulations were characterised in terms of gel times, bond strength in and adhesion strength on concrete highlighting the potential of the newly designed Dual Cure RadP-ROMP and Single Cure RadP systems in the application as chemical anchors.

2.1 CHEMICAL ANCHORS

Post-installed fastening systems have been on the market for decades. However, there is still a great interest in improving these systems. In contrast to cast-in-place anchors, the post-installation of anchors facilitates the design, planning and construction of load-bearing structures.^{1,2} Post-installed anchors transfer the load to the concrete for example mechanically with expanding anchor rods or undercuts. Another option are bonded anchors which are based on a threaded rod and chemical mortar, also known as chemical anchors. The mortar works as bonding agent filling the space between the rod and the borehole completely and hence, prevents the corrosion of the rod.³ These anchors can also be used in porous substrates maintaining the outstanding load bearing capacity.

Chemical anchors are often referred to as adhesives. Besides bonding by adhesion and cohesion, the anchors make use of mechanical keying via micro- and macro-undercuts which are found at the rough borehole wall and the threaded rod, respectively (Figure 1).⁴

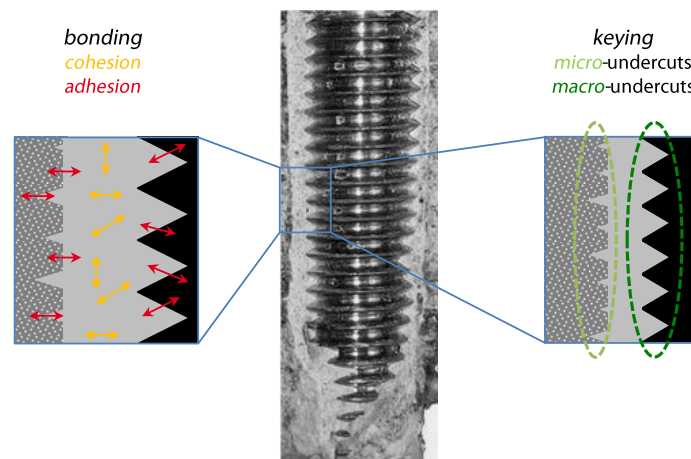


Figure 1. The principle of operation of chemical anchors (redrawn from reference 4).

Two types of chemical anchors are used, namely adhesive capsules and injection systems. Both are based on a two component system separating resin from hardener. Fillers and several additives (reactive diluents, inhibitors, etc.) are used in both components. Adhesive capsules are glass or plastic tubes which are placed in the borehole. The resin and hardener compounds are mixed upon installation by the rotating threaded rod with a blade edge at the tip. In injection systems, the mortar is stored in a two component cartridge. The formulations are applied with a dispensing device and resin and hardener are mixed homogeneously in a static mixer tip. Subsequently, the threaded rod is implemented.¹

The setting process of chemical anchors includes drilling, cleaning, injecting and setting. Each step might influence the performance of the final anchor and has to be taken into account when designing a new anchor system. Boreholes are usually drilled with a hammer or diamond core drill. The choice of drill influences the roughness of the borehole wall. Diamond core drilled boreholes have a smoother surface (less micro-undercuts) compared to hammer drilled ones. In this case, keying is less pronounced and an enhanced adhesion of the mortar to the concrete is

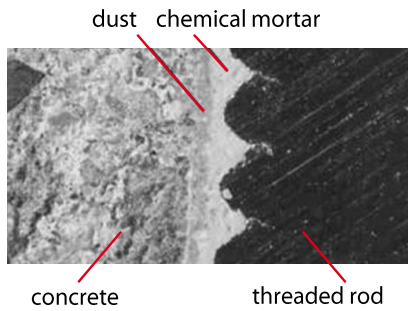


Figure 2. Uncleaned borehole with a dust layer between concrete and chemical mortar, taken from reference 2.

required. The following cleaning step is crucial for the performance of a chemical anchor and must be followed carefully. Residual bore dust fills the micro-undercuts in the borehole wall and works as lubricant decreasing the bond strength by half (Figure 2). Similarly, the bond strength of anchors set in water soaked concrete or water filled boreholes is reduced by 60% compared to those in dry concrete. In the injection and setting step several aspects have to be considered. As described before, the compounds of adhesive capsules are mixed by the rotating threaded rod.

In the case of injection systems, the two components are mixed in the static mixer tip attached to the cartridge. The first 20 g of formulation are discarded to assure homogeneous mixtures in all boreholes. About 2/3 of the borehole are filled with the formulation. The threaded rod is inserted within the specified working time and the load must not be applied until the end of the stated curing time. The curing time depends on the surrounding temperature and the heat transfer across the interfaces.^{1,4,5,6}

The performance of the fully cured anchors is affected by various parameters like the applied load and in-service temperature. Also chemical resistance is an important property as concrete is an alkaline medium. If the bond strength of the anchor is higher than the tension load resistance of the concrete, a concrete cone breaks out along the full length of the anchor (Figure 3, A). The rod might also be a source of error (Figure 3, B). The anchor itself fails if the load is too high or if its bond strength is weakened over time. Depending on the source of error, the bond fails either at the mortar/concrete or the mortar/rod interface (Figure 3, C and E). Mixed failure at both interfaces may occur too (Figure 3, D). A small concrete failure cone is typically observed close to the surface in the all three cases.⁷

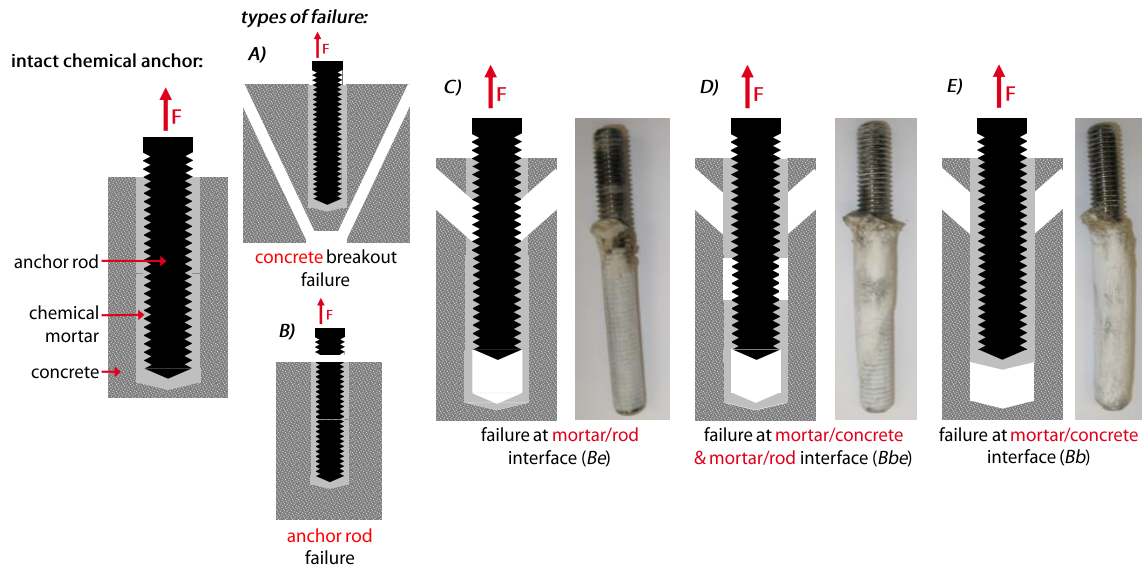


Figure 3. Types of failure under tension load (redrawn from reference 7).

Commercially available chemical anchors are mostly based on epoxy-amine and methacrylate systems (Figure 4). The first system is based on the polyaddition of epoxy-resin with di- and tri- amines. It exhibits low polymerisation shrinkage, good adhesion to concrete and is typically used for higher load applications (steel beams, silos, ...). However, epoxy-amine systems require higher temperatures and cures slower compared to a methacrylate-based system. At low temperature increased viscosity and decreased reactivity lead to very long curing times and an insufficient degree of curing. Careful handling is necessary due to the hazardous chemicals including caustic amines and sensitising epoxy-monomers.

The second system is known as “fast cure”-system exhibiting high performance also at low temperature. The chemical reaction is based on the free radical polymerisation of methacrylate-functionalised monomers. Fastening of façade-substructures and railings are two typical applications of this system. The main weak spot is the significant polymerisation shrinkage which can lead to inner stress in and hence, weakening of the chemical anchor.^{6,8}



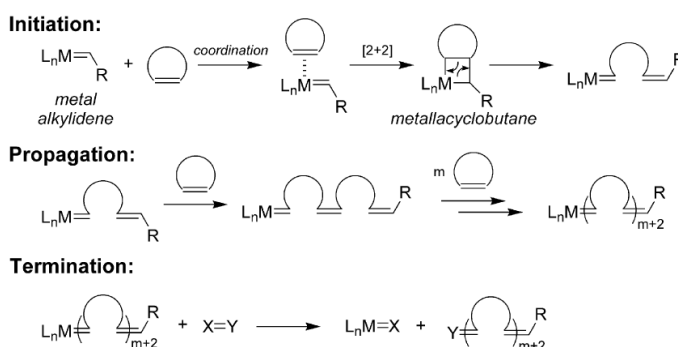
Figure 4. Typical methacrylate- (HIT-HY 200-A) and epoxy-amine- (HIT-RE 500 V3) based products by Hilti AG.

2.2 COMBINING ROMP WITH CONTROLLED RADICAL POLYMERISATION

The development of living and controlled polymerisation techniques allowed for the synthesis of complex polymers with well-defined architecture. The combination of those polymerisation methods gave rise to sophisticated macromolecular structures and networks. The following section outlines the research on combination of ring opening metathesis polymerisation (ROMP) with controlled radical polymerisation (CRP).

2.2.1 ROMP

ROMP itself is based on a transition metal catalysed carbon-carbon bond formation.⁹ The reaction follows the general mechanism of olefin metathesis by Chauvin starting with the coordination of a cyclic olefin to a metal alkylidene (Scheme 1).^{10,11} The double bond undergoes redistribution through a metallacyclobutane-

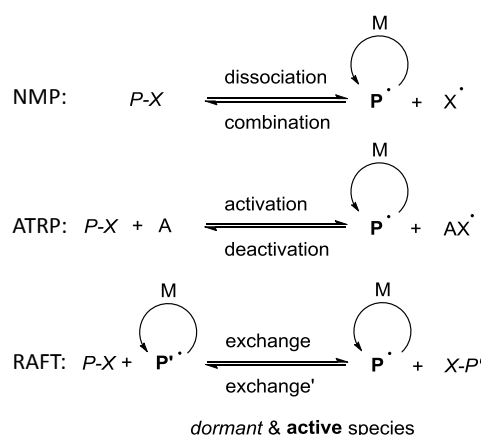


Scheme 1. General mechanism of ROMP (taken from reference 11).

intermediate and ring opening takes place. Propagation proceeds in a living manner with an active Ru-complex at the beginning of the growing chain. Termination is achieved by an olefinic reagent which cleaves the polymer chain from the Ru-initiator. The driving force of the polymerisation is the release of ring strain (ca. 5 - 30 kcal·mol⁻¹).¹² ROMP exhibits low polymerisation shrinkage due to the opening of the ring system.

2.2.2 CRP

The mechanism of CRP reactions (Scheme 2) is based on the reversible activation of a dormant species (P-X) to an active species (P[•]) which reacts with the monomer (M).¹³ The equilibrium is on the dormant side and the concentration of polymer-chain-radicals is lowered. Hence, the chance of termination reactions is decreased enabling controlled reaction conditions. The three main CRP, namely nitroxide mediated polymerisation (NMP), atom transfer radical polymerisation (ATRP) and reversible addition fragmentation chain transfer (RAFT) polymerisation, differ slightly in the specific mechanism switching between active and dormant species. CRP reactions facilitate the synthesis of well-defined polymers with low PDIs.



Scheme 2. Reversible activation of dormant species in NMP, ATRP & RAFT (redrawn from reference 13).

2.2.3 COMPATIBILITY OF ROMP AND CRP REACTANTS

Combining ROMP and CRP reactions allow for the built-up of copolymeric networks under controlled conditions. Several researchers have successfully accomplished this challenge, as will be described in chapter 2.2.4. However, the parallel implementation of these polymerisations is not at all an easy task. In fact, the selectivity of the reactive species and inertness of all compounds, which are technically not involved in the respective other reaction, is a main issue.

The following section focuses on the contribution of typical ROMP and CRP monomers, namely norbornenes and (meth)acrylates, in radical polymerisation and olefin metathesis, respectively. Comparing various publications revealed that the results are very sensitive to the specific reaction conditions. It is therefore not possible to give a universally valid statement. Further on, the role of ruthenium catalysts in radical polymerisation reactions will be elucidated.

THE ROLE OF NORBORNENE IN RADICAL POLYMERISATION

The role of norbornenes in radical polymerisation in solution has been examined extensively in the literature. *Sveum* and co-workers analysed the thermally initiated radical copolymerisation of norbornene (NB) and various (meth)acrylates.¹⁴ NB did hardly copolymerise with *tert*-butyl methacrylate (tBMA) reflected in the respective consumption of 5% and 95% in 300 min reaction time (0.88 M NB, 1.08 M tBMA in dioxane-*d*₈ at 70 °C). The result was a little different for the combination of NB with *tert*-butyl acrylate (tBA). Approximately 85% of tBA and 18% of NB were consumed within 400 min (0.90 M NB, 0.92 M tBA, in dioxane-*d*₈ at 70 °C). The higher affinity of acrylates towards NB is due to the lower electron density and smaller steric hindrance resulting in an increased crosspropagation. The copolymerisation of methyl acrylate (Me-A) with NB via ATRP was investigated by *Elyashiv-Barad et al.* (2.0 g (NB+Me-A) at 90 °C).¹⁵ At low NB concentrations in the monomer feed (NB:Me-A 1:5 and 1:10) the homopolymerisation of Me-A is preferred. The amount of norbornane units in the final polymer is still rather low, also at higher NB concentrations in the monomer feed (feed: 1:1 and 2:1 NB:Me-A; polymer composition: 1:3 and 1:2 NB:Me-A, respectively). The homopolymerisation of NB yielded only trace amount of polymer with this initiation system. These results show that the reactivity of the NB double bond in ATRP is rather low. The variation of initiator and ligand did not affect the resulting copolymer composition. The free radical polymerisation initiated with AIBN at 60 °C resulted in similar polymers concerning their composition (NB:Me-A ratio in the polymer) but with higher molecular weight and polydispersity indices (PDI) which is due to the uncontrolled process (10.6 mmol NB, 11.6 mmol Me-A, in 2 mL chlorobenzene at 60 °C). *Tanaka et al.* focused on the copolymerisation of various olefins, especially NB with BA and MMA, via ATRP as well as activators regenerated by electron transfer (ARGET) ATRP, in which tin (2-ethylhexanoate) (Sn(Oct)₂) is used as reducing agent (in anisole (20% v/v vs. monomer) at 80 °C).¹⁶ Even at a feed ratio of 1:1, the norbornane content in the final polymer was no higher than 24%. *Ihara et al.* explored the effect of incorporating norbornane units in the main chain of butyl acrylate (PBA)

via a thermally initiated radical copolymerisation of BA with 2-substituted norbornenes (in toluene at 85 °C).¹⁷ The higher the amount of norbornane units in the main chain, the higher is the T_g compared to the homopolymerised PBA. The same is true for the copolymerisation of NB with Me-A initiated by AIBN in THF at 70 °C.¹⁸ In contrast to NB, the polymeric double bond of PNB does not take place in ATRP as explored in the grafting from synthesis of PtBA in toluene at 90 °C.¹⁹

Liaw et al. explored the radical polymerisation in solution of bifunctional monomers bearing both a norbornene and a (meth)acrylic functionality. Cross-linking involving the norbornene moiety was observed in the photopolymerisation after a critical time of irradiation,²⁰ but thermally initiated polymerisation of another bifunctional monomer yielded polymers with a methacrylic backbone and norbornene side chains.²¹ ATRP of the bifunctional 5-norbornene-2-methyl methacrylate was performed by *Wooley's* research group in anisole at 70 °C.²² A theoretical analysis using Alfrey-Price equation suggested significantly higher reactivity of the methacrylate (MA) group compared to the NB unit. Hence, ATRP of the monomer should result in norbornene functionalised PMMA-homopolymers. The well-defined polymeric structure could be obtained with some restrictions. Controlled conditions could be achieved up to 50% conversion of the MA. Above this value, the side reaction incorporating the NB group could not be avoided.

In the course of investigations on grafting-through copolymers, the preparation of norbornenyl-functionalised macromonomers by ATRP was examined. *Wooley* and co-workers analysed ATRP of St and several (meth)acrylates in solution at elevated temperature using a norbornenyl-functionalised initiator.²³ As they aimed at controlled conditions, the reactivity of the norbornene double bond in α -position of the growing polymer chain should best be negligible compared to that of the vinyl-monomers (NB:vinyl = 1:200). ATRP of St, tBMA and MMA led to linear polymers with an intact norbornene end group indicating “inertness” of the norbornene double bond. Minor reactivity of the norbornene was observed in the ATRP of Me-A and tBA resulting in mixed linear and branched macromonomers. It is important to note that this effect seems to be very sensitive to the reaction conditions and partners. As mentioned above, free NB did not take part in ATRP of Me-A at a NB:vinyl ratio of 1:5 and showed only minor reactivity compared to Me-A at a ratio of 1:1 and 2:1.¹⁵ Two research groups presented alternative procedures to avoid the involvement of NB in ATRP. *Morandi et al.* prepared α -cyclobutenyl macromonomers by ATRP using a cyclobutenyl-functionalised initiator (in toluene at 60 - 100 °C).²⁴ *Grubbs' group* circumvented the problem by preparing a norbornene-free graft side chain via ATRP, introducing an azide end group and clicking it with an alkyne-functionalised norbornene dicarboximide.²⁵

THE ROLE OF (METH)ACRYLATES IN OLEFIN METATHESIS

Grubbs and his co-workers studied the cross metathesis (CM) of several classes of olefins, including (meth)acrylates.²⁶ Acrylates show only low tendency to homodimerise via CM and methacrylates do not homodimerise. Both were tested in CM with various other olefins but unfortunately, not with the same ones. Norbornenes were not included as reaction partners in this publication. CM of acrylates with different olefins such as St gave considerable high yields. Methacrylates on the other hand reached only low to moderate yields. *Lexer et al.* took advantage of the CM potential of acrylates and used them as terminating agents for asymmetric end-functionalisation of ROM polymers.²⁷ After ROMP of norbornene monomers the acrylate was added in excess. Depending on the residues on the acrylate, around 75% of the polymer chains were functionalised with the acrylate and 25% with the methylene group. *Liaw et al.* investigated the ROMP of bifunctional monomers bearing both norbornene and acrylic units.²¹ They obtained polynorbornene homopolymers with unreacted acrylic pendant groups. The functional groups did not undergo CM reactions.

The results are also quite concordant when the reactivity of methacrylates is evaluated. Various studies in literature state that the shielded double bond is not participating in ROMP making it an attractive functional group for further modification in the side chain of the polymer. *Liaw et al.*, for example, performed ROMP of a bifunctional norbornene-methacrylate monomer initiated with G1. The reaction turned out to be a norbornene-selective as confirmed by nuclear magnetic resonance spectroscopy and qualitatively by the lack of gel formation.²⁰ *Wooley* and co-workers demonstrated the efficient ROMP of a norbornene-functionalised macromonomer using the G3 initiator in toluene and MMA which was used as a cosolvent (40 vol%).²⁸ In contrast to the methacrylate, they showed that Me-A as cosolvent caused incomplete conversion attributed to chain termination by the acrylate. In another study they underlined these results. They carried out the norbornene-selective ROM homopolymerisation of the bifunctional 5-norbornene-2-methyl methacrylate in diluted conditions (1.3 mM).²² NMR spectroscopy and gel permeation chromatography (GPC) confirmed that little to no CM of the methacrylate unit has occurred. However, performing ROMP with another functionalised norbornene in presence of MMA (30vol%) did not work out that easily.²⁹ A sluggish course of polymerisation, a broad MWD and different control experiments indicated chain transfer to MMA by CM. A similar conclusion could be drawn from the observations of *Maughon* and *Grubbs*.³⁰ They conducted ROMP of 5-methacryloyl-1-cyclooctene (MA-CO) with a G1-like catalyst in various solvents. But instead of yielding linear polymers with pendant MA groups on every eighth carbon, they isolated a presumably highly cross-linked polymer insoluble in all common solvents. The polymer exhibited a broad and multimodal MWD and a polydispersity index (PDI) up to 15. The polymerisation yield increased while the PDI decreased (> 3) by increasing the monomer:catalyst ratio. Several control experiments have been conducted to elucidate the mechanism causing the cross-linking. In presence of MMA (9.0 eq), ROMP of MA-CO (1.0 eq) proceeded in an unaltered manner. The

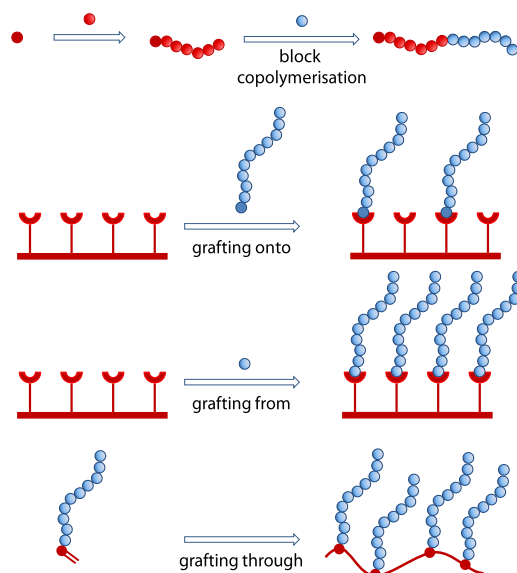
interaction of MMA with the catalyst would have caused chain coupling and hence, higher molecular weights. Mixing of the catalyst with MMA alone did not result in any reaction. Altogether, metathesis could be excluded as origin of the topical problem. The influence of *para*-methoxyphenol, a free radical inhibitor, on the polymer properties suggested cross-linking through a free radical mechanism.

THE ROLE OF RUTHENIUM COMPLEXES IN RADICAL POLYMERISATION

In the 1990s, great effort was made in the field of metal-catalysed CRP. Transition-metal complexes played a central role as controlling agent activating reversibly the dormant, terminally halogenated polymer chain. Prominent examples were based on Cu, Ni and Fe but also Ru catalysts were developed. *Sawamoto* reported the CRP of MMA mediated by $\text{RuCl}_2(\text{PPh}_3)_3$ in the presence of an Al cocatalyst.^{31,32,33} By using a multifunctional initiator multiarmed polymers could be produced with controlled MWD. In contrast, *Noels* and co-worker developed a class of Ru catalysts for ATRP of various methacrylates and St without the need of a cocatalyst.^{34,35} They varied the ligands of $[\text{RuCl}_2(\text{L})(\text{L}')]]$ and $[\text{RuCl}_2(=\text{CHPh})(\text{L})(\text{L}')]]$ complexes including several phosphates, 4-isopropyl toluene and N-heterocyclic carbenes (NHC). The polymerisation of BA and vinyl acetate did not meet the requirements of CRP. *Opstal* and *Verpoort* presented highly ATRP and ROMP active Ru- Schiff base complexes bearing varying carbene ligands (indenylidene, Fischer-type carbene, NHC).³⁶ *Grubbs* explored that various Ru benzylidene complexes turned from metathesis-active to metathesis-inactive when treated with alkyl halogens at elevated temperature.³⁷ The decomposed catalyst with the general structure $\text{Ru}_x\text{Cl}_y(\text{PCy}_3)_z$ exhibited excellent performance in atom transfer radical addition (ATRA) reactions.

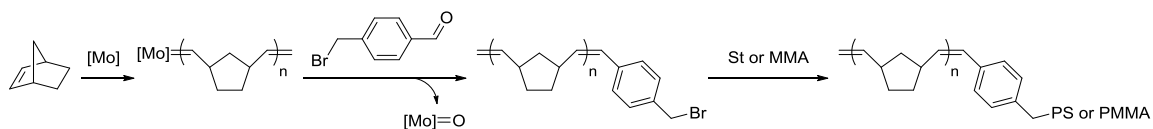
2.2.4 ROMP - CRP COPOLYMERS

A high variety of polymeric structures based on copolymerisation by ROMP and CRP are presented in the literature. Scheme 3 depicts the different synthetic route to block and graft copolymers.

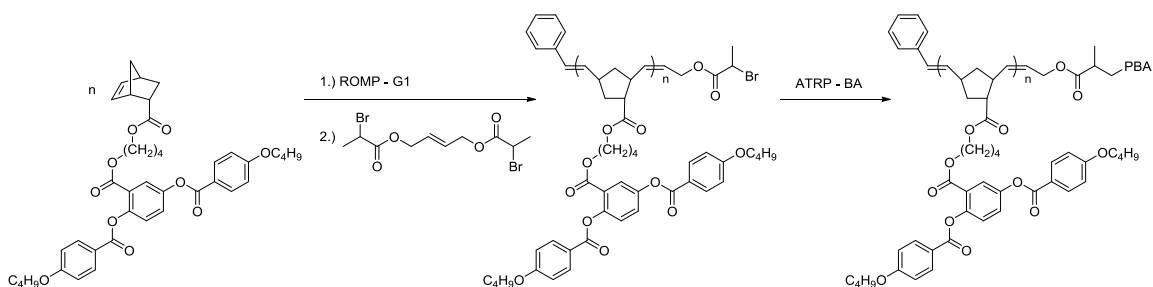


Scheme 3. Block copolymerisation and different types of graft copolymerisation (adopted from reference 38).

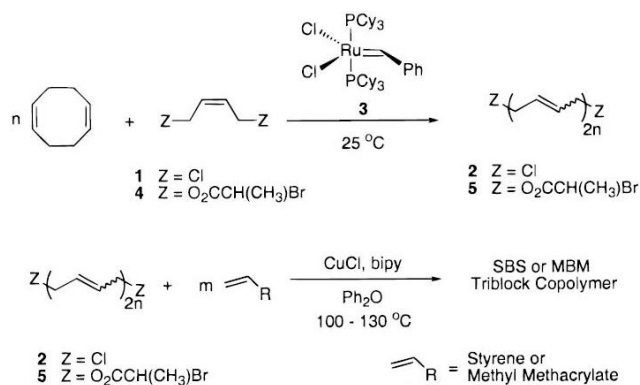
Block copolymers are prepared sequentially by homopolymerisation of the single blocks. The functional group capable to initiate the succeeding polymerisation is either introduced by chain-transfer agents (CTA) during polymerisation or by post-polymerisation functionalisation using termination agents. *Matyjaszewski* and co-workers were the first to present the successful preparation of block copolymers by ROMP and ATRP (Scheme 4).³⁹ They performed ROMP of norbornene (NB) or dicyclopentadiene (DCPD) with a molybdenum initiator terminated with a brominated benzaldehyde derivative. The halide species worked as initiator in the ATRP of styrene (St) or Me-A. Similarly, *Li et al.* prepared liquid crystalline (LC) block polymers (Scheme 5).⁴⁰ First, the LC block was synthesised by ROMP which was terminated with a halide-bearing ATRP-initiator molecule. Then, the isotropic block was prepared by ATRP of *n*-butyl acrylate (BA). These copolymers self-assembled into lamellar mesophases and exhibited thermally induced transitions similarly to LC-homopolymers. *Grubbs et al.* used difunctional CTAs, namely 1,4-dichloro-*cis*-but-2-ene and 1,4-(bis-2'-bromopropionate)-*cis*-but-2-ene, for the preparation of telechelic 1,4-polybutadiene (PB) by ROMP of 1,5-cyclooctadiene (COD) (Scheme 6).⁴¹ This difunctional macroinitiator was utilised for the preparation of ABA triblock copolymers by ATRP of St and methyl methacrylate (MMA). *Katayama et al.* performed ROMP of NB in the presence of several bromo- and chloro-vinyl ethers to introduce the desired end-functionality (Scheme 7).⁴² Although the presented vinyl ethers are easily prepared, this approach seems less practical as polymers with a broad molecular weight distribution (MWD) are obtained.



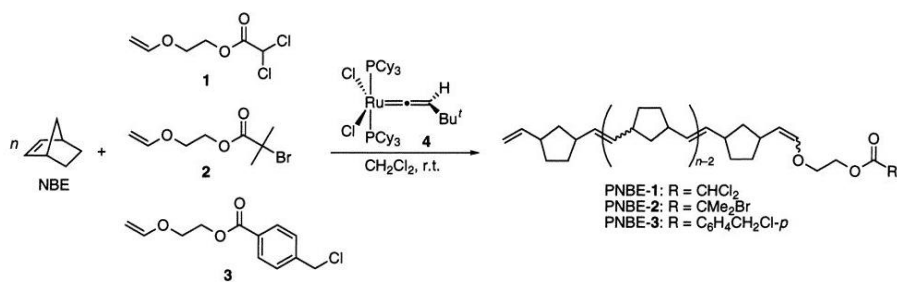
Scheme 4. Block copolymers via ROMP and ATRP (redrawn from reference 39).



Scheme 5. Preparation of liquid crystalline block copolymers (redrawn from reference 40).



Scheme 6. Preparation of ABA triblock copolymers via ROMP of COD with a chain transfer agent and ATRP of styrene or methyl methacrylate (adopted from reference 41).



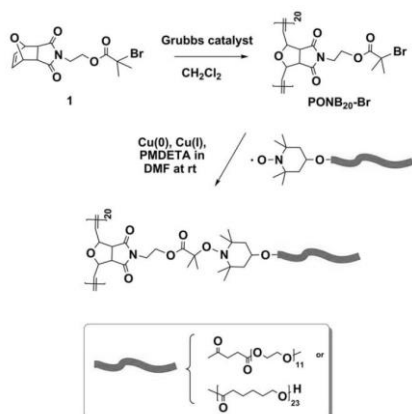
Scheme 7. Preparation of end-functionalised polynorbornene for the ATRP of styrene and methyl methacrylate (adopted from reference 42).

Graft copolymerisation gave rise to more enhanced polymeric structures. Few examples of **grafting onto** polymers prepared by ROMP and radical coupling are found in literature. *Tunca* and co-workers presented the grafting of poly(ethylene glycol) (PEG) or poly(ϵ -caprolactone) (PCL) onto ROMP-based poly(7-oxanorbornene-2,3-dicarboximide) (PONB) (Scheme 8).⁴³ PEG and PCL were end-capped with 2,2,6,6-tetramethylpiperidinyloxy (TEMPO) and reacted with PONB carrying a pendant bromide group via a nitroxide radical coupling reaction.

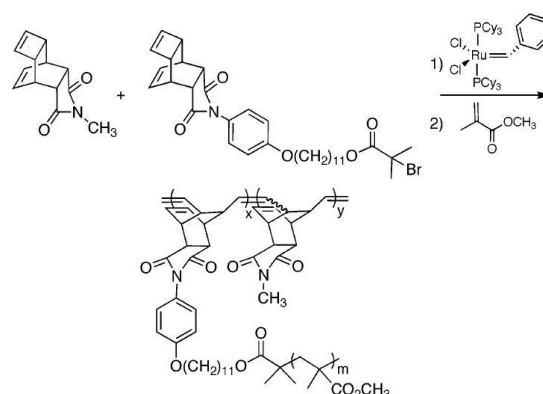
More emphasis was put on the development of **grafting from** copolymers. The high functional group tolerance of modern ROMP initiators¹⁰ allows for the preparation of a polymeric backbone containing radical initiation sites in the side chain.

The first papers on graft copolymers combining ROMP and ATRP were published in 2004. The working groups of *Weck* and *Novak* presented the random copolymerisation of ROMP monomers with and without a terminal bromide.^{19,44} The halide group worked as initiator for ATRP. *Weck's* group grafted *tert*-butyl acrylate (tBA) from poly(norbornene carboxylates) (Scheme 9). The grafted side chains were further modified by selective hydrolysis with trifluoroacetic acid (TFA) to give poly(acrylic acid) (PAA). The ester in α -position to the norbornene is less prone to hydrolysis due to the hydrophobic nature of the polynorbornene (PNB) backbone. *Novak's* group used cyclobutene monomers based on tricyclo[4.2.2.0]deca-3,9-dienes for the preparation of poly(buta-1,4-diene) (PBD) from which they grafted MMA (Scheme 10). Similarly, *Fontaine* and co-workers made PBD from cyclobutene which was 3,4-disubstituted with terminal ATRP initiating sites.⁴⁵ After ROMP of this inimer, two polystyrene (PS), poly(methyl methacrylate) (PMMA) and poly(*tert*-butyl acrylate) (PtBA) side chains per repeating unit were grafted from the backbone via ATRP. *Cheng* from *Wooley's* group investigated the combination of ROMP and ATRP in a one-pot one-feed approach (Scheme 12).²⁹ They synthesised the 5-norbornene-2-methyl ether terminally functionalised with an ATRP initiator. The Ru-based Grubbs 1st generation (G1) catalyst worked both as ROMP initiator and ATRP controlling agent. The ability of Ru complexes to work as catalyst in radical polymerisations has been demonstrated by the groups of *Sawamoto* and *Noels* (*cf.* chapter 2.2.3).^{31,34} The goal of *Cheng et al.* was to polymerise the norbornene moiety of the inimer and simultaneously build up the PMMA grafts. Unfortunately, the one-feed approach resulted in poor yields and broader MWD. Control experiments showed that the observed problem of ROMP could be assigned to chain transfer of MMA by CM. Also, ATRP was hampered as the amount of Ru-catalyst was optimised for ROMP but too low compared to the initiator for ATRP. They were forced to change their synthetic route to a one-pot but two-feed procedure. After successful ROMP of the norbornene-based inimer, another portion of the Ru-catalyst and MMA (30v% in toluene) were added for ATRP to obtain the graft chains.

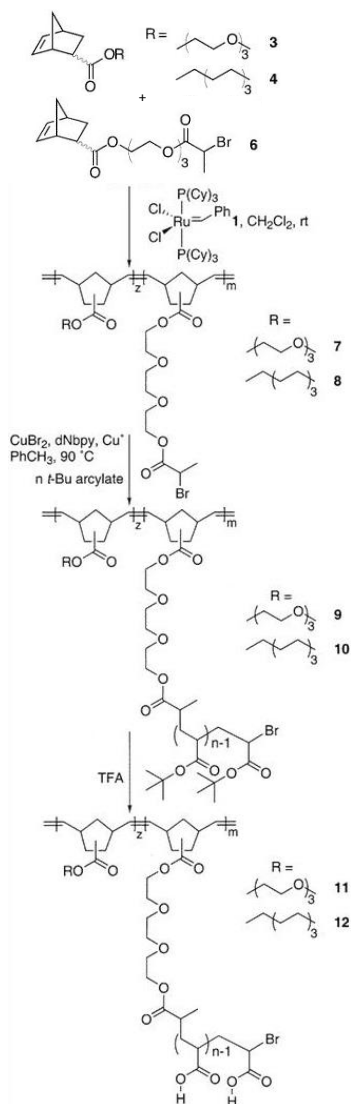
Wooley's group also presented core-shell brush graft copolymers based on ROMP and NMP.^{46,47} Starting from monomers with a norbornene moiety on one side and a nitroxide on the other side,



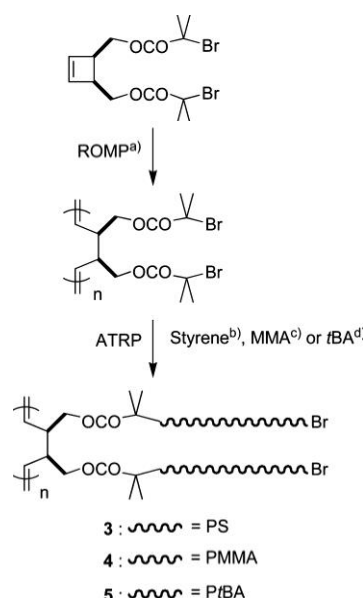
Scheme 8. Grafting onto polymers prepared by ROMP and nitroxide coupling reaction (taken from reference 43).



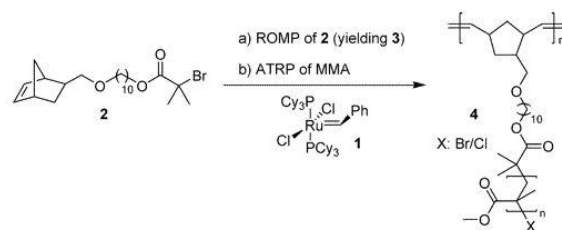
Scheme 10. Grafting from copolymers combining ROMP and ATRP (adopted from reference 44).



Scheme 9. Grafting from copolymers combining ROMP and ATRP (adopted from reference 19)



Scheme 11. Grafting from copolymers combining ROMP and ATRP (adopted from reference 45).



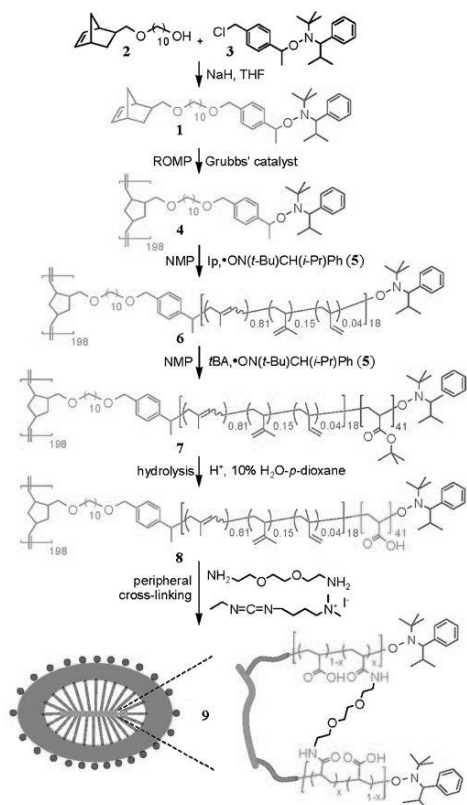
Scheme 12. Grafting from polymerisation via ROMP and ATRP starting from a bifunctional monomer (taken from reference 29).

ROMP was conducted and sequentially, isoprene (Ip) and tBA were grafted from the backbone via NMP (Scheme 13). Further modification of the polymer was achieved by cross-linking of either the polyisoprene (PIp) – or PtBA block and hydrolysis cleaving off the PNB-backbone along with the PIp block. Thereby, crosslinked and even hollowed nanoparticles were obtained. They also prepared graft copolymers via ROMP and RAFT in a one-pot synthesis (Scheme 14).⁴⁸ They polymerised a norbornene-functionalised RAFT agent via ROMP and subsequently, grafted St and maleic anhydride via RAFT random copolymerisation from PNB backbone. Amphiphilic core-shell brush copolymers were produced by hydrolysis of the anhydride. *Zhang et al.* used the ROMP-RAFT approach for the preparation of cobaltocenium-containing molecular brushes (Scheme 15).⁴⁹ ROMP of 5-norbornene-2,3-dicarboximide carrying a RAFT-active side chain was followed by RAFT polymerisation of cobaltocenium-containing methacrylate.

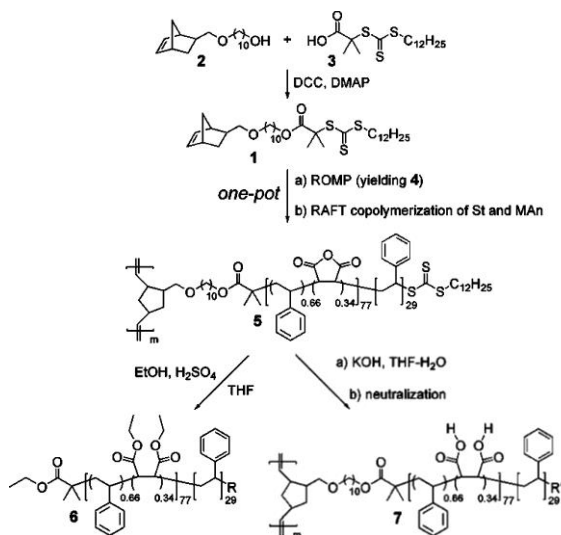
Another prominent strategy is the **grafting through** copolymerisation. The preparation of norbornene-terminated macromonomers via CRP is followed by ROMP. These macromonomers can be synthesised in two different ways: Polymerisation of a norbornene-functionalised initiator (inimer) or incorporation of a norbornene-end group after the polymerisation. The first approach, yielding an α -functionalised macromonomer, requires high tolerance against the norbornene double bond of the respective polymerisation method. This can be achieved by living polymerisation, for example anionic and cationic polymerisation or various CRP. The second approach towards macromonomers is based on the postpolymerisation-functionalisation of graft chains. However, a high degree of functionalisation yields are a main issue in this context and hard to reach.²³

The reactivity of vinyl-terminated macromonomers decreased with increasing molecular weight of the macromonomer.²³ In contrast to this, ROMP of the terminal norbornene group also works efficiently with macromonomers having a molecular weight up to 10 000 g·mol⁻¹. The release of ring strain (27.2 kcal·mol⁻¹)⁵⁰ and the less densely packed branching grafts compared to vinyl-type polymers makes ROMP of norbornene-type macromonomers thermodynamically and sterically favourable.

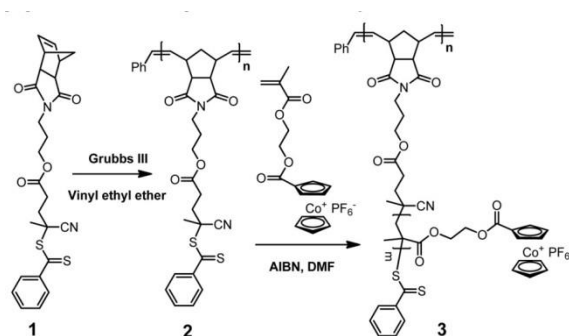
Fontaine and co-workers applied the same bifunctional monomer they used for grafting from polymerisation also in the grafting through approach combining ATRP and ROMP sequentially (Scheme 16).^{24,51} Two PS-co-PtBA block copolymers on cyclobutene were built up via ATRP. Optionally, the *tert*-butyl groups of PtBA were cleaved off with TFA yielding a PAA block as demonstrated by *Weck's* group.¹⁹ Brush copolymers with a PBD backbone were generated by ROMP of the macromonomers. *Grubbs* and co-workers developed a three-step strategy involving ATRP, a “click” reaction and ROMP (Scheme 17).²⁵ They performed ATRP of Me-A, St and tBA and transformed terminal bromines to azides. Then, they coupled these polymer chains with an alkyne-functionalised 5-norbornene-2,3-dicarboximide followed by ROMP to prepare the brush polymers.



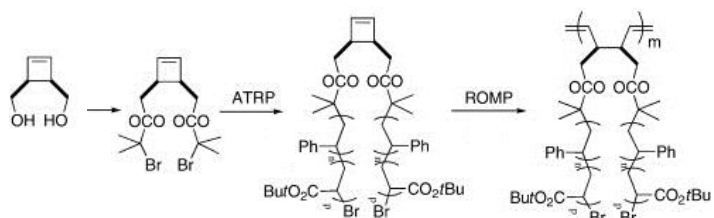
Scheme 13. Core-shell brush graft copolymers based on ROMP and NMP (taken from reference 46).



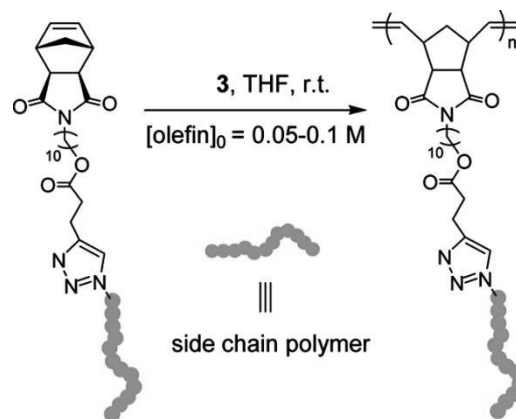
Scheme 14. Grafting from copolymers prepared via ROMP and RAFT (taken from reference 48).



Scheme 15. Preparation of metallocene-containing molecular brushes via ROMP and RAFT (taken from reference 49).



Scheme 16. Grafting through copolymerisation via ATRP and ROMP (adopted from reference 51).

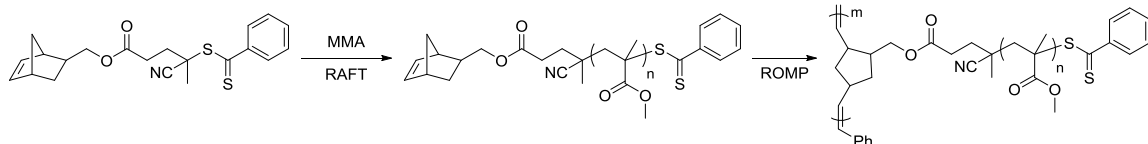


Scheme 17. ROMP of a norbornenyl macromolecule with a side chain polymer prepared via ATRP which was clicked to the norbornene derivative using copper-catalysed azide-alkyne chemistry (taken from reference 25).

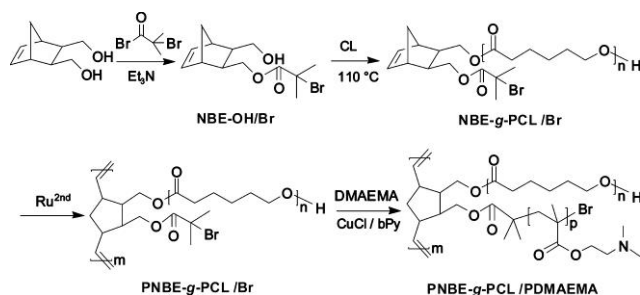
Similarly to what they showed for grafting from ROMP-RAFT copolymers, *Wooley's* group explored in the grafting through RAFT-ROM polymerisation (Scheme 18).^{28,52} Using a bifunctional monomer functionalised with NB and a RAFT-active trithiocarbonate unit, various PNB with either PMMA, PtBA or PAA graft chains could be synthesised.

Xie et al. combined ROP with ROMP and ATRP representing a **mixed grafting through - grafting from** approach (Scheme 19).⁵³ They transformed selectively only one hydroxyl of the 2,3-dihydroxymethyl-5-norbornene into an bromobutryl group giving a trifunctional inimer. First, the remaining hydroxy group was used to initiate ROP of ϵ -caprolactone. Second, the macromonomers were then polymerised via ROMP (grafting through) and lastly, ATRP of 2-(dimethylamino)ethyl methacrylate (DMAEMA) was conducted (grafting from). With this method, amphiphilic brush polymers containing both a PCL and a PDMAEMA chain on each repeating unit of the backbone could be synthesised.

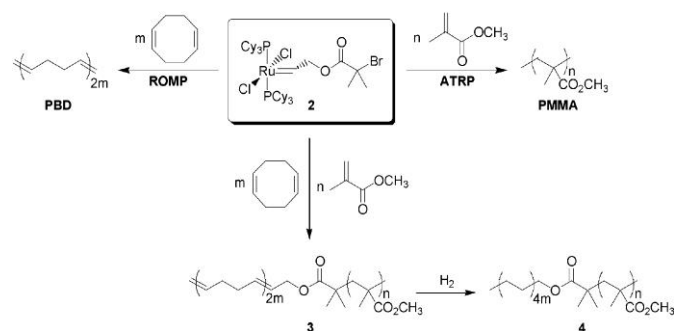
Tandem copolymerisation combining the mechanistically distinct reactions allows for the preparation of well-defined polymeric structures in a one-feed one-pot way. *Wooley's* approach of a one-feed tandem ROMP-ATRP polymerisation using a G1 initiator failed to work in a controlled manner.²⁹ In contrast, *Grubbs* modified the G1 initiator by exchanging benzylidene with allyl 2-bromo-3-methyl propionate (Scheme 20).⁵⁴ This bifunctional initiator was employed to simultaneously perform ROMP of COD and ATRP of MMA yielding a PBD-co-PMMA. Hydrogenation, giving polyethylene-co-PMMA, was achieved by transforming the residual Ru catalyst into a hydrogenation catalyst under a hydrogen atmosphere. Researches in *Héroguez's* group performed tandem ROMP-ATRP polymerisations in miniemulsions.^{55,56} They used three different routes involving two modifications of the G1 initiator (Table 1). Two modifications of the G1 initiator were used as ROMP initiator and ATRP control agent in routes 1 and 2 and additionally as ATRP initiator in route 3. Route 1 is the simultaneous homopolymerisation of NB and MMA. Graft copolymers were prepared via route 2 using norbornene functionalised ATRP initiator. Route 3 unifies both initiator systems in one molecule yielding star-like copolymers. *Ding et al.* synthesised a phosphoamidate featuring a ROMP-active 7-membered cycloolefin and two ATRP initiators (Scheme 21).⁵⁷ ROMP and ATRP, which involves DMAEMA, could be performed either in a communitive way or in a tandem one-pot reaction. The latter was conducted in a two-feed procedure using Grubbs 3rd generation (G3) and G1 catalysts for ROMP and ATRP, respectively.



Scheme 18. Grafting through RAFT-ROMP copolymerisation (redrawn from reference 52).



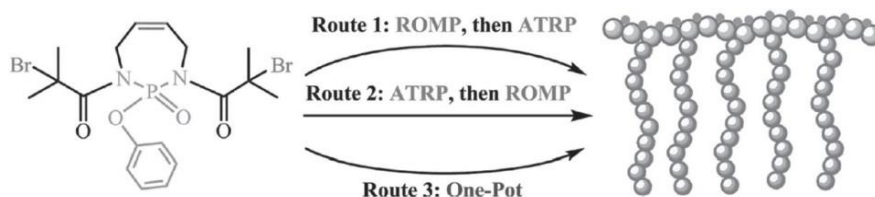
Scheme 19. Mixed grafting through - grafting from approach (taken from reference 53).



Scheme 20. Tandem ROMP and ATRP with a bifunctional Ru-complex for ROMP and ATRP initiation (taken from reference 54).

Table 1. Different synthetic routes combining a Ru-based ROMP initiator + ATRP control agent and ATRP initiator for the copolymerisation of NB and MMA in aqueous miniemulsions (redrawn from reference 55).

route	ROMP initiator + ATRP control agent	ATRP initiator
1		
2		
3		



Scheme 21. Synthetic routes to brush copolymers via ROMP and ATRP (taken from reference 57).

3 ROMP FOR CHEMICAL ANCHORS

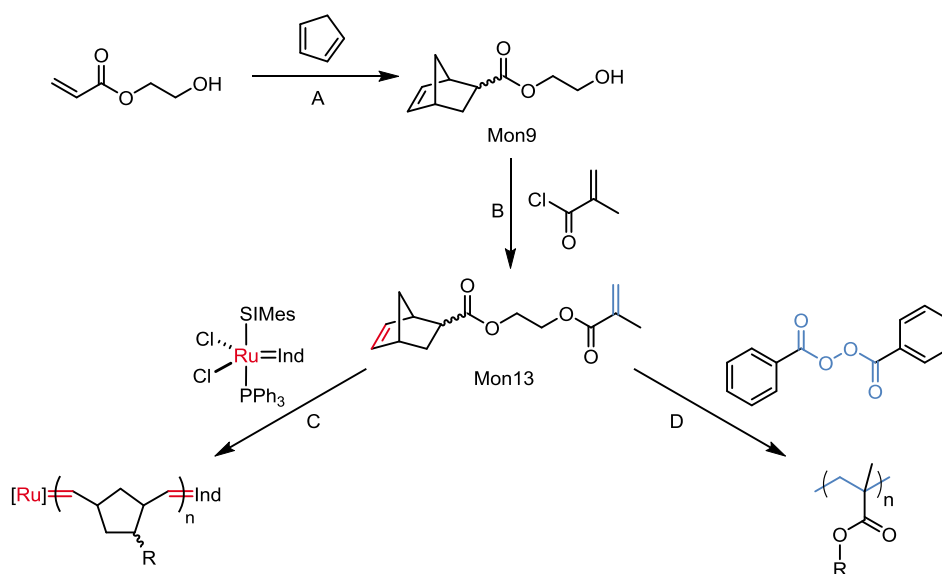
A feasibility study conducted in the course of the preceding master's thesis explored the potential of the ring opening metathesis polymerisation (ROMP) in the field of chemical anchors. ROMP of cyclic olefins is a living, exothermic polymerisation driven by the release of ring strain and exhibits low polymerisation shrinkage making it an interesting reaction for the investigated application. ROMP in bulk with various monomers like dicyclopentadiene and multifunctional norbornene monomers was tested extensively. It turned out that appealing working and curing times could be achieved by the choice of the appropriate Grubbs type catalyst. Alkali resistant polymers with high E-moduli (up to 1.8 GPa) and glass transition temperatures ($T_g > 70\text{ }^\circ\text{C}$) were successfully prepared at high curing temperature around $80\text{ }^\circ\text{C}$. As the application aims for the curing at room temperature or even below $0\text{ }^\circ\text{C}$ improvements are necessary.

3.1 DEVELOPING A DUAL CURE CHEMICAL ANCHOR SYSTEM

The initial idea was to make use of the synergetic potential of ROMP and radical polymerisation techniques in a Dual Cure system leading to a new product with advanced properties. We aimed for a fast curing system for the application also at low temperature with a high network density yet low polymerisation shrinkage.

Such Dual Cure systems would also facilitate to fulfil the requirements of two component formulations for the application as chemical anchor. Commercially available products consist generally of two components in the volumetric ratio of 3+1 or 5+1. This would pose a problem for ROMP-only systems. Whereas it is easy to prepare the component A containing the ROMP-monomer with fillers, it would be far more challenging to fabricate the required amount of component B as it would consist only of the very small amount of ROMP initiator needed and fillers. Radical initiated formulations involve two initiation molecules (e.g. peroxide and tertiary amine) which are both dissolvable in the monomer but stored separate from each other. We required a second component or system which is in best case inert in regard to the ROMP initiator but reactive during the polymerisation. In this context, a methacrylate based composition with the mentioned two-compound radical initiation system - similar to Hilti HIT-HY systems - would fulfil these requirements. Acrylates would be the more reactive monomers for the radical polymerisation but the terminal olefin would be prone to cross metathesis.^{26,27} Compared to acrylates, methacrylates are supposed to be less active in metathesis reactions due to the sterical hindrance of the adjacent methyl group.^{28,20,22}

We came up with the idea of a bifunctional molecule bearing both a norbornene moiety for ROMP (Scheme 22, C) and a methacrylate group for radical polymerisation (RadP, Scheme 22, D). Thereby, cross linking is promoted and a higher network density and glass transition temperature is achieved. The first monomer of this kind we dealt with was 2-(methacryloyloxy)ethyl-*endo,exo*-5-norbornene-carboxylate (Mon13). It is based on 2-hydroxyethyl-*endo,exo*-5-norbornene-carboxylate (Mon9), the Diels-Alder product of 2-hydroxyethyl acrylate (HEA) and cyclopentadiene (Cp) which is further esterified with methacryloyl chloride (Scheme 22, A and B; cf. chapter 3.3).



Scheme 22. Two step synthesis of Mon13 (A, B) and polymerisation via ROMP (C) or RadP (D).

The potential of a Dual Cure system compared to exclusive ROMP or free radical polymerisation (RadP) was investigated. Tensile tests were conducted revealing the mechanical properties of the polymers (Figure 5 and Table 2). Shoulder test bars were prepared using Mon13 and either the ROMP initiator M20 (50 ppm), the thermally activated radical initiator dibenzoyl peroxide (BPO, 1wt%) or both of them. Curing was performed either at room temperature (only ROMP) or at 80 °C for 24 h. Even at 80 °C, ROMP of Mon13 led to rather low E-moduli ($E < 120$ MPa) as only linear polymers can be built up. A 6-fold increase in the E-modulus was achieved by combining both types of polymerisation. Unfortunately, these values could not be compared to Poly13 cured via radical polymerisation only. The prepared shoulder test bars were solid but too brittle. Removing the samples from the steel mould was hard to achieve, as the specimen did not shrink upon curing. This was somewhat unexpected as the radical polymerisation of methacrylates involves pronounced volumetric shrinkage.⁵⁸ The specimen did swell upon storing in DCM revealing the norbornene double bond as an active side.

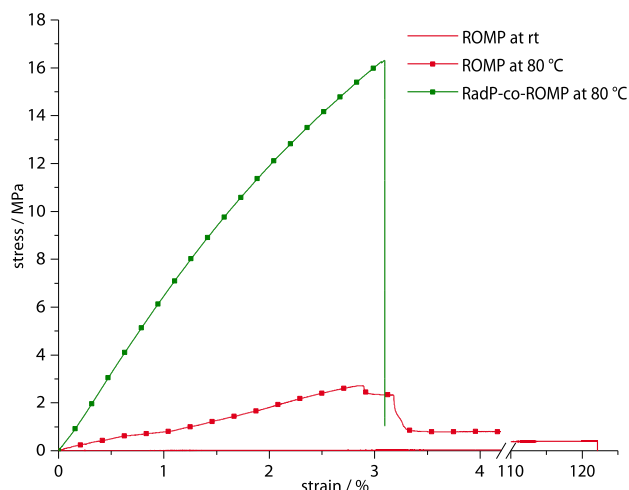


Table 2. Mechanical properties of Poly13 polymerised via ROMP, RadP-co-ROMP and RadP.

polymerisation	temperature	E / MPa
ROMP	rt	0.8 - 1.1
ROMP	80 °C	100 - 120
RadP-co-ROMP	80 °C	650
RadP	80 °C	-

Figure 5. Tensile test of Poly13 polymerised via ROMP or RadP-co-ROMP.

These results encouraged us to investigate both the Single Cure as well as the Dual Cure approach further, but focusing on curing at room temperature and low temperature performance. We therefore proceeded with preliminary curing tests which will be described in the following section.

3.1.1 PRELIMINARY CURING TESTS

The feasibility of a Dual Cure system combining ROMP with radical polymerisation was evaluated in preliminary curing tests. Several types of radical initiation systems apart from the thermally initiated BPO were investigated. Additionally to the RadP-initiation system used in Hilti HIT-HY products, we drew attention to two multi-compound initiation systems for controlled radical polymerisation (Table 3), namely single electron transfer (SET) and atom transfer radical addition (ATRA). These systems consist both of an initiator and a copper species with a ligand transferring the growing polymer chain reversibly into a dormant species.

Table 3. Compounds of the radical initiation systems SET, ATRA and RadP.

compounds	SET	ATRA	RadP
initiator	ethyl α -bromoisobutyrate (BiBEE)	BiBEE	dibenzoyl peroxide (BPO)
copper species	Cu	copper (2-ethylhexanoate) (Cu(Oct) ₂)	-
reducing agent	-	tin (2-ethylhexanoate) (Sn(Oct) ₂)	<i>N,N</i> -dimethyl- <i>para</i> -toluidine (DMpT) ^a
ligand	pentamethyldiethylene triamine (PMDETA)	2,2'-bipyridine (Bipy)	-
inhibitor ^b	4-hydroxy-2,2,6,6-tetramethyl piperidinyloxyl (Tempol)	Tempol	Tempol
accelerator	2-methyl-hydroquinone (MeHQ)	-	-

[a] needed only for curing at room or lower temperature; [b] was not used in preliminary tests.

Several mono- and bifunctional monomers (2-hydroxyethyl methacrylate, methyl methacrylate, Mon13 and Mon9) were used for these tests. The progress and success of curing was examined qualitatively in terms of the change in colour and condition of the formulations (Table 4).

Table 4. Change in condition of the formulation upon curing.

Category	Consistency of curing formulation
0	no apparent change in viscosity
5	slightly viscous
10	viscous
15	more viscous
20	highly viscous
25	stacked, highly viscous, sticky
30	gelation, soft & sticky
35	solid, gel-like, slightly sticky
40	solid, gel-like, not sticky
50	solid, very elastic
60	solid, rather elastic
70	solid, elastic
80	solid, slightly elastic
90	solid, hardly elastic
95	solid, barely elastic
100	solid, fully cured

SINGLE CURE SET SYSTEM

The potential of SET was investigated in preliminary tests polymerising mixtures of HEMA and MMA as well as Mon13 and Mon9 in bulk (Table 5 and Figure 6). The single components were mixed in a glass vial and the mixture was subjected to ultrasonication to achieve a homogeneous distribution of the Cu(0) powder. The change in colour and condition (viscosity, gelation) was followed over time. Homopolymerisation of HEMA was characterised with a sudden change of the colour to green indicating the formation of a Cu(I)/PMDETA complex as stated in the literature.⁵⁹ Gelation occurred within minutes; an elastic, solid polymer was obtained until the next day but a 1 mm thick, dark red layer on top remained. The suspension based on MMA only became greenish yellow at first and brown within 3 hours but stayed liquid. This difference could be assigned to the hydrophobic nature of MMA causing reduced rates of activation, polymerisation and disproportionation, whereas polar additives enable the latter.⁶⁰ SET polymerisation of mixed HEMA-MMA (75:25 – 10:90, w/w) formulations resulted in dark red liquids with slightly increased viscosity at higher HEMA-content. The attempt of homopolymerisation of Mon13 and Mon9 was similarly unsuccessful. The formulations turned dark green but stayed liquid. The viscosity of the Mon13-formulation increased slightly.

Table 5. Composition of a SET formulation.

compound	proportions / wt%
monomer	100
Cu	0.63
MeHQ	0.37
Tempol	0.05
BiBEE	1.10
PMDETA	1.10

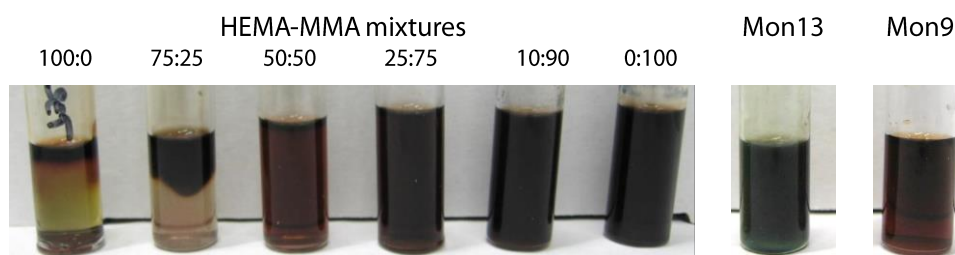


Figure 6. SET polymerisation of HEMA-MMA mixtures, Mon13 and Mon9.

Due to these unsatisfying results and the inconvenience of a solid compound in this liquid system, the SET LRP approach was discarded.

SINGLE CURE ATRA SYSTEM

A two-component approach was chosen for preliminary tests examining ATRA as potential radical initiation system (Table 6 and Figure 7). Initially, all compounds were mixed in a single vial by ultrasonic bath. Repetition of the tests revealed significant reproducibility problems (insufficient mixing). By switching to a two component test set-up, the obstacle could be eliminated.

The solid compounds $\text{Cu}(\text{Oct})_2$ and Bipy were dissolved in $\frac{3}{4}$ of the required amount of monomer using ultrasonication to accelerate this process (component A). The liquid compounds $\text{Sn}(\text{Oct})_2$ and BiBEE were mixed with residual aliquot of the monomer (component B). Depending on the monomer, the $\text{Cu}(\text{II})/\text{Bipy}$ complex dyed the solution in blue to green colours, as stated in the literature.⁶¹ In case of HEMA and MMA the colour changed to brown upon mixing of the two components as the reducing agent $\text{Sn}(\text{Oct})_2$ reacts with the $\text{Cu}(\text{II})$ complex to form $\text{Cu}(\text{I})$.^{62,63} This effect was not observed with Mon13. The exothermic polymerisation of HEMA yielded a solid polymer within minutes featuring a high degree of shrinkage. The polymerisation of MMA and Mon13 were less successful. The polymerisation of MMA was characterised by the brown colour of the $\text{Cu}(\text{I})$ but hardly notable exothermic behaviour and only a minor change in viscosity. In case of Mon13, the formulation turned light green and yellow and was still liquid in the beginning and only a slight increase in viscosity within 24 h.

Table 6. Composition of a two-component ATRA formulation.

component A	component B
0.75 g monomer	0.25 g monomer
0.64 wt% $\text{Cu}(\text{Oct})_2$	0.98 wt% $\text{Sn}(\text{Oct})_2$
0.24 wt% Bipy	0.60 wt% BiBEE

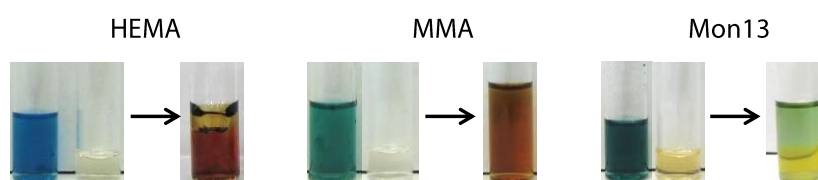


Figure 7. ATRA polymerisation of HEMA, MMA and Mon13; change of colour and condition upon mixing of the two components.

The observed differences in reactivity between HEMA, MMA and Mon13 could be related to the varying polarity of the monomers as mentioned in the literature.^{64, 65,66} The influence of polarity was investigated by polymerising mixtures of HEMA and Mon13 (Figure 8, see Experimental Table 33). The respective components A were coloured from deep blue to green as the polarity did also affect the colour of the $\text{Cu}(\text{II})/\text{Bipy}$ complex. The polymerisation start was judged qualitatively as colour and temperature were changing. Generally, the higher the content of HEMA, the earlier the polymerisation started. The homopolymerisation of HEMA led to a solid formulation within 1.5 min (Table 6, 1.5 min, the sample is turned upside down). The more HEMA was in the formulation the more pronounced was the change to a brown (or brown

greenish) colour. At least 50% HEMA was needed to obtain solid polymers within 15 min. The polymerisation of formulations with a lower HEMA-content was substantially slower and gave gelatinised or solid, but very elastic polymer within 15 min and fully cured, bright green samples after 24 h.

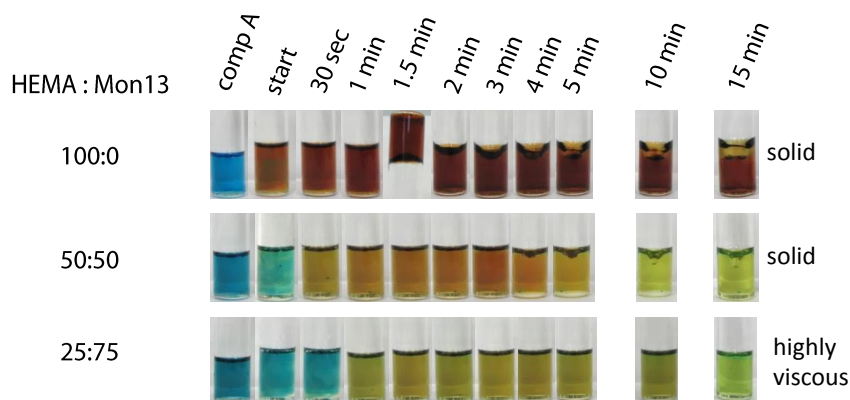


Figure 8. Change of colour and condition upon ATRA polymerisation of HEMA-Mon13 mixtures.

Further tests were conducted at 5 °C and -20 °C in order to evaluate the specific influence of temperature on the performance of HEMA-, Mon13- and mixed HEMA-Mon13 (75:25 – 10:90, w/w) formulations (see Experimental Table 33). Generally, the homopolymerisation of HEMA was unperturbed by the lower reaction temperatures. A fast increase in temperature (higher than 80°C) was observed and a fully cured polymer was obtained after 10 min. Increasing the amount of Mon13 in the formulation led to a delay of the polymerisation start. At a reaction temperature of 5 °C fully cured samples were obtained within 24 h but a smear layer was observed on samples with $\geq 50\%$ Mon13. At a reaction temperature of -20 °C solid samples were obtained within 24 h. The samples with a Mon13-content of $\geq 50\%$ were very elastic by that time indicating incomplete curing. However, curing for further 24h at the same temperature led to fully cured samples. It was concluded that the polymerisation is slowed down but not stopped. Again, a smear layer was observed on samples with $\geq 50\%$ Mon13. The samples were subsequently stored in DCM for three days to extract residual monomers which were qualitatively confirmed via NMR spectroscopy (Figure 9). Swelling of the samples (formulations $\geq 50\%$ Mon13) indicated cross-linkages and thus, the contribution of the norbornene group in the radical polymerisation. At a Mon13-content of $< 50\%$ swelling was not observed.



Figure 9. Extraction and swelling test of ATRA-polymers based on HEMA-Mon13 mixtures.

The participation of the norbornene double bond in the radical polymerisation was further studied using mixture of HEMA and Mon9 (Figure 10, see Experimental Table 32). The latter is the hydroxy-functionalised Mon13-precursor resembles HEMA replacing the methacrylate group by a norbornene (Scheme 22). Solid polymers were obtained with a feed ratio up to 25:75 with increasing elasticity with higher ratios of Mon9. The same trend was observed when samples were polymerised at 5 and -20 °C. This is in accordance with HEMA-Mon13 formulations. The increasing elasticity could be assigned to unreacted Mon9 serving as a plasticiser in the final sample. Formulation with 90% Mon9 became highly viscous indicating some extend of polymerisation. The homopolymerisation of Mon9 was not achieved. These findings were in line with the literature stated above and demonstrated that the norbornene double bond is taking part in the propagation in the presence of methacrylates.

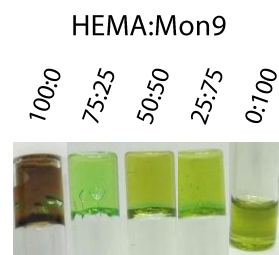


Figure 10. Formulations of HEMA-Mon9 mixtures with ATRA initiation system after 24 h at room temperature.

DUAL CURE ATRA-ROMP SYSTEM

The combination of ATRA and ROMP asked for a three-component system at that stage (Table 7). Component A and B were similar to the single cure ATRA system and component C was prepared as a stock solution of M20 in DCM. The aliquot amount of component C and A were simultaneously added to component B.

Table 7. Composition of a three-component ATRA-ROMP formulation.

component A	component B	component C
0.75 g monomer	0.25 g monomer	50 ppm M20
0.64 wt% Cu(Oct) ₂	0.98 wt% Sn(Oct) ₂	30 μL DCM
0.24 wt% Bipy	0.60 wt% BiBEE	

The preliminary tests yielded fully cured HEMA-Mon13 polymers at any ratio within 24 h. The curing behaviour was generally very similar to those of the single cure ATRA system (see Experimental Table 36).

SINGLE CURE RADP SYSTEM

Another promising option for Dual Cure system would be to combine ROMP with RadP initiated at room temperature with BPO and a tertiary amine.⁶⁷ The peroxide is activated by the amine which is made up of the general structure aryl-*N,N*-dialkyl-amine. This initiation system is well-studied and used in commercially available chemical anchors. The main advantage is its reduced complexity compared to multi-compound systems like ATRA and SET. It's a rather robust initiation system exhibiting good performance also at lower curing temperature. Ideally, BPO should be homogeneously distributed in the component in terms of finely-dispersed particles. In the dissolved state, BPO would degrade slowly generating radicals also at room temperature. Unfortunately, the latter is the case in Mon13 leading to solid materials within two weeks. For the evaluation of the Single Cure RadP, preliminary curing tests were performed using BPO either as thermal initiator or as redox couple in combination with *N,N*-dimethyl-*para*-toluidine (DMpT).^{68,69} Curing of HEMA, Mon9 as well as Mon13 led to solid materials within 24 h.

The radical curing behaviour of Mon13 in comparison to difunctional butane-1,4-diol dimethacrylate (BDDMA) was additionally examined by means of dynamic scanning calorimetry (DSC) and thermogravimetric analysis (TGA). For DSC measurements, both Mon13 and BDDMA were freshly mixed with peroxide which is activated by manganese dioxide. Isothermal DSC measurements were conducted at 5 °C and 25 °C for one hour (Figure 11, A, B). In both cases, the polymerisation of Mon13 started earlier than the one of BDDMA (at 5 °C 4 and 7 min, at 25 °C 18 and 32 min, respectively). In the case of curing at 5 °C, an exothermic peak was observed upon heating up from 5 °C to 100 °C indicating a post-curing process. TGA coupled with IR spectroscopy of the monomer showed that monomer components are evaporating from 140 °C on (Figure 11, C). The fully cured samples were analysed using the same set-up. Polymerised BDDMA lost 12% of its weight in two steps, releasing water at first and some kind of methacrylic ester at higher temperature. Polymerised Mon13 provided the similar results with 16%, the obtained IR spectra gave no explicit information about the released chemicals.

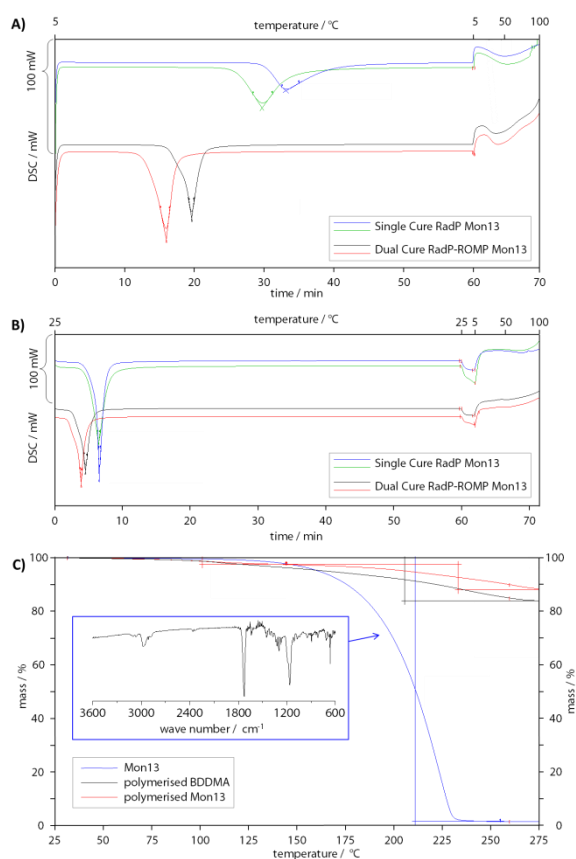


Figure 11. Thermal analysis of BDDMA and Mon13; A) isothermal DSC at 5 °C; B) isothermal DSC at 25 °C; C) TGA and IR spectrum of Mon13.

COMPARATIVE STUDY

In order to improve our understanding, specimen of Mon13 were produced with the polymerisation techniques we investigated so far (except for SET) and mechanical and thermal properties were determined (Table 8). The E-Moduli of ROMP - samples were quite low as the methacrylate is not contributing and hence, the polymers are lacking cross-links as discussed above. ATRA of Mon13 at room temperature and RadP by thermal initiation with BPO at 80 °C resulted in higher E-moduli. The mechanical properties of dual cure ATRA-ROMP samples could not be determined due to the brittleness of the samples. Interestingly enough, the storage modulus G' , determined below the T_g , was rather the same for all samples. The evaluation of the thermal properties showed that the T_g of Mon13-based polymers increased in the following order:

$$\begin{aligned} & \text{ROMP} < \text{ATRA-ROMP} < \text{ATRA (all cured at room temperature)} \\ & < \text{ROMP} < \text{RadP} < \text{RadP-ROMP (all cured at 80 °C)} \end{aligned}$$

Overall, two divergent conclusion could be drawn from the presented data. At room temperature, single cure ATRA gave the best results, whereas RadP-ROMP at 80 °C demonstrated the true potential of a dual cure system.

Table 8. Mechanical and thermal properties of polymers of Mon13 and DCPD prepared via various polymerisation techniques.

monomer	initiation system	curing temp.	E / MPa	G' ^a / Pa	T_g / °C
Mon13	ROMP	rt	0.8 - 1.1	$5 \cdot 10^8$	-12
	ATRA-ROMP	rt	-	$2 \cdot 10^8$	45
	ATRA	rt	400	$7 \cdot 10^8$	70 ^b
	ROMP	80 °C	100 - 120	-	-
	RadP	80 °C	-	$8 \cdot 10^8$	82
	RadP-ROMP	80 °C	650	$5 \cdot 10^8$	100

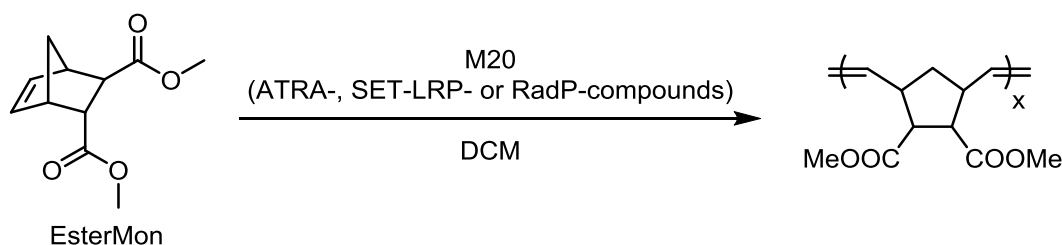
[a] determined at 30 °C, if $T_g > 40$ °C; [b] 80 °C when heated up to 180 °C.

3.1.2 STABILITY OF THE ROMP INITIATOR

A very crucial parameter in the designed two component (2K) Dual Cure system is the stability of the ROMP initiator dissolved in the one of the components. Apart from the fact, that the ROMP initiator must be clearly stored apart from the ROMP-monomer, there is still the question which are the best storage fellows for the probably most sensitive compound in the new system. But also, dissolving of the ROMP initiator could already lead to decomposition reactions and was investigated in the following study.

STANDARD BENCHMARK ROMP REACTION

The ROMP of the model monomer EsterMon was performed in order to evaluate the stability of the initiator M20 in solution and the influence of the single compounds of the radical initiation systems (ATRA, SET-LRP and RadP, Table 3) on the performance of M20 (Scheme 23 and Figure 12; for more details see Experimental Table 47).



Scheme 23. ROMP of EsterMon initiated by M20 in the absence and presence of ATRA-, SET- and RadP-compounds.

The reactions were conducted in dichloromethane (0.1 M) at room temperature and monitored via TLC. Stock solutions were used for a more precise addition of M20 (M:I = 300:1). The work-up was performed either after full conversion of the monomer or after a specific reaction time (17, 24 or 72 h). In case of incomplete conversion, the monomer:polymer ratio (M:P) of the reaction solution was analysed with ^1H NMR spectroscopy. The obtained polymers were examined via GPC in chloroform.

At first, the storage stability of M20 in solution was investigated. Four polymerisation reactions were started, two subsequent after the preparation of the M20-stock solution and two after a storage time of 15 h of the same stock solution. The first ones led to polymers with a molecular weight around $80\,000 - 100\,000 \text{ g}\cdot\text{mol}^{-1}$ within about one hour (Figure 12, blank, solid bars). As the target molecular weight ($63\,000 \text{ g}\cdot\text{mol}^{-1}$), calculated from the M:I ratio, is lower, incomplete initiation has occurred as expected from the slow initiation but fast polymerisation rate of this initiator. Storing of the stock solution led a change of colour (from red to brown) indicating a degradation of the initiator in solution. Further, the polymerisations started with this solution did not reach full conversion (M:P = 1:300) in respect of monomer within 24 hours. The polymers had much higher molecular weights ($235\,000 - 370\,000 \text{ g}\cdot\text{mol}^{-1}$) resulting from the reduced

amount of active initiator (Figure 12, blank, dashed bars). It became very clear that M20 is stable in solid state but is rather instable in solution, degraded possibly by the present oxygen.

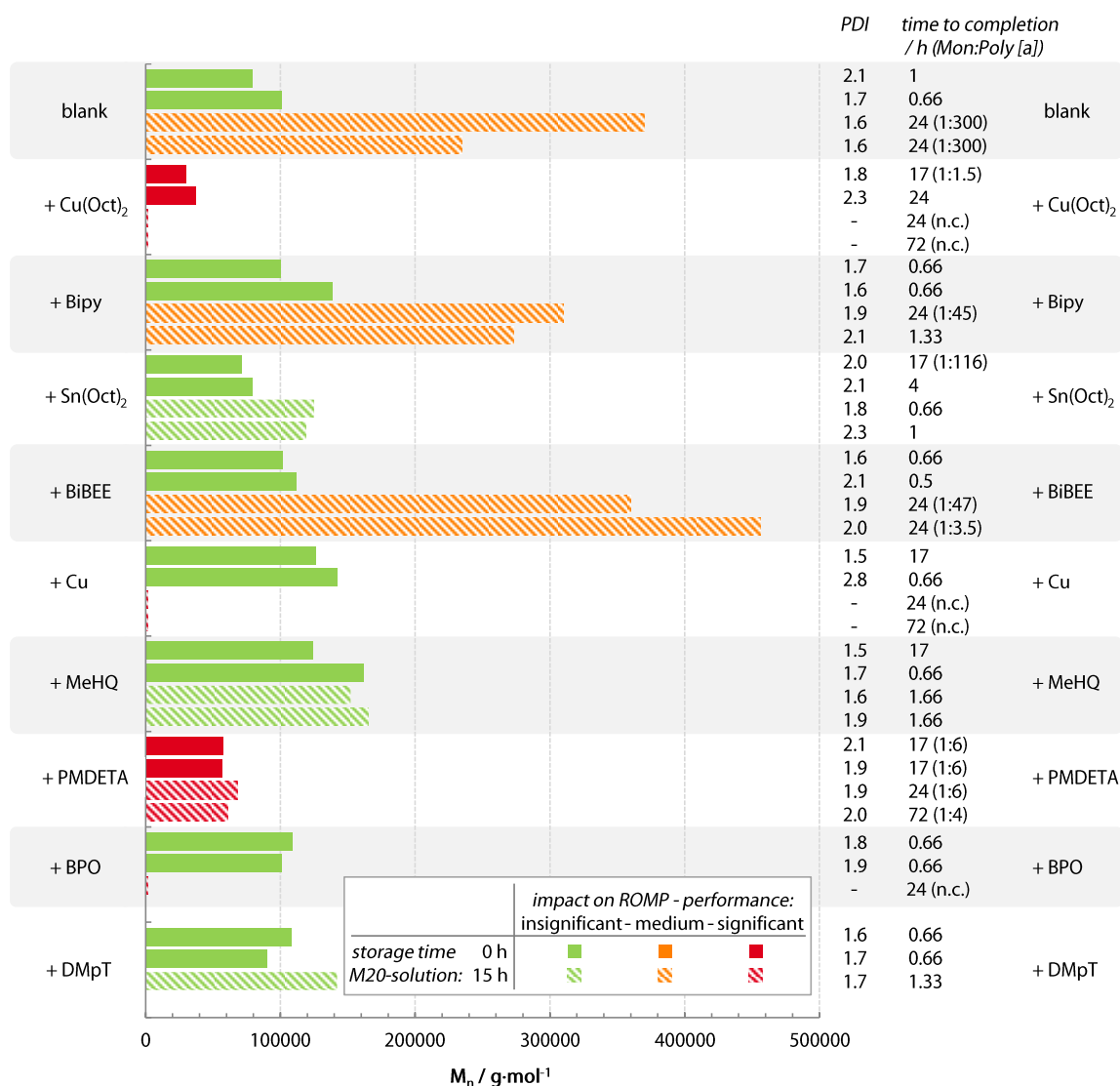


Figure 12. Molecular weight and PDI of polymers obtained in the stated reaction time via ROMP of EsterMon initiated by M20 in the absence (blank) and presence of single compounds of the radical initiation systems, [a] monomer:polymer-ratio after stated reaction time if full conversion was not reached.

Next, the influence of single compounds of ATRA-, SET-LRP- and RadP-initiation systems on the performance of M20 was analysed. Therefore, two approaches were used. The compounds were either mixed with the monomer-solution and then the freshly prepared M20-stock solution was added (Figure 12, solid bars) or the compounds were mixed with the freshly prepared M20-stock solution and stored for 15 h before added to the monomer-solution (Figure 12, dashed bars).

The addition of BPO und Cu to the monomer-solution had no significant effect on the polymerisation, whereas storing of these compounds with M20 for 15 h led to an almost complete

breakdown of the activity of the ROMP initiator. In the presence of PMDETA, polymers with a lower molecular weight of 57 000 – 68 000 g·mol⁻¹ were obtained, but the conversions within 24 h were relatively low (M:P = 1:6) in any case. PMDETA coordinates competitively with the olefin to the Ru-centre and thereby, it has a retarding effect on the propagation. Even worse was the result with Cu(Oct)₂. The addition of this compound to the monomer-solution prior to initiation gave polymers with low molecular weight (30 000 – 37 000 g·mol⁻¹) and conversions were also rather low. When stored with M20 for 15 h, no conversion was detected at all.

More favourable results were reached with the other compounds. Bipy, with its rigid structure, is known to be a poor ligand for Grubbs 1st generation catalysts,⁷⁰ and BiBEE had no effect on the polymerisation performance at all. Sn(Oct)₂, MeHQ and DMpT showed little effect on the polymerisation when mixed to the monomer-solution prior to initiation. Positive effects were observed when these compounds were mixed to the M20-solution and stored for 15 h. In all three cases, full conversions were reached in maximum 1.66 h). The molecular weight of these polymers was close to those from the blank reaction initiated with a freshly prepared M20-solution suggesting a conserving effect of the initiator in solution. Additionally, the M20-solution with Sn(Oct)₂ did not change its colour indicating no degradation of the initiator.

Sn(Oct)₂ is already known as a reducing agent by Matyjaszewski and co-workers in ATRP conducted in presence of air.⁷¹ Oxygen oxidises the activator Cu(I) to Cu(II) which is reactivated to Cu(I) by the reducing agent. Thereby, the present oxygen is consumed and eventually, the polymerisation starts. We became particularly interested in the potential of Sn(Oct)₂ as oxygen scavenger and performed further investigations by means of UV/Vis and NMR spectroscopy.

UV/VIS SPECTROSCOPY

UV/Vis spectroscopic experiments were conducted to monitor the degradation process of M20 which is accompanied by a change of colour from red to brown. Solutions of M20 with and without Sn(Oct)₂ were prepared in DCM and UV/Vis spectra were recorded repeatedly. In both cases, a fast decay of a peak at 400 nm and a shoulder at 500 nm was observed within one hour (Figure 13, A and B). Plotting the intensity at 400 nm vs. time showed a very fast decay running into a plateau after about 2 h in the absence of Sn(Oct)₂. Either the initiator is completely degraded or the dissolved oxygen is consumed within this time frame. In presence of the reducing agent, the degradation process is not inhibited but retarded running into a plateau after about 7 h (Figure 13, C).

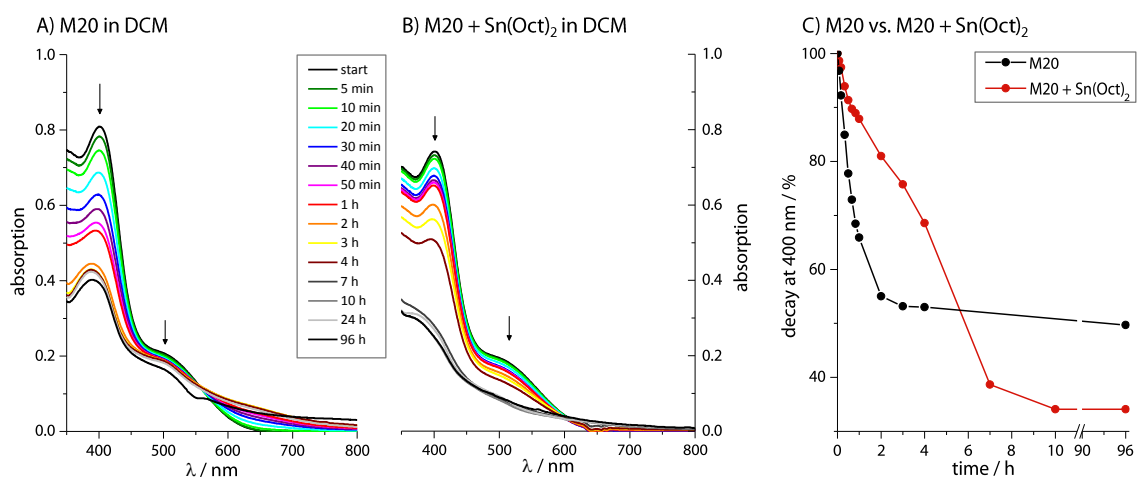


Figure 13. Decreasing intensity due to degradation process of M20 in absence and presence of $\text{Sn}(\text{Oct})_2$ (A and B: absorption spectra over time; C: decay at 400 nm over time).

^1H - AND ^{31}P -NMR SPECTROSCOPY

^1H - and especially ^{31}P -NMR spectroscopic studies were performed to gain information about the chemical process leading to the degradation of M20. It was suggested that this process originates from the labile nature of the coordination of triphenylphosphine to the Ru-centre.

^1H -NMR spectra (Figure 14) revealed small amounts of degradation products already at the beginning. Either the degradation process takes place subsequently and rather fast after dissolution in CDCl_3 or degradation products were already present in the unsolved initiator to some extent.

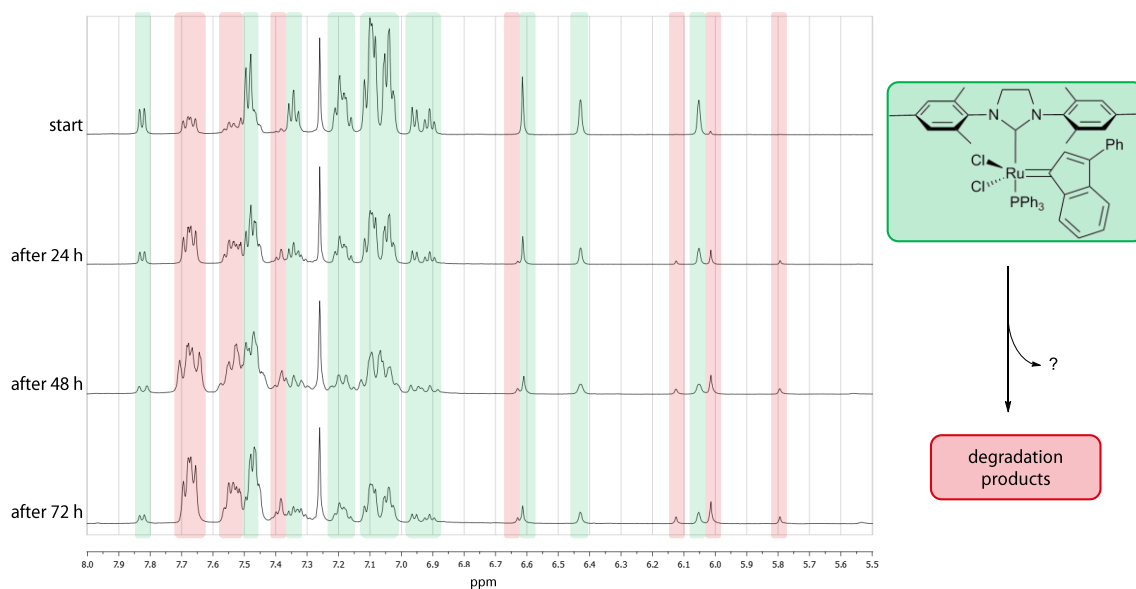


Figure 14. Degradation of M20 detected by ^1H -NMR spectroscopy in CDCl_3 at 25 °C.

More information about the degradation mechanism were gained from the ^{31}P -NMR spectroscopic study (Figure 15). M20 was dissolved in CDCl_3 (with or without $\text{Sn}(\text{Oct})_2$) and ^{31}P -

NMR spectra were measured repeatedly. In absence of $\text{Sn}(\text{Oct})_2$, the signals of the coordinated phosphine ligand (Ru-PPh_3 , 26 ppm) and of phosphine oxide (OPPh_3 , 29 ppm) but no free PPh_3 (-6 ppm) could be detected at the beginning (Figure 15, A). After 24 h Ru-PPh_3 and OPPh_3 were present in equal amounts. Storing for several days led to further increase of the OPPh_3 signal compared to the one of Ru-PPh_3 . In contrast to this, hardly any OPPh_3 but a small amount of free PPh_3 could be detected in the presence of $\text{Sn}(\text{Oct})_2$ at the beginning (Figure 15, B). Successive measurements displayed no free PPh_3 -signal after 48 h and the constant increase of OPPh_3 . However, the amount of OPPh_3 compared to Ru-PPh_3 was still rather small after 72 h. These findings underline the proposed degradation mechanism (Figure 15, C). The labile phosphine ligand dissociates, is subsequently oxidised to OPPh_3 by the dissolved oxygen and does not coordinate to the Ru-centre. Further information about chemical composition and follow-up chemistry of the degrading Ru-initiator was not gained. In the literature, Grubbs and co-workers proposed a decomposition mechanism resulting in the dimerization of the initiator.⁷²

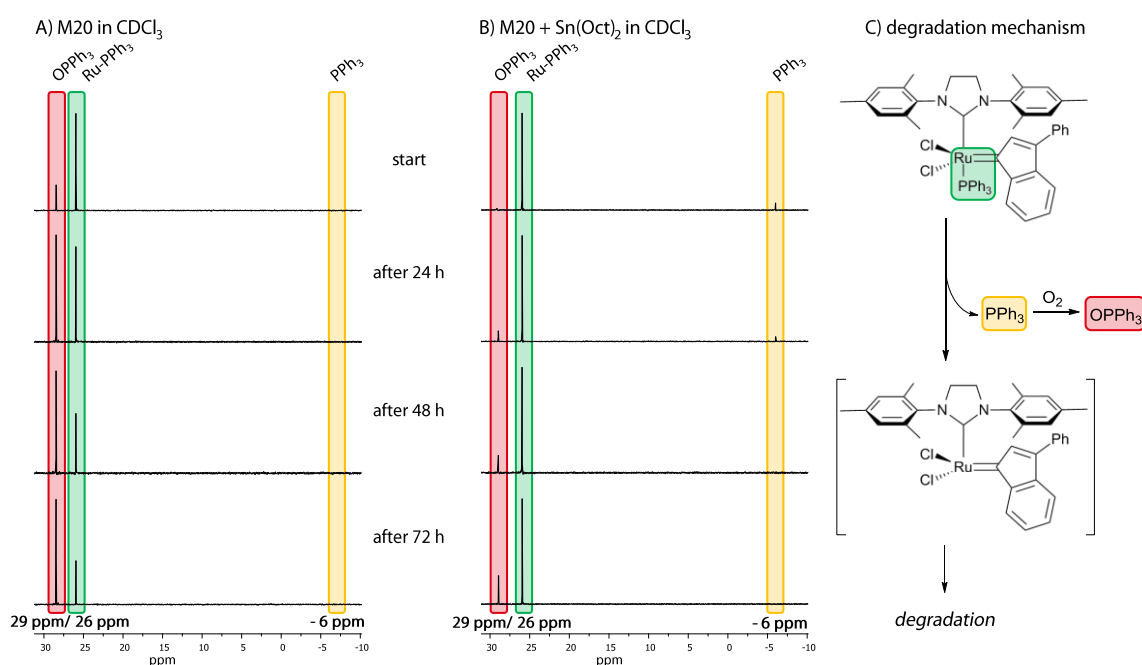
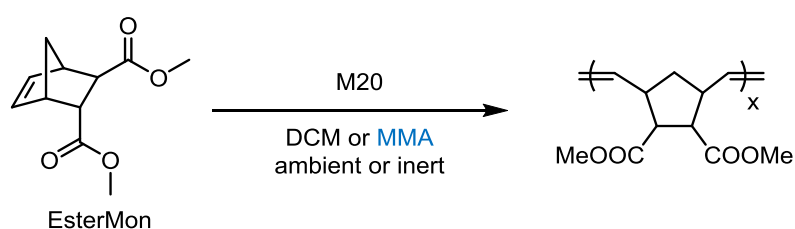


Figure 15. Irreversible formation of OPPh_3 detected by ^{31}P -NMR spectroscopy in absence (A) and presence (B) of $\text{Sn}(\text{Oct})_2$ in CDCl_3 at 25 °C, proposed degradation mechanism (C).

In the context of Dual Cure ATRA-ROMP, $\text{Sn}(\text{Oct})_2$ added in excess would simultaneously serve the role as antioxidative and reducing agent. Preliminary tests with Single Cure ATRA methacrylate systems showed that increasing the amount of $\text{Sn}(\text{Oct})_2$ up to 4-fold of the original level leads to an accelerated formation of $\text{Cu}(\text{I})$. At higher concentration neither accelerating nor retarding effects could be observed.

3.1.3 INTERACTION OF THE ROMP INITIATOR AND METHACRYLATE

Several research groups have investigated intensively the role of methacrylates in olefin metathesis or the role of ruthenium complexes in radical polymerisation reactions (*cf.* chapter 2.2.3). The results depended strongly on the specific reactants and reaction conditions. Therefore, a universal conclusion could not be drawn from those investigations. We decided to analyse the interaction of the ROMP initiator M20 with the methacrylate double bond performing the standard benchmark ROMP reaction (*cf.* chapter 3.1.2) in neat methyl methacrylate under ambient or inert conditions (Scheme 24). The polymerisation progress was monitored by means of TLC and the resulting polymers were characterised with GPC (Figure 16 and Experimental, Table 48).



Scheme 24. ROMP of EsterMon initiated by M20 in either DCM or MMA under ambient or inert conditions.

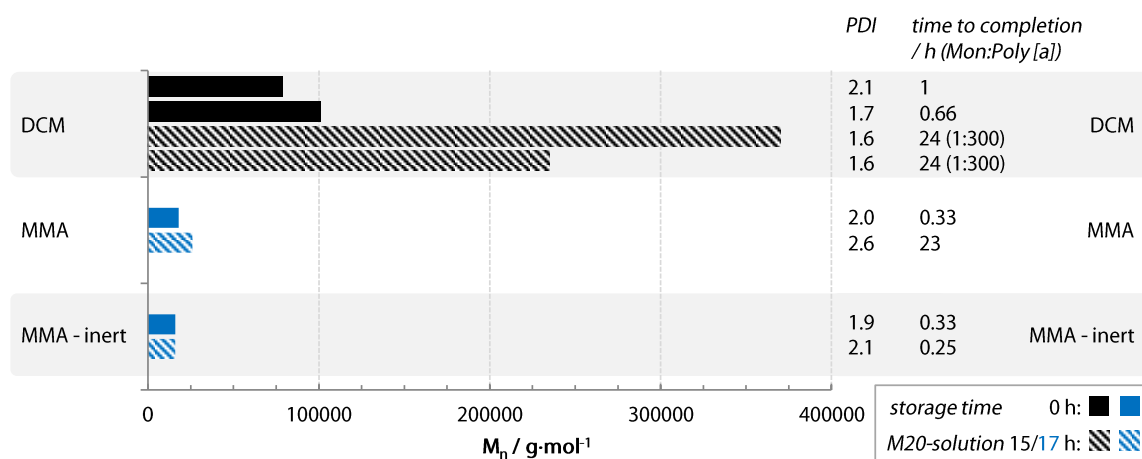
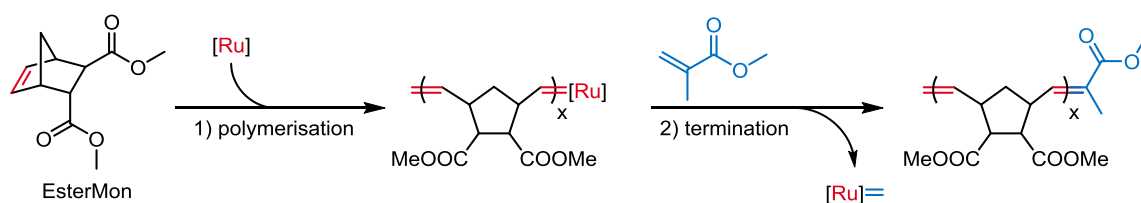


Figure 16. Molecular weight and PDI of polymers obtained in the stated reaction time via ROMP of EsterMon initiated by M20 in DCM, MMA or MMA-inert, [a] monomer:polymer-ratio after stated reaction time if full conversion was not reached.

First, M20-stock solutions in MMA were prepared and immediately added to the EsterMon-solutions working under either ambient or inert conditions. These polymerisation reactions proceeded faster than in DCM in terms of full conversion of EsterMon within 20 min (Figure 16, blue bars). A second set of polymerisation was started 17 h later but with the same M20-stock solutions. Under ambient conditions, the polymerisation progress slowed down compared to the first reaction. This could be assigned to the degradation of the initiator in solution leading to a reduced amount of active M20. In contrast to the polymerisation in DCM, full conversion of the monomer was achieved within 23 h (hatched bars - DCM and MMA). A different picture

emerged in the case of the M20-stock solution prepared in the inertly distilled MMA and stored under inert conditions (hatched bar - MMA-inert). Full conversion was reached within 15 min and the polymer reached the same molecular weight as with the freshly prepared initiator solution.

Generally, the molecular weight of the polymers prepared in MMA was between 18 000 and 26 000 g·mol⁻¹ instead of 63 000 g·mol⁻¹ as calculated from the M:I-ratio. The reduced molecular weight indicated that the methacrylate double bond was interacting with the initiator. For example, MMA could interfere in propagation acting a terminating reagent (Scheme 25), similarly to what was shown for acrylates.²⁷ The performed experiments could not provide information about the mechanism but a clear evidence of the contribution of methacrylates in bulk reactions.



Scheme 25. Possible reaction pathway with MMA acting as termination reagent in the ROMP of EsterMon.

It is important to note that these results depict the interaction of the Ru-initiator with methyl methacrylate in high excess compared to the norbornene. They can only give a hint about the processes going on in formulations with a NB:MA-ratio 1:1.

3.1.4 COMPOSITION OF A DUAL CURE SYSTEM

The composition of 2K Dual Cure formations was designed based on the compatibility of the ROMP initiator with compounds of the radically cured system (Table 9). A methacrylate was used as reactive diluent in component B, although some kind of interaction between the Ru-initiator and the methacrylate double bonds was observed. However, sufficient ROMP-activity in the respective two component systems is expected.

Table 9. Composition of 2K Dual Cure systems combining ROMP with radical initiation systems (ATRA, SET, RadP).

polymerisation	component A	component B
ROMP	norbornene	ROMP - initiator
radical polymerisation		methacrylate
ATRA initiator	Cu(Oct) ₂ Bipy	Sn(Oct) ₂ BiBEE
SET initiator	Cu MeHQ	PMDETA BiBEE
RadP initiator	BPO	DMpT

3.1.5 INVESTIGATIONS ON THE REACTIVITY OF ROMP-MONOMERS

Although the preliminary tests of the bi-functional Mon13 (Figure 17, A) showed rather good results (cf. chapter 3.1), there was still the demand for improvements on the ROMP part of a Dual Cure system. We tried to enhance the reactivity in ROMP of the monomer itself. The linker, especially the position of the carbonyl group to the norbornene double bond, is a prominent candidate in this context. This was already investigated in a Single Cure ROMP approach of Mon6 and Mon12 (Figure 17, B). A carbonyl group in α -position to the norbornene moiety is able to coordinate to the Ru-centre (Figure 17, C). In the propagation step, a second free coordination site is vacant for the addition of a norbornene double bond from a second monomer-molecule. In the instance of Mon6 and Mon13, the intramolecular carbonyl group can competitively coordinate at the second free coordination site. Thereby, the propagation is retarded and the overall performance is impaired. By altering the position of the carbonyl groups in Mon6 to the γ -position in Mon12 an immense increase in reactivity was achieved. The ROMP of Mon12 required a less active ROMP initiator to prevent a start of polymerisation before the initiator is evenly distributed. From a mechanistic point of view, coordination of the carbonyl group in the γ -position to the Ru-centre would lead to an entropically unfavoured 8-membered ring.

The influence of the anchoring group was intensively investigated by *Slugovc et al.*^{70,73} Polymerisation reactions of the 2,3-difunctionalised norbornene derivatives Mon I and Mon II with the initiators G1 (Grubbs 1st generation) and G3 (Grubbs 3rd generation) were monitored via ¹H-NMR spectroscopy and polymer properties were analysed with GPC in THF (Figure 17, D and Table 10). Independent of the used initiator, the polymerisation of Mon II proceeded faster than of Mon I reflected in $t_{1/2}$. Combining G1 and Mon I led to a polymer with a molecular weight close to the calculated value and a moderate PDI. Replacing Mon I by Mon II resulted in both high molecular weight and PDI. The latter indicates fast propagation combined with a low

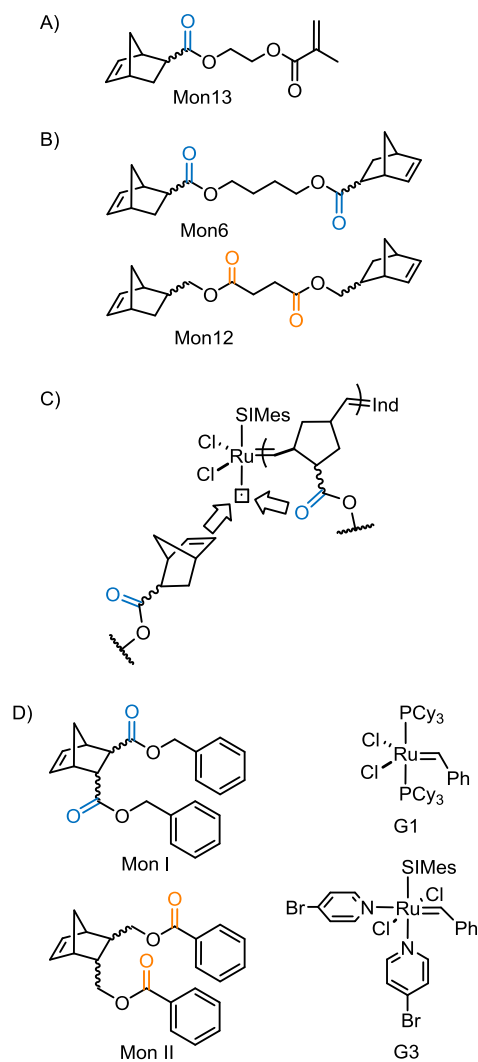


Figure 17. A) bi-functional Mon13; B) di-norbornenes Mon6 and Mon12 for Single Cure ROMP; C) competitive coordination of a norbornene double bond and the carbonyl group on the growing polymer chain; D) monomers and initiators investigated by *Slugovc et al.*⁷⁰

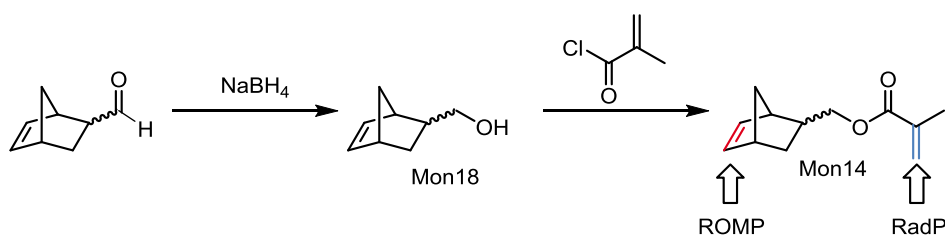
initiation rate and thus, incomplete initiation. The outcome was quite different when using G3 as initiator. The reaction speed increased significantly, but molecular weights were just around the calculated value and PDIs lower than with G1, demonstrating the qualitative advantages of this class of initiators.

Table 10. Molecular weight and PDI of polymers obtained via ROMP of Mon I and Mon II in DCM using different initiators, determined by GPC and reported relative to polystyrene standards.

monomer	initiator	M:I	$t_{1/2}^a$ / s	$M_n(\text{calc.})$ / $\text{g}\cdot\text{mol}^{-1}$	$M_n(\text{GPC})^b$ / $\text{g}\cdot\text{mol}^{-1}$	PDI
Mon I	G1	300:1	2100	109 000	105 000	1.4
	G3	300:1	48	109 000	84 000	1.1
Mon II	G1	300:1	240	109 000	433 000	2.1
	G3	300:1	12	109 000	120 000	1.2

[a] M:I = 20:1, solvent: CDCl_3 ; [b] in THF.

Based on the concept discussed above, another bifunctional monomer, *endo,exo*-5-norbornene-2-methyl methacrylate (Mon14), was designed (synthesis see chapter 3.3). Mon14 is quite similar to Mon13 but with a carbonyl group in the γ -position to the norbornene moiety. This monomer was synthesised starting either from 5-norbornene-2-carboxaldehyde or from also commercially available 5-norbornene-2-methanol (Mon18; Scheme 26).



Scheme 26. Two step synthesis of Mon14 starting from 5-norbornene-2-carboxaldehyde.

PRELIMINARY CURING TESTS

An increased reactivity was expected for the ROMP-based system with Mon14 but for comparison reasons, the single cure ATRA approach was tested first (see Experimental, Table 34 and Table 37). The (co)polymerisation of HEMA-Mon14 mixtures (100:0 – 0:100, w/w) at room temperature showed an enhanced reactivity and solid polymers were obtained within 10 min. Only, the homopolymer of Mon14 was slightly elastic within this time frame which is still an improvement compared to the very elastic Mon13-homopolymers. Polymerisations at 5 °C and -20 °C provided an even clearer picture. Copolymers (100:0 - 0:100, w/w) cured at 5 °C were already solid after 15 minutes. At -20 °C, polymers containing no more than 50% Mon14 were fully cured after 24 h. The copolymer HEMA-Mon14 (25:75, w/w) and the Mon14-homopolymer were solid but slightly elastic. Finally, the Dual Cure approach combining ATRA and ROMP gave the best results. The increased reactivity of Mon14, also in ROMP, was reflected in the curing performance. It was neither altered by the HEMA-Mon14 ratio nor by the chosen reaction temperature yielding completely cured samples after 24 h.

KINETIC NMR STUDY

As shown above, Slugovc et al. investigated the role of the anchoring group of 2,3-norbornene derivatives.^{70,73} Since we are dealing with 2-monofunctionalised norbornene derivatives, we decided to investigate the kinetics of this class of monomers in ROMP in more detail. For this purpose, Mon13 and Mon14 are no monomers of choice as the methacrylate double bond might interfere in ROMP. Instead, we used the two constitutional isomers 2-ethyl-5-norbornene-carboxylate (Mon16) and 5-norbornene-2-methyl acetate (Mon17) with an analogue position of the carbonyl group as in Mon13 and Mon14 (Figure 18). Additionally, the diastereomeric forms, namely *endo* and *exo*, were not separated but differences in reactivity were investigated in the presence of each other. A Grubbs 3rd generation type initiator, M31, was used allowing for complete activation of the initiator, controlled polymerisation conditions and a narrow MWD similar to G3. However, 5 eq of pyridine with respect to the initiator were added to slow down the polymerisation⁷⁰ in order to gain more information about the reaction kinetics before $t_{1/2}$. The reactions were performed directly in a NMR tube in CDCl₃ without stirring and NMR spectra were recorded repeatedly. Conversions were determined from the integrals of the signals for the disappearing monomeric and appearing polymeric double bond at 6.2 - 5.8 and 5.4 - 5.1 ppm, respectively (Figure 18).

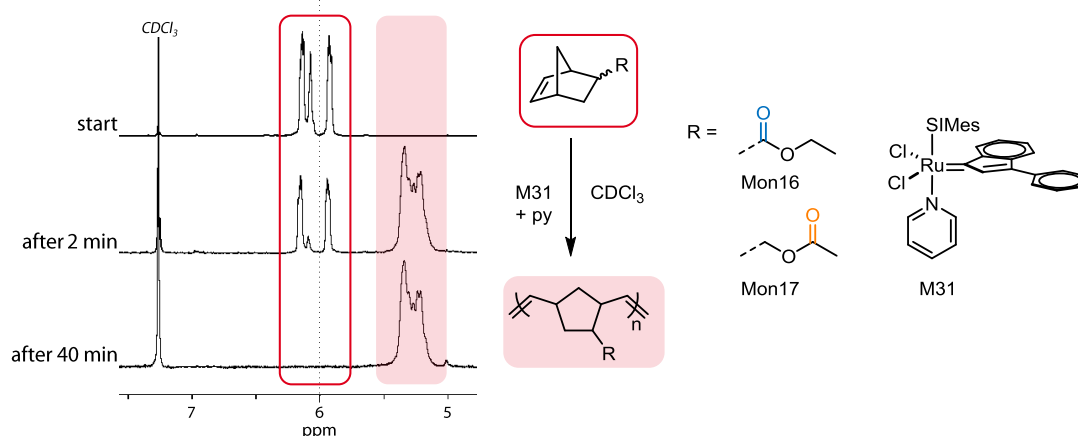


Figure 18. Following the polymerisation of Mon16 and Mon17 initiated with M31 in CDCl₃ via ¹H-NMR spectroscopy.

At a first glance, the results from this study were quite surprising. Although significant differences were expected, the reaction of Mon16 and Mon17 seemed to be unaffected by the chemical structure of the monomers as it proceeded at the same speed (Figure 19, solid and dashed lines and Table 11). However, the analysis of the respective polymers (Poly16 and Poly17) via GPC revealed substantial differences. The molecular weight of Poly17 is twice to three times higher than of Poly16. The MWD of Poly16 is rather narrow (PDI = 1.1), whereas the PDI of Poly17 is quite broad (2.6). Further, the obtained molecular weight of Poly16 is close to the calculated values. These data indicate controlled polymerisation conditions (initiation is faster than propagation) in case on Mon16. In contrast to this, only about a third of the initiator

becomes active in presence of Mon17 before the fast proceeding propagation starts. Therefore, less polymer chains with high molecular weight are built and the overall consumption of Mon17 is similar to that of Mon16.

Taking a closer look at the conversion of the *endo*- and *exo*-isomers of both monomers (Figure 19, lines with square and triangular symbols, respectively) revealed notable differences in reactivity. The *exo*-isomers react much faster than the *endo*-isomers – also in mixtures of both isomers. This is in line with the trends reported in literature, in which the phenomenon is assigned to the reduced steric hindrance at the olefin.^{70,73,74,75,76}

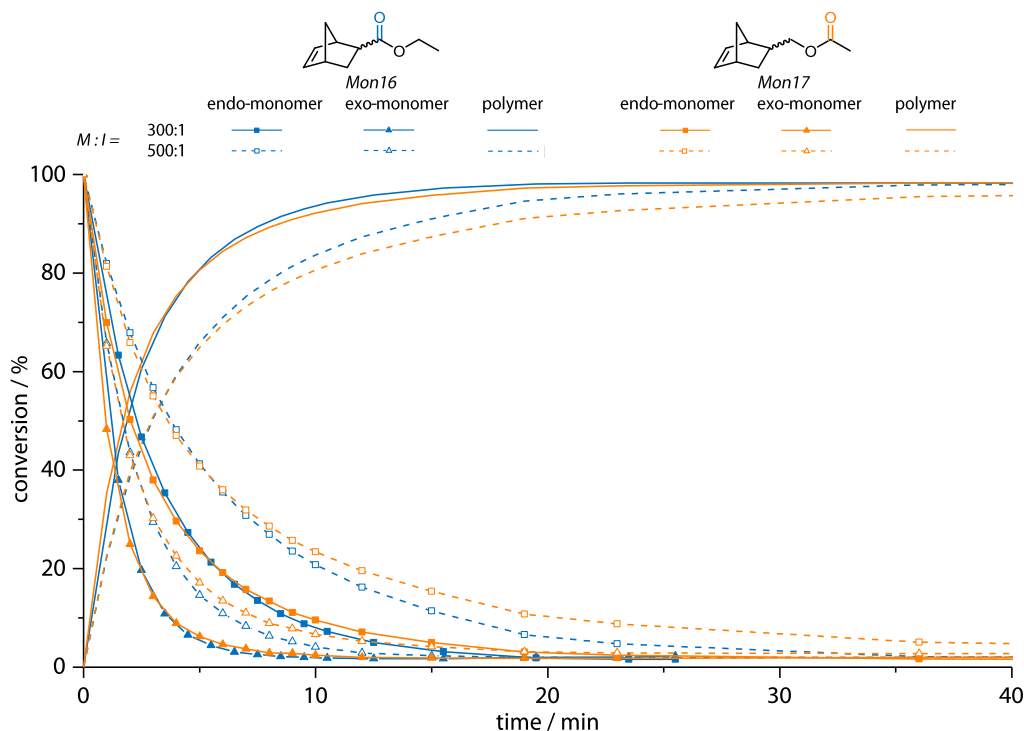


Figure 19. Conversions of *endo*- and *exo*-Mon16 and Mon17 to the respective Poly16 and Poly17; the reactions were performed in CDCl₃ (0.1 M) at different M:I-ratios using M31 as initiator (+5 eq pyridine).

Table 11. Molecular weight and PDI of polymers obtained via ROMP of Mon16, Mon17 in CDCl₃ using different M:I-ratios, determined by GPC and reported relative to polystyrene standards.

monomer	initiator ^a	M:I	t _{1/2} / s	M _n (calc.) / g·mol ⁻¹	M _n (GPC) ^b / g·mol ⁻¹	PDI
Mon16	M31	300:1	113	50 000	56 000	1.1
		500:1	176	83 000	86 000	1.2
Mon17	M31	300:1	103	50 000	123 000	2.6
		500:1	174	83 000	241 000	2.7

[a] M31 + 5 eq pyridine with respect to initiator in CDCl₃; [b] in THF.

Transferring these findings to the ROMP of Mon13 and Mon14 in bulk, the higher reactivity of monomers based on an inverse ester originates in the fast propagation compared to the initiation. This means that a lower amount of active initiator is needed to start a curing process which still leads to high conversions. It is therefore expected that Mon14 will give better results in Dual Cure formulations used as chemical anchors compared to Mon13.

3.1.6 COMPARATIVE STUDIES ON UNFILLED FORMULATIONS

Preliminary curing tests and the compatibility study showed that a Dual Cure system incorporating such complex systems as ATRA and SET bears several disadvantages mostly concerning storage stability and cross reactions with the ROMP initiator. As a result, the main focus changed to Single Cure RadP as well as ROMP and Dual Cure Rad-ROMP systems. In the following, several curing parameters and material's characteristics of the unfilled formulations were determined.

RHEOKINETICS

Rheokinetic measurements were performed in order to compare the curing behaviour of the Single Cure RadP or Dual Cure RadP-ROMP approach. It is a powerful technique monitoring the change in viscosity in terms of the storage modulus G' and the loss modulus G'' upon time (Figure 20). One of the most important parameters is the gel time defined as the time frame between the mixing of the components and either the onset of G' or the G''/G' cross over point. Further information about the curing behaviour can be gained from the curve characteristic of the increasing G' and G'' . Unfortunately, the maximum value of G' of most formulations could not be determined as it was running into the detection limit of the instrument at $1 \cdot 10^7$ Pa.

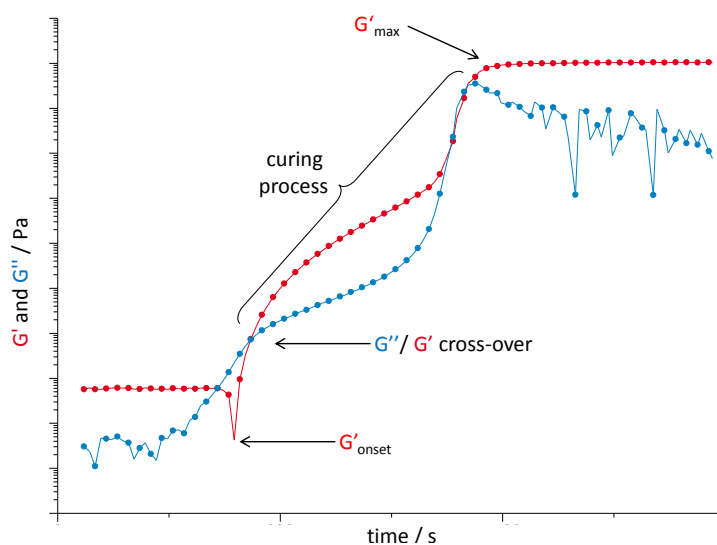


Figure 20. Characteristics of a rheokinetic measurement.

The formulations were freshly prepared before each experiment (Table 38). The experiments (triple determination) were conducted in using a plate-plate oscillatory rheometer applying a stress of 0.5% dynamic deformation at 1.0 Hz and 23 °C. Data points were measured every 15 sec. At a G' level higher than 10^6 Pa the applied stress was lowered to 0.01% dynamic deformation to avoid slipping of the polymer on the metal plates. The obtained results are stated in Figure 21 and Table 12.

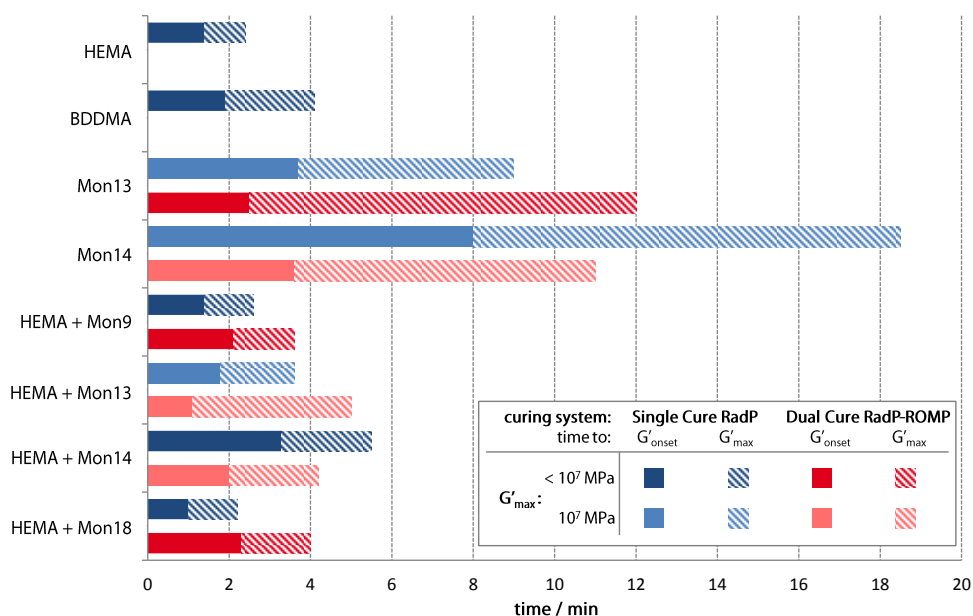


Figure 21. Time to G'_{onset} and G'_{max} of curing via Single Cure RadP and Dual Cure RadP-ROMP of various monomers.

Table 12. Rheokinetic parameters of RadP and RadP-ROMP cured monomers and monomer mixtures.

monomers	MA:NB	Single Cure RadP			Dual Cure RadP-ROMP		
		$G'_{\text{onset}} / \text{min}$	$G'_{\text{max}} / \text{min}$	$G'_{\text{max}}^a / \text{Pa}$	$G'_{\text{onset}} / \text{min}$	$G'_{\text{max}} / \text{min}$	$G'_{\text{max}}^a / \text{Pa}$
HEMA	1:0	1.4	2.4	$8 \cdot 10^6$	-	-	-
BDDMA	1:0	1.9	4.1	$1 \cdot 10^7$	-	-	-
Mon13	1:1	3.7	9.0	$1 \cdot 10^7$	2.5	12.0	$5 \cdot 10^6$
Mon14	1:1	8.0	18.5	$1 \cdot 10^7$	3.6	11.0	$1 \cdot 10^7$
HEMA + Mon9	1:1	1.4	2.6	$1 \cdot 10^5$	2.1	3.6	$7 \cdot 10^4$
HEMA + Mon13	3:1	1.8	3.6	$1 \cdot 10^7$	1.1	5.0	$1 \cdot 10^7$
HEMA + Mon14	3:1	3.3	5.5	$7 \cdot 10^6$	2.0	4.2	$1 \cdot 10^7$
HEMA + Mon18	1:1	1.0	2.2	$9 \cdot 10^6$	2.3	4.0	$3 \cdot 10^5$

[a] detection limit of G' at $1 \cdot 10^7 \text{ Pa}$.

The curing onset (G'_{onset}) in Single Cure RadP was observed after less than four minutes except for the Single Cure RadP Mon14 formulations and followed no distinct trend. The curing process started much faster in the Dual Cure approach than in Single Cure, except for HEMA-Mon9- and HEMA-Mon18-formulations. These results showed that ROMP contributes to a faster start of polymerisation in case of bi-functional monomers. Comparing both curing approaches, it became clear that the curing of pure Mon13- and Mon14-formulations bearing both functional groups of interest on one molecule exhibited the later curing onsets (Mon13 < Mon14).

The curing onset times obtained with this method provided an indication to those in the final application in the bore hole. In both cases, the thickness of the applied material was around 1 mm and the heat released upon polymerisation was dissipated at the interfaces. This was also the main differences to curing investigations in the Geltimer, which is a standard method for such investigation. However, only unfilled formulations were investigated in this comparative study to avoid side effects due to fillers. The curing onset of filled formulations which were used for

chemical anchors would occur much later as less of the reactive compounds ($\approx 40\text{wt}\%$) were present.

The interpretation of the G'_{max} data was complicated by the fact that many formulations would reach G'_{max} values higher than $1 \cdot 10^7$ Pa but ran into the detection limit of the instrument at this point. Only HEMA-Mon9-formulations in both Single and Dual Cure as well as HEMA-Mon18-formulations in the Dual Cure approach exhibited G'_{max} values between $1 \cdot 10^4$ and $1 \cdot 10^6$ Pa. The time frame to reach G'_{max} was also rather inconclusive following only the trend of G'_{onset} as Mon13- and Mon14-formulations are reaching this point later than other the formulations.

The curve shape of G' was another considerable parameter showing a generally valid trend for all samples investigated (Figure 22). Formulations consisting of mono-functional monomers only (e.g. Single Cure RadP HEMA) featured a single-step before reaching G'_{max} . By contrast, each formulation containing a bi-functional monomer (e.g. Single Cure RadP Mon13 & Mon14) exhibited a two-step curing curve until G'_{max} was reached. The described trend was also true for the not bi- but difunctional BDDMA which was behaving like a mono-functional monomer in this context.

Another interesting phenomenon monitored with the rheokinetic apparatus was the contraction of the formulations due to polymerisation shrinkage. Generally, the corresponding normal force can be observed only in the case of polymers that are adhering also to the metal plates. In this particular study, the normal force was constantly 0 N in the beginning and increased (negative values) at a distinct point (Figure 22). In the case of a single-step curing curve, the normal force drops rapidly as G' reaches its maximum values (e.g. Single Cure RadP HEMA). In contrast to this, the normal force started to descend at the inflection point in the case of two-step curing curves. This holds true for samples with a longer induction period (e.g. Single Cure RadP Mon13 & Mon14).

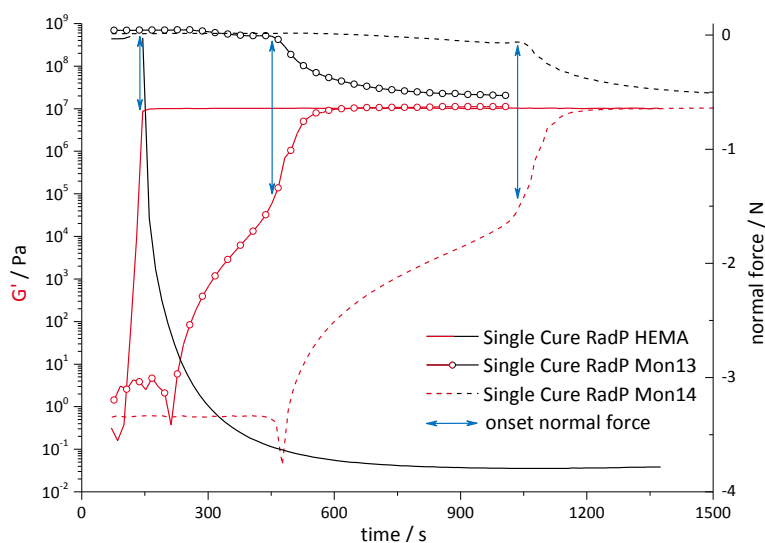


Figure 22. G' and the depending onset of the decrease of the normal force of various formulations.

It is important to note that only qualitative information could be gained by this means but a certain trend was revealed by comparison of the obtained data (Figure 23 and Table 13). Formulations with an equimolar MA:NB mixture reached a significantly lower normal force than those with a ratio of 3:1. Therefore, it could be concluded that a higher NB content leads to less polymerisation shrinkage. This is in line with the investigations on Hilti HIT-HY 200-A and its analogues containing Mon13 instead of BDDMA. The only exception of this rule was provided by the Single Cure RadP HEMA-Mon18 formulations.

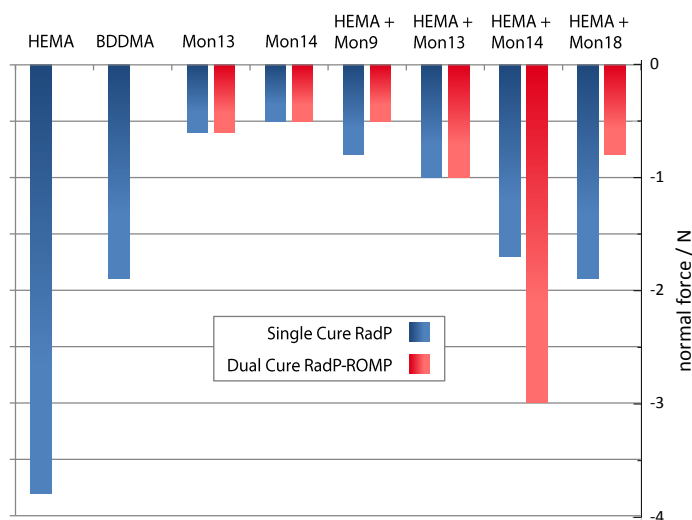


Figure 23. Normal force for Single Cure RadP and Dual Cure RadP-ROMP systems at the end of the curing processes followed by rheokinetic measurements.

Table 13. Comparison of MA:NB ratio and normal force_{max} of Single Cure RadP and Dual Cure RadP-ROMP systems.

monomers	MA:NB	Single Cure RadP	Dual Cure RadP-ROMP
		normal force _{max} / N	
HEMA	1:0	-3.8	-
BDDMA	1:0	-1.9	-
Mon13	1:1	-0.6	-0.6
Mon14	1:1	-0.5	-0.5
HEMA + Mon9	1:1	-0.8	-0.5
HEMA + Mon13	3:1	-1.0	-1.0
HEMA + Mon14	3:1	-1.7	-3.0
HEMA + Mon18	1:1	-1.9	-0.8

SHRINKAGE TEST

Polymerisation shrinkage which is caused by the closer packing of the monomers forming the polymer and thus, leading to reduced free volume is an intrinsic phenomenon in radical polymerisation.^{58,77,78} This effect has the power to compromise the strength of the chemical anchor. Either the bond strength is simply reduced as the formulation shrinks “away” from the borehole wall or, in the case of formulations that adhere on both concrete and metal rod, the shrinkage is hampered and internal stress is built up. Several experiments in this contribution discussed above indicate that monomers containing a norbornene double bond reduce this effect. Furthermore, ROMP is a low shrinkage-polymerisation technique as the linking of the monomers is coupled to the ring opening of the cyclic monomers.⁷⁹

A facile set-up for the measurements of polymerisation shrinkage of unfilled formulations was developed to investigate the effect of distinct monomer moieties and polymerisation methods (Figure 24). The formulations were composed similar to those in the preliminary curing tests in two and three components for Single Cure RadP, ROMP and Dual Cure RadP-ROMP systems, respectively. Upon mixing, exactly 1.0 mL of the formulation was transferred with a scaled syringe (1.0 mL/0.01 mL) into a hand-scaled 3.0 mL glass vial marked at 1.0 and 2.0 mL and cured for 24 h at room temperature. The vials were closed with a plastic cap during the curing process which was opened easily in case of overpressure. In order to determine the polymerisation shrinkage, the amount of water needed to reach the 2.0 mL mark was measured with a scaled syringe (1.0 mL/0.01 mL).

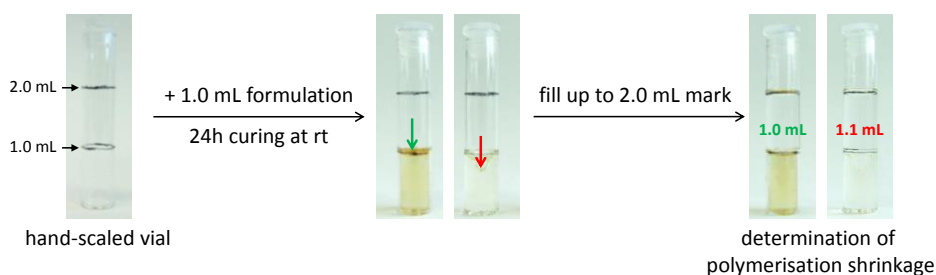


Figure 24. Determination of polymerisation shrinkage.

With this set-up the volumetric shrinkage upon polymerisation could be measured and formulations with various components could be compared. Small deviations in the behaviour of the formulations were observed but classified as uncritical concerning the comparability of the obtained values. For example, smear layers which were observed in the case of the Single Cure RadP HEMA-formulation stayed on the sample in the vial. Thus, the determined values are not altered by an accidental removal of the smear layer. All samples exhibit a more or less pronounced exothermic behaviour upon polymerisation, whereas adhesion on glass was observed only in the case of the Single Cure RadP of HEMA and partially of BDDMA. The polymers of Dual Cure RadP-ROMP HEMA-Mon14-formulations were prepared successfully only once. The

initiation occurred very early and the transfer of 1.0 mL with the syringe was not achieved. The preparation of Single Cure ROMP Mon14 samples was not achieved for the same reason.

Generally, the measured values for the polymerisation shrinkage vary between almost 0% and 10% (Table 14). Dual Cure RadP-ROMP led to lower shrinkage values than Single Cure RadP. Apparently, the lowest polymerisation shrinkage was achieved with the Single Cure ROMP system followed by Mon14-formulations in the Dual Cure approach. Radical polymerisation of HEMA showed to the highest shrinkage (10%), whereas the shrinkage of BDDMA formulations was significantly lower and comparable to other Single Cure RadP samples.

Table 14. Polymerisation shrinkage of Single Cure RadP and Dual Cure RadP-ROMP, colour-coding: 10% - 0%.

monomers ^a	Single Cure ROMP			Single Cure RadP			Dual Cure RadP-ROMP		
	shrinkage / %	± SD ^b / %	sample size	shrinkage / %	± SD ^b / %	sample size	shrinkage / %	± SD ^b / %	sample size
HEMA	-	-	-	10.0	0.0	5	-	-	-
BDDMA	-	-	-	4.2	0.8	5	-	-	-
Mon9	0.0	0.0	5	-	-	-	-	-	-
Mon13	0.0	0.0	5	4.8	1.6	3	2.3	1.5	3
Mon14 ^c	-	-	-	5.7	2.2	6	0.5	0.8	6
HEMA + Mon9	-	-	-	3.8	1.0	4	3.0	1.6	5
HEMA + Mon13	-	-	-	6.0	1.0	3	2.2	0.8	5
HEMA + Mon14	-	-	-	8.5	1.9	6	2.0	-	1

[a] mixed formulations in molar ratio = 1:1; [b] SD = standard deviation; [c] failed due to fast initiation.

The statistical error caused by the use of 1.0 mL syringes (1.0 mL/0.01 mL) was investigated gravimetrically with water at three different volumes to determine the accuracy of the obtained values. The statistical errors increased with decreasing volume as follows: 0.5%, 0.6% and 7.9% for 1.0, 0.05 and 0.01 mL, respectively. These errors alter neither the general trend nor the range of the measured shrinkage values (0% < x < 11%) in a significant way. Therefore, the presented set-up for the measurement of the polymerisation shrinkage of unfilled formulations is considered as reasonable.

DYNAMIC MECHANICAL ANALYSIS

The glass transition temperature (T_g) is a crucial parameter of polymers and thus, an interesting key value to compare the quality of the different formulations and polymerisation methods. The dynamic mechanical analysis (DMA) is a powerful tool to analyse the mechanical properties of polymers upon heating determining the T_g . There are several different definitions of the T_g -value stated in the literature (Figure 25).⁸⁰ First, the E' onset is related to the mechanical failure of the polymer. Second, at E''_{\max} polymers are getting in motion leading to thermally induced changes of the physical property. The third and most commonly used is the maximum of $\tan \delta$ which is the E''/E' -ratio. It reflects the transition point between the glassy and rubbery state of polymers. The last one was chosen for this contribution.

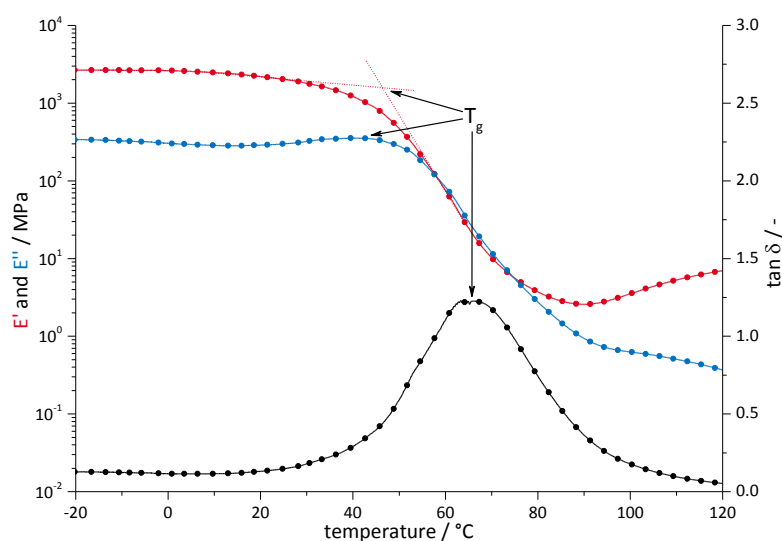


Figure 25. Dynamic mechanical analysis with the definition of different glass transition temperatures.

In the presented study, the specimens (3 x 5 x 22 mm) were cured generally in closed Teflon[®] moulds at least for 24 h at room temperature. Single Cure ROMP DCPD samples were cured at 80 °C and the ROMP initiator M2 was used instead of M20. The specimens were placed on a 3-point-bending clamp with a clamping length of 10 mm. An axial force was applied in oscillating mode with a deformation amplitude of 25 μm and a frequency of 1.0 Hz. The DMA measurements were started about 40 °C below the expected T_g and a heating ramp (3 °C/min) was applied. The obtained data is depicted in Figure 26, and the glass transition temperature at the maximum of $\tan \delta$ is summarised in Table 15.

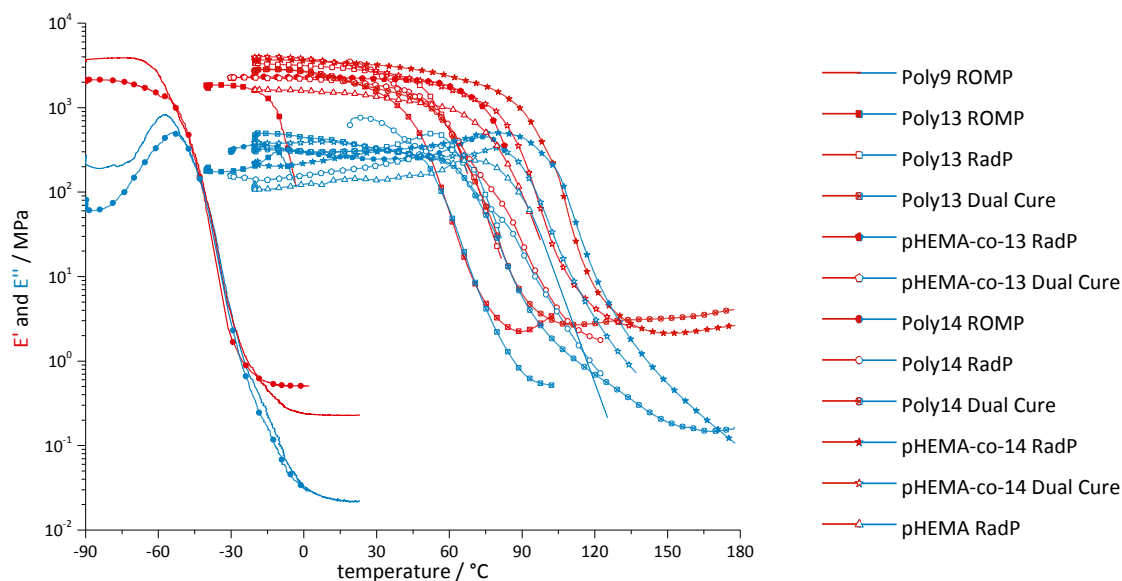


Figure 26. E' and E'' of polymers based on various monomers (Mon9, Mon13, Mon14 and HEMA) and polymerisation techniques (ROMP, RadP and Dual Cure).

Table 15. Glass transition temperatures depending on the polymerisation method and monomers used.

monomers	Single Cure ROMP	Single Cure RadP	Dual Cure RadP-ROMP
	T_g at $\tan \delta_{max}$ / °C		
Mon9	-34	-	-
Mon13	-8	80	70
Mon14	-40	100	90
HEMA	-	98	-
HEMA + Mon13	-	80	66
HEMA + Mon14	-	114	100

The E' - and E'' -values below the T_g were generally higher than 10^3 and 10^2 MPa, respectively. Single Cure ROMP Mon9, Mon13 and Mon14 formulations exhibited T_g s below 0 °C. More precisely, the T_g of Mon13 (-8 °C) was much higher than of Mon9 and Mon14 (-40 and -34 °C). ROMP of these monomers leads to linear polymers with large plasticising side groups resulting in low glass transition temperatures. T_g s well above 60 °C were reached with the Dual Cure RadP-ROMP system. This increase arises from the use of the two initiation systems leading to simultaneous polymerisation at both olefinic structures. However, Single Cure RadP systems gave higher T_g -values in any case. This is quite astonishing but reveals the impact of the role of the norbornene group in the radical polymerisation once more. In contrast to the Single Cure ROMP systems, Mon14 exhibited generally higher T_g s compared to Mon13. The T_g s of Mon14 and Mon13 differed about 20 °C comparing to the single systems. Formulations containing a mixture of HEMA and Mon13 or Mon14 in a 1:1-molar ratio (MA:NB = 3:1) showed an even more significant difference of 34 °C. The thermal properties of Single Cure RadP and Dual Cure RadP-ROMP HEMA-Mon14-formulations reached T_g s higher than 100 °C demonstrating the great potential of the new systems.

3.2 FILLED DUAL CURE FORMULATIONS FOR CHEMICAL ANCHORS

The Dual Cure RadP-ROMP approach has proven to be a competitive alternative to Single Cure RadP systems. In extensive investigations on unfilled formulations (*cf.* chapter 3.1), the compatibility of the two initiation systems, favourable curing behaviour and excellent thermal properties of the formed polymers could be demonstrated. Although the complexity of the new system bears the risk of intrinsic problems like storage instability, the beneficial effects of the implementation of ROMP in a chemical anchor system, above all the reduced polymerisation shrinkage, is presented. The next steps towards the target application are described in the following section.

3.2.1 DEVELOPING FILLED DUAL CURE FORMULATIONS

The two component (2K) Dual Cure system was developed based on a 2K radically curing reference system. Component A of the latter (Table 16) consists of an aliquot amount of the monomer (or mixed resin), Tempol as inhibition agent to adjust the gel time and diisopropyl-*para*-toluidine (Dippt) which forms a redox couple with BPO (in component B) generating the initiator radicals. Component A contains with several fillers with a filling degree of 60%. Cab-O-Sil TS-720 is hydrophobic fumed silica working as thickening agent to prevent sedimentation. Quarzsand F32, quartz sand, is a commonly used filler. Secar 80 is a calcium aluminate cement used to bind water from component B. Component B is composed of the residual amount of monomer, 6 wt% BPO and fillers (same fillers and filling degree). Due to safety reason, Perkadox 20S consisting of 20 wt% BPO on inert fillers ($\text{MgCO}_3/\text{Mg}(\text{OH})_2$, CaSO_4) is added instead of neat BPO.

Table 16. Composition of component A of the radically curing reference system.

comp. A	materials	role	proportion ^a	% (w/w) ^b
1	monomer	resin	100 wt%	
2	Tempol	inhibition agent	0.46 wt%	40
3	Dippt	radical initiator A	1.73 wt%	
4	Cab-O-Sil TS-720	filler		
5	Quarzsand F32	filler		60
6	Secar 80	filler		

[a] related to $\text{Mon13}/\text{Mon14} = 100\text{wt}\%$; [b] related to overall composition;

CURING TESTS

Preliminary curing tests were performed using unfilled 2K Dual Cure formulations (Table 17). The composition had to be rearranged in comparison to the radically curing system (Table 16) for several reasons. The bifunctional monomers containing both methacrylate and norbornene moiety had to be stored separate from the ROMP initiator and hence, could be used for compound A only. BDDMA was chosen for component B as a reactive diluent which participates

in the radical polymerisation. The two radical initiation compounds switched places compared to the reference system. BPO is added in a dispersed form (20 wt% in Perkadox 20S) to the monomer in component A as a larger volume was required. In component B the liquid dimethyl-*para*-toluidine (DMpT) was used instead of the solid Dippt due to easier handling of the liquid amine and the very slow dissolving behaviour of the latter in the used methacrylates. For practical reasons Tempol was shifted to component B too. Varying amount of Tempol and M20 were used to investigate the influence of those compounds on the gel time. Tempol works as an inhibiting agent in the radical initiation mechanism as it scavengers the initial radicals. As Tempol is consumed in this process, the amount of Tempol added to the formulation correlates to the inhibition period. The amount of Tempol was adjusted in order to achieve a reasonable gel time. But clearly, also the amount of M20 influences the gel time of the whole system. Special attention needed to be paid in case of Mon14 as too high loadings result in inhomogeneous distribution of the ROMP initiator. Fillers were left out for these tests as only the interaction of the active compounds should be investigated. Generally, they should be inert to the system but retard the polymerisation start and lower the reaction heat.

Table 17. Adopted composition of a preliminary Dual Cure system without fillers.

comp. A	materials	role	proportion^a
1	Mon13 or Mon14	resin	100 wt%
2	Perkadox 20S ^b	radical initiator A	30 wt%
comp. B	materials	role	proportion^a
1	M20	ROMP - initiator	0-200 ppm
2	BDDMA	reactive diluent	5 wt%
3	Tempol	inhibition agent	0-0.35 wt%
4	DMpT	radical initiator B	1.05 wt%

[a] related to Mon13/Mon14 = 100wt%; [b] 20 wt% BPO in Perkadox 20S.

The preliminary curing tests with Mon13-formulations were performed in small scale (10 g monomer) and with half the amount of Tempol compared to the radically cured reference system (Table 18 and Figure 27, for more details see Experimental Table 43). The Dual Cure Approach (entry 2 – 7) led to a shorter gel time compared to the Single Cure RadP system (entry 1). The addition of 25 – 100 ppm M20 resulted in a reduction of the gel time by 0.5 min, whereas higher loadings (150 and 200 ppm) led to a reduction by 1.5 min. There is no obvious explanation why the reduction of gel time is not directly correlated to the initiator loading but more or less stepwise. Further, the temperature started to increase significantly only after the gelation of the formulation. It was suggested that ROMP started earlier than RadP leading to the gelation but RadP started successfully afterwards indicated by the distinct rise in temperature. The effect of a higher amount of Tempol on the curing behaviour was investigated too (entry 1, 8 and 9). The results were in line with the expected trend as an increase of Tempol led to a delay in gelation and solidification. This information was very important to adjust the working time of the mixed formulation in following experiments.

As Mon13 and Mon14 showed very significant differences in reactivity in ROMP (*cf.* chapter 3.1.5), the curing of Mon14-formulations was investigated likewise (Table 18 and Figure 27, for more details see Experimental Table 43). The gel and solidification time of Single cure RadP of Mon14 was four times longer at the same concentration of Tempol as of Mon13 (Table 18 entry 10 and 1, respectively). The addition of M20 led to a gel time reduced by half (entry 11). More important, the viscosity of the formulation increased tremendously upon mixing of the two components. The level of viscosity then stayed the same until gelation. A homogeneous distribution of M20 in the mixed formulation was not achieved at 75 and 100 ppm M20. Instead, ROMP started already in some parts (solid formulation) while the surrounding formulation stayed liquid.

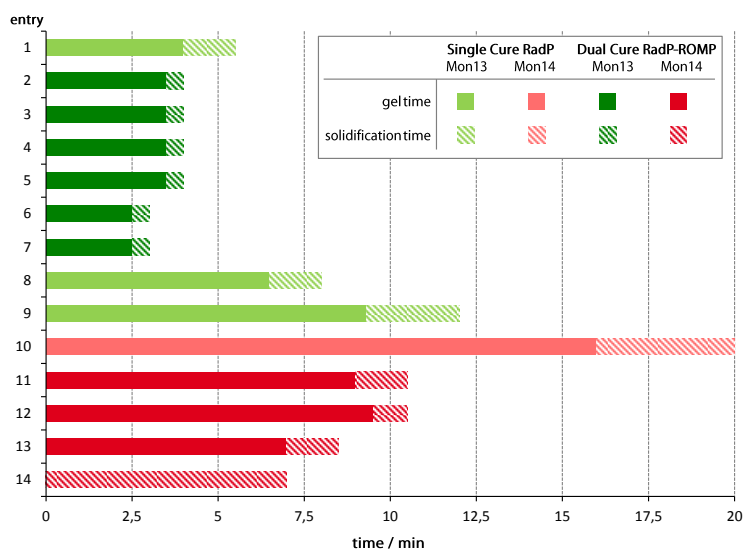


Figure 27. Gel time and solidification time upon Single Cure RadP and Dual Cure RadP-ROMP, entry 1-14 correspond to those in Table 18.

Table 18. Influence of the Tempol- and M20-content on the gel and solidification time of Mon13- und Mon14-formulations (entry 1-9 and entry 10-14, respectively).

entry	monomer	Tempol / mg	M20 / ppm (mg)	gel time; solidification time / min
1		23	-	4.0; 5.5
2		23	25 (0.93)	3.5; 4.0
3		23	50 (1.86)	3.5; 4.0
4		23	75 (2.79)	3.5; 4.0
5	Mon13	23	100 (3.72)	3.5; 4.0
6		23	150 (5.58)	2.5; 3.0
7		23	200 (7.44)	2.5; 3.0
8		30	-	6.5; 8.0
9		35	-	9.3; 12.0
10		23	-	16.0; 20.0
11		23	50 (2.42)	9.0; 10.5
12	Mon14	23	60 (2.91)	9.5; 10.5
13		23	75 (3.63)	7.0; 8.5 ^a
14		23	100 (4.84)	-; 7.0 ^a

[a] inhomogeneous distribution of M20, immediate start of polymerisation.

GELTIMER MEASUREMENTS

The gel times of unfilled and filled formulations were investigated with a Geltimer. The formulations are prepared freshly, mixed homogeneously and filled into two glass test tubes which are placed in water bath thermostated at 25 °C. The temperature profile and gelation of the curing formulations were measured with thermal (GTT) and mechanical (GTM) sensors placed in the middle of the test tubes.

Both unfilled and filled Mon13- and Mon14-formulations were prepared with 0.35 and 0.23 wt% Tempol and 50 ppm M20, respectively (Table 19). Compared to the filled reference system, Secar 80 was replaced by Millisil W12 (quartz powder) as the new formulations were water-free. The filled formulations were prepared by adding the fillers homogeneously only to component A and mixing with the unfilled, liquid component B using a speed mixer in both cases. These two component formulations were subsequently filled into a single component (1K) cartridge and hence, termed 1K formulations in the following experiments.

Table 19. 1K Dual Cure RadP-ROMP system with(out) fillers.

comp. A	materials	proportion ^a	% (w/w) ^b	
1	Mon13 or Mon14	100 wt%		
2	Perkadox 20S ^c	30 wt%	20	
comp. B	materials	proportion ^a	% (w/w) ^b	
1	M20	50 ppm		
2	BDDMA	10 wt%		
3	Tempol	0.35/0.23 wt%	20	
4	DMpT	1.05 wt%		
fillers	materials	proportion ^a	% (w/w) ^b	
5	Cab-O-Sil TS-720	7.8 wt%	3	
6	Quarzsand F32	96.7 wt%	37	60
7	Millisil W12	53.3 wt%	20	

[a] related to Mon13/Mon14 = 100wt%;

[b] related to overall composition;

[c] 20 wt% BPO in Perkadox 20S.

The obtained data was compared with previous measurements of the reference system Hilti HIT-HY 150 (Figure 28 and Table 20). Generally, the gel time of the unfilled formulations of Mon13 and Mon14 was a bit longer than of the reference system but within a favourable time range (solid lines with unfilled dots). A rise in temperature up to ≈ 35 °C was observed associated to the ROMP before the fast increase in temperature associated to the radical polymerisation. Fillers prolonged the gel time by 4-5 minutes and reduced the maximum temperature but the curve characteristics are preserved (solid lines). In case of the reference system, the fillers led to reduced maximum temperature only (black line with filled dots).

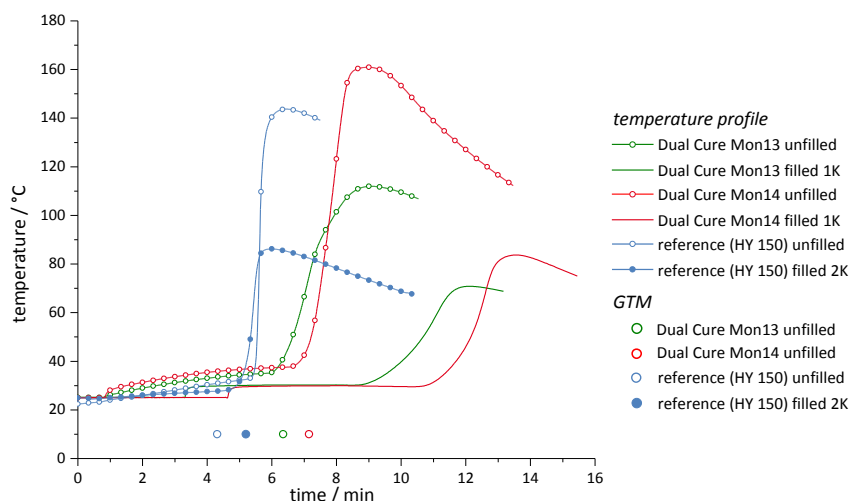


Figure 28. Gel times of Dual Cure RadP-ROMP and reference formulations determined with a thermal (lines) and mechanical sensor (GTM, dots).

Table 20. Gel times of Dual Cure RadP-ROMP and reference formulations determined with thermal (GTT at +10 °C and at 50 °C) and mechanical (GTM) sensors.

system	composition	Tempol wt%	GTT +10°C min	GTT 50°C min	GTM min
Dual Cure RadP-ROMP Mon13	unfilled	0.35	5.83	6.65	6.35
	filled 1K		9.57	10.68	-
Dual Cure RadP-ROMP Mon14	unfilled	0.23	3.73	7.21	7.15
	filled 1K		11.37	12.15	-
reference (HY 150)	unfilled	0.46	5.10	5.55	4.31
	filled 2K		5.12	5.35	5.20

The Geltimer measurements showed that the developed 2K formulations have reasonable working times for the preparation of chemical anchors and analysis of several characteristic parameters (bonding strength, adhesion, shrinkage).

PULL OFF TESTS

Pull off tests are a facile method to determine the adhesive properties of a cured formulation on concrete. The formulations were filled into metal jagged-edged moulds on concrete plates and cured for 24 h. The bond strength is measured by pulling off the stamps from the concrete plate.

Unfilled Mon13- and Mon14-formulations were freshly prepared analogously to those for Geltimer measurements (Table 19, comp. A + comp. B). The pull off tests were performed using dry concrete plates. Mon13-formulations showed higher bond strength compared to those with Mon14. However, the moulds were not completely filled and the measured values were caused by cohesive failure (Table 21 and Figure 29, left). The latter might be caused (or at least promoted) by stress induced by the sharp edges of the moulds. The values for the adhesive failure were above those of the cohesive failure and thus, not measurable with this set-up. In contrast to Mon13,

formulations with Mon14 exhibited adhesive failure only. There was also a thin layer of concrete on each samples indicating penetration of the formulation into the concrete before gelation.

Table 21. Adhesion strength of unfilled Dual Cure RadP-ROMP Mon13- and Mon14-formulations.

monomer	sample	strength at failure / MPa	type of failure
Mon13	1	1.79	cohesive, incomplete filling
	2	2.23	
	3	3.27	
	4	2.94	
Mon14	1	1.78	adhesive
	2	0.79	
	3	1.20	

The pull off tests were repeated on wet concrete plates (Figure 29). Complete filling of the moulds was achieved with both formulations but the adhesive force of the Dual Cure formulations was rather low. In fact, the maximum adhesive force was below the preload force. A thin layer of concrete was observed on all samples indicating penetration into the wet concrete.

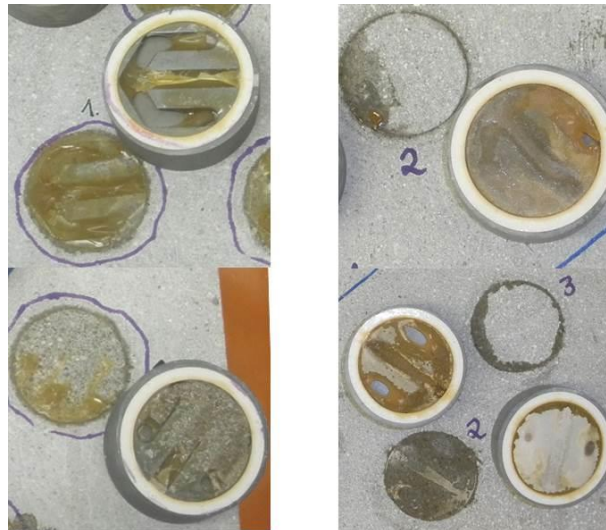


Figure 29. Unfilled Mon13- (top) and Mon14- (bottom) formulations on dry (left) and wet concrete after pull off tests.

Standard methacrylate-based systems exhibit an adhesive failure at > 3 MPa which is considered a very good value. Compared to this, the new Dual Cure system with Mon13 and Mon14 showed a high potential but still some improvements need to be done.

3.2.2 APPLICATION OF FILLED DUAL CURE FORMULATIONS AS CHEMICAL ANCHORS

After the successful development of filled 2K Dual Cure RadP-ROMP Mon13- and Mon14-formulations (*cf.* chapter 3.2.1), the composition was adjusted to 2K 10+1 cartridges (Table 22, more details see Experimental Table 45) and chemical anchors were prepared in concrete for the very first time. In order to evaluate the impact of ROMP in the new system, a Single Cure RadP Mon13 formulation, lacking only M20, was tested too. Additional experiments were performed to analyse the gel time, adhesive properties and shrinkage of the respective batches.

Table 22. Composition of filled 2K Dual Cure RadP-ROMP and Single Cure RadP formulations for 10+1 cartridges.

comp. A	materials	proportion ^a	% (w/w) ^b	
1	Mon13 or Mon14	100 wt%	31	40
2	Perkadox 20S ^c	30 wt%	9	
3	Cab-O-Sil TS-720		3	
4	Quarzsand F32		37	60
5	Millisil W12		20	
sum			≈ 300 mL	
comp. B	materials	proportion ^a	% (w/w) ^b	
1	BDDMA	11.7 wt%	36	40
2	Tempol	0.23 wt%	0.7	
3	DMpT	1.05 wt%	3.2	
4	M20 ^c	50 ppm	0.1	
5	Cab-O-Sil TS-720		3	
6	Quarzsand F32		37	60
7	Millisil W12		20	
sum			≈ 30 mL	

[a] related to Mon13/Mon14 = 100wt%; [b] related to overall composition of each component; [c] 20 wt% BPO in Perkadox 20S; [d] only in case of Dual Cure RadP-ROMP systems.

PULL OUT TESTS

The application of the newly designed formulations as chemical anchors in concrete was examined. The 10+1 cartridges were equipped with a static mixer tip to obtain homogeneous mixing of the two components upon filling of the boreholes in a standard type concrete (C20/25). Subsequently, a threaded rod ($\varnothing = 12$ mm) was embedded in 72 mm depth and the formulations were cured for 48 h. Five different borehole conditions were chosen to investigate the performance in more detail (Table 23).

Table 23. Varying borehole conditions (differences to reference conditions are greyed out).

borehole type	F1Ref	F1b	oversized	-5 °C	+5 °C
base material temperature	rt	rt	rt	-5 °C	+5 °C
mortar temperature	rt	rt	rt	+5 °C	+5 °C
borehole diameter	14 mm	14 mm	18 mm ^a	14 mm	14 mm
borehole cleaning procedure ^b	CAC	½ CAC	CAC	CAC	CAC
concrete	dry	wet	dry	dry	dry

[a] 16 mm for Mon13 - batch 1 and 2; [b] CAC: 2x blow (6 bar), 2x brush, 2x blow (6 bar).

Every time a new static mixer tip was needed, the first 20 g of mixed formulation were rejected to ensure equal mixing quality of each anchor. Three boreholes per formulation and condition were filled and the anchors were cured for 48 h before being pulled out. The pull out tests of chemical anchors cured at -5 °C were performed after 6 days, as these samples were hardly cured after 48 h. In general, a narrow confinement (26 mm) for F1Ref, F1b, +5 °C boreholes and a more wider one (30 mm) for oversized boreholes was chosen and the bond strength was determined.

In the course of the study, three distinct Dual Cure RadP-ROMP Mon13-formulations (batch 1-3), one Single Cure RadP Mon13-formulation (batch 3) and one Dual Cure RadP-ROMP Mon14-formulation were prepared. Batch 1 and 2 of Mon13 were used to analyse the influence of the setting temperature and interval of the chemical anchors on their performance. Batch 3 was utilised for the preparation of both a Dual Cure RadP-ROMP and a Single Cure RadP formulation. The direct comparison of these two formulations should give a better insight into the influence of ROMP on the mechanical properties. The obtained data for Dual Cure RadP-ROMP Mon13- and Mon14- and Single Cure RadP Mon13-formulations were compared to the values of the epoxy-amine system Hilti HIT-RE 500 V1 (averaged reference values) and the radically initiated methacrylate system Hilti HIT-HY 200-A (Figure 30, Table 24, for more details see Experimental, Table 46).

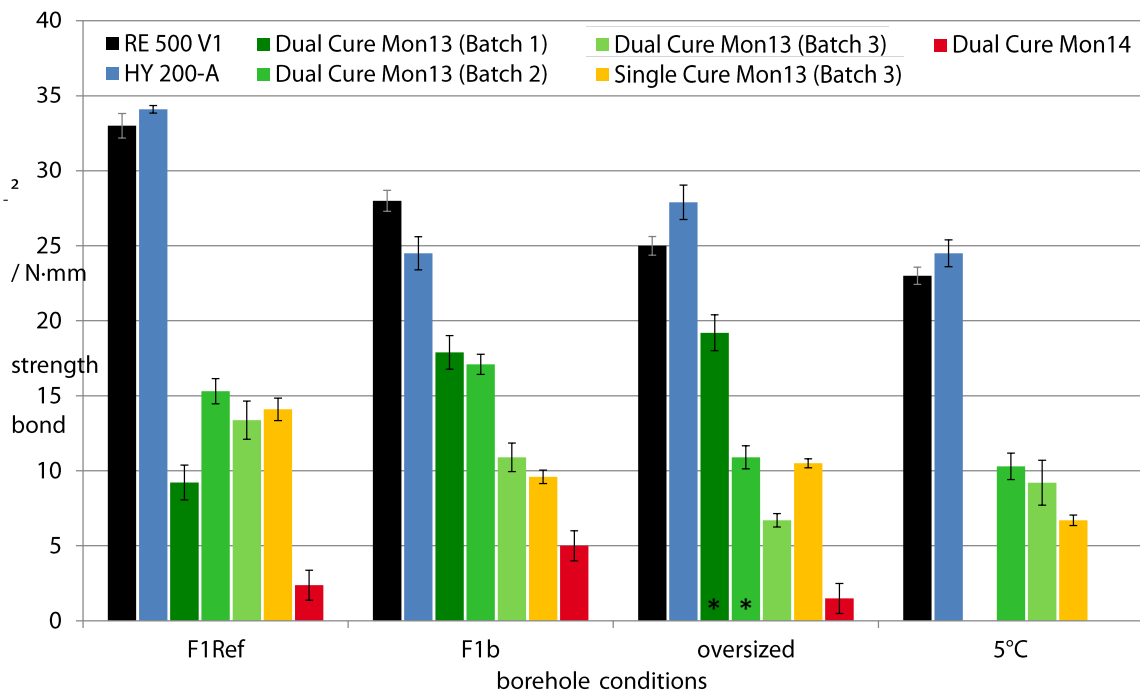


Figure 30. Bond strength of reference systems RE 500 V1- (epoxy-amine) and HY 200-A- (RadP) and filled 2K Dual Cure RadP-ROMP Mon13- and Mon14- and Single Cure RadP Mon13-formulations at different borehole conditions determined in pull out tests (RE 500 V1: averaged reference values, 5% SD; * borehole diameter = 16 mm).

Table 24. Force, bond strength and type of failure of RE 500 V1- (epoxy-amine) and HY 200-A (RadP) and filled 2K Dual Cure RadP-ROMP Mon13- and Mon14- and Single Cure Rad Mon13- formulations determined in pull out tests.

system	borehole condition	force / kN	bond strength / N-mm ²	cause of failure ^a
RE 500 V1 (epoxy-amine) ^b	F1Ref		33.0	
	F1b		28.0	
	oversized		25.0	
	+5 °C		23.0	
HY 200-A (RadP)	F1Ref	90.5 ± 1.0	34.1 ± 0.5	Be
	F1b	65.9 ± 6.9	24.5 ± 2.2	Be
	oversized	74.6 ± 5.9	27.9 ± 2.3	Be
	+5 °C	65.9 ± 3.9	24.5 ± 1.8	Be
Dual Cure RadP-ROMP Mon13 (batch 1)	F1Ref	25.0 ± 4.8	9.2 ± 1.8	Bb
	F1b	48.6 ± 6.1	17.9 ± 2.2	Be & Bbe
	oversized ^{c,d}	52.1 ± 6.6	19.2 ± 2.4	Be & Bbe
	-5 °C ^e	0.07	0.03	Be
Dual Cure RadP-ROMP Mon13 (batch 2)	F1Ref	41.7 ± 4.5	15.3 ± 1.7	Bb & Bbe
	F1b	46.5 ± 3.6	17.1 ± 1.3	Be & Bbe
	oversized ^c	30.3 ± 4.3	10.9 ± 1.5	Bbe
	+5 °C	28.3 ± 4.9	10.3 ± 1.8	Be & Bb
Dual Cure RadP-ROMP Mon13 (batch 3) ^f	F1Ref	35.7 ± 7.0	13.4 ± 2.6	Bb
	F1b	29.3 ± 5.0	10.9 ± 1.9	Bb & Bbe
	oversized ^c	17.7 ± 2.5	6.7 ± 0.9	Bb
	+5 °C	24.7 ± 8.1	9.3 ± 3.0	Bb & Bbe
Single Cure RadP Mon13 (batch 3) ^f	F1Ref	38.2 ± 4.0	14.1 ± 1.5	Be & Bbe
	F1b	25.3 ± 2.1	9.6 ± 0.9	Bb & Bbe
	oversized ^c	28.3 ± 1.5	10.5 ± 0.6	Bb & Bbe
	+ 5 °C	18.0 ± 2.0	6.7 ± 0.8	Bb & Bbe
Dual Cure RadP-ROMP Mon14	F1Ref	6.4 ± 1.2	2.4 ± 0.4	Bb
	F1b ^f	5.0	1.8	Bb & Bbe
	oversized ^{c,d}	4.1 ± 1.3	1.5 ± 0.5	Bb
	-5 °C ^e	0.09	0.03	Be

[a] Bb: failure at borehole wall; Be: failure at rod; Bbe: failure at both borehole wall and rod; [b] averaged reference values (5% SD); [c] borehole diameter = 16 mm; [d] 1st value rejected; [e] one measurement only; [f] maximum value of force and bond strength before failure, expanding anchor after failure.

The presented data demonstrate the high potential of Dual Cure RadP-ROMP systems as formulations with Mon13 reached remarkable values except for curing at -5 °C. Both Mon13 and Mon14 exhibited poor performance due to insufficient curing at low temperature. After 6 days of curing, the threaded rod could still be pulled out manually (< 0.1 kN) and was therefore not included in Figure 30. Although, Mon13 and Mon14 are both bifunctional monomers their performance at room temperature differed largely and will be discussed in the following.

The first set of chemical anchors based on **Dual Cure RadP-ROMP of Mon13 (batch 1**, Figure 30, dark green bars) exhibited excellent bond strength in F1b and oversized (only 16 mm due to shortage of material) boreholes (up to 50 kN) and reached almost ¾ of those of the reference systems (RE 500 V1: black bars; HY 200-A: blue bars). Surprisingly, the bond strength of the

chemical anchors set in the reference boreholes (F1Ref) was much lower. This might be traced back to the fact that the anchors were set at different times. The oversized boreholes were filled one hour after preparation of the formulation, whereas F1b and F1Ref were filled 21 and 25 h later. Comparing F1b and F1Ref indicated that the negative effect becomes significantly more pronounced with longer storage time. During this time, BPO, which is unstable once dissolved, might decompose to a certain extent. The same is true for M20 as the labile triphenylphosphine ligand might dissociate and be oxidised to phosphine oxide by ambient oxygen. However, it is not clear which of these compounds is responsible for the decreased reactivity of the system.

A **second batch** (Figure 30, mid green bars) was prepared and all chemical anchors were set subsequently to exclude the temporal deterioration of their performance. For the assessment of low temperature performance a fourth set of anchors were set at +5 °C instead of -5 °C. The performance in F1b boreholes remained the same compared to batch 1. Elevated values in the reference borehole showed the potential of the system although they were still lower than in F1b. In the case of oversized boreholes - again only 16 mm due to shortage of material - a decrease of the bond strength by half was detected. Chemical anchors cured at +5 °C failed at around the same level as in oversized boreholes and the smell of monomer indicated incomplete or retarded curing.

The results of the **third batch** (Figure 30, light green bars) in the F1Ref and 5 °C borehole were similar to those of the second batch. A poorer outcome compared to batch 1 and 2 was observed in F1b and oversized boreholes. It must be noted that an increased diameter was used in the oversized boreholes which might be the reason for the lower values.

Generally, the deviating results between the batches might be also explained by possible inhomogeneities due to insufficient mixing during preparation of the single components and in the static mixer tip upon filling of the boreholes. The rather large standard deviation of the three anchors per borehole condition support this suggestion.

The bond strength of **Single Cure RadP Mon13** formulations (Figure 30, yellow bars) was about in the same range as those of the Dual Cure analogue. That was a very interesting result. The Single Cure system is lacking the ROMP initiator and a structurally different polymeric network is built-up. In respect of the requirements of the future application, this less complex system has the clear advantage as the storage stability of the Ru-complex would be a main issue.

The results of **Dual Cure RadP-ROMP Mon14**-formulations (Figure 30, red bars) were somehow disappointing. The bond strength was decreased significantly compared to those with Mon13. The chemical anchors stuck to the anchor rod and were removed entirely from the borehole in the pull out test. The smell of monomer and the brittle consistency at the surface indicated incomplete curing of these anchors at the interface to the concrete wall. The failure of the anchors was detected between 3 and 8 kN. The overall strength was supposedly higher as the anchors were expanding in the borehole. These bad results were unexpected as the Mon14-formulations exhibited a good curing behaviour in the preliminary curing tests (*cf.* chapter 3.2.1).

However, there were two significant differences compared to the Mon13-formulations. First, the gel times of Mon14 were much longer. In the Dual Cure approach using 50 ppm M20 gelation of Mon13 and Mon14 occurred after 3.5 and 9 min, respectively. In the case of the exclusively radically initiated polymerisation, the difference was even larger (4 min and 16 min). Second, increasing the M20-loading in the Dual cure formulation above 60 ppm failed as a homogeneous distribution of the ROMP initiator was not achieved due to an immediate start of polymerisation. This observation was somehow contradicting to the longer gel times but might be associated to the differing reactivity of the monomers in ROMP. As discussed in chapter 3.1.5, the position of the carbonyl group to the norbornene double bond influences the ROMP performance. The kinetic NMR study of the monofunctional norbornene ester and inversed ester corresponding to Mon13 and Mon14 showed that the overall polymerisation speed is similar (*cf.* Figure 19). But, incomplete initiation yet fast propagation proceeding to high conversions was observed for the monomer with the carbonyl group in γ -position to the norbornene. Transferred to the Dual Cure Mon14-formulation, it could be suggested that ROMP started earlier than the radical polymerisation impeding complete conversion.

Another important parameter for the evaluation of the quality of a chemical anchor is the cause of failure (*cf.* Figure 3). The reference system HY 200-A showed only failure at the rod which is the preferred type of failure. For the Single Cure and Dual Cure systems the result was a little different. Mostly, mixed failure occurring both at the rod and the borehole wall was observed. This could be related to (partially) insufficient chemical bonding and/or mechanical keying to the concrete wall and indicated the need for further improvement.

In the direct comparison to HY 200-A system the Single Cure and Dual Cure systems come off worse. In this context, it is important to include the resin composition into this evaluation. The new systems are based on bi- and difunctional monomers (9:1 w/w) only, whereas HY systems consist of mono- and difunctional monomers and also prepolymers. The latter are added to build up a more rigid network with improved mechanical and thermal properties. Additionally, the lower double bond density compared to neat monomeric systems leads to a reduced polymerisation shrinkage. Therefore, the comparison to a HY 200-A system based on BDDMA only might be more suitable. Another fact that needs to be considered in this discussion is the composition of the initiation system. Preliminary curing tests were performed to determine the gel time at varying concentration of the ROMP initiator M20 and the radical inhibitor Tempol. Further optimisation by tuning of the radical initiation system and adjusting with the ROMP initiator could result in reduced polymerisation shrinkage, high conversion, a higher network density and hence, a tougher material.

The good performance of the Single Cure system drew attention on the norbornene based monomers for radical systems. Mon13 and Mon14 were tested as substituents of the difunctional BDDMA in the HY 200-A formulation as will be described in chapter 3.2.3.

GELTIMER AND YOKOGAWA MEASUREMENTS

Geltimer measurements were conducted to evaluate the gel time of filled 2K Dual Cure RadP-ROMP systems used for chemical anchors. For these measurements the same Mon13 (batch 1 and 2)- and Mon14-formulations were used as in the pull out tests described above (Table 22, for more details see Experimental, Table 45).

The results were compared to the unfilled and filled 1K Mon13- and Mon14-formulations and the reference system HY 150 (Figure 31, left and Table 25). The filled 2K Mon13-formulations (batch 1 and 2) exhibited gel times similarly those of the reference system. Unfortunately, the Tempol-content in the filled 2K Mon13-formulations was lower as used in its 1K formulations (0.23wt% instead of 0.35wt%) and therefore, the gel times are not comparable. The Mon14-formulations showed longer gel times than any other sample although the amount of Tempol was lower. Especially the prolonged gel time of the filled 2K Dual Cure Mon14-formulation compared to the Mon13 ones (batch 1 and 2) indicated a decreased reactivity, but all samples were fully cured in the end. Therefore, these measurements gave only a hint where the problems in the pull out tests came from.

Additionally, the gel time in an entirely filled borehole of filled 2K Dual Cure RadP-ROMP Mon13 (batch 2 and 3)- and Single Cure RadP Mon13 (batch 3)-formulations was determined with a Yokogawa thermal sensor (Figure 31, right and Table 25). Compared to the Geltimer measurements, the ambient temperature in the borehole was about 2 °C lower; more heat dissipates across the interface formulation/concrete and the boreholes have a different radius. Both the Dual Cure and Single Cure systems had distinctively shorter gel times compared to the reference system HY 200-A and exhibited a 2-step increase in temperature. The maximum temperature of all systems was between 38 and 57 °C was reached shortly after the onset.

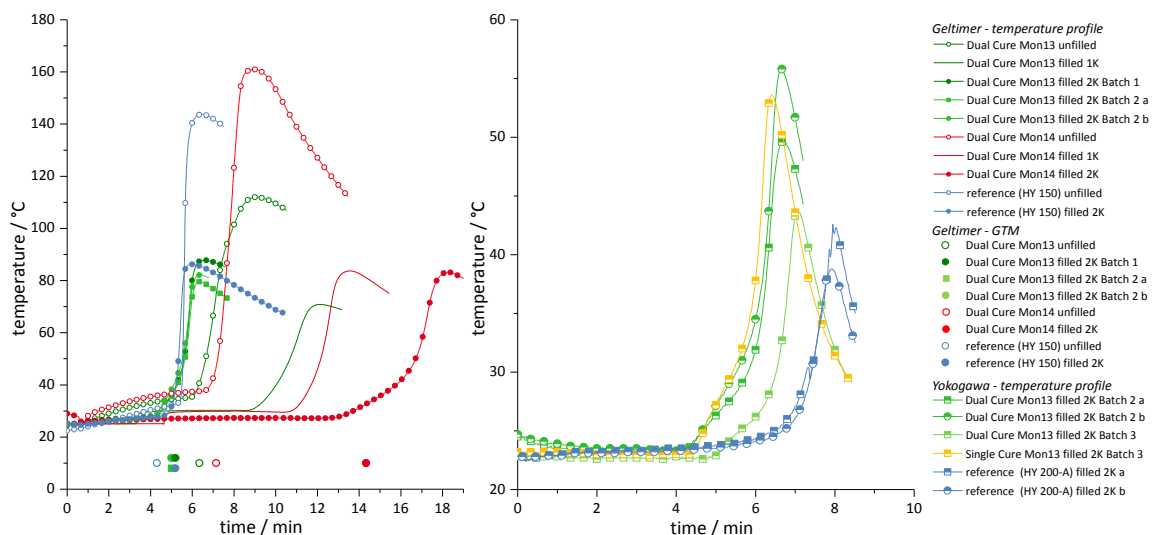


Figure 31. Left: Geltimer measurement of unfilled and filled 2K Dual Cure RadP-ROMP Mon13- and Mon14- and reference (HY 150) formulations, GTM: gel time determined with a mechanical sensor; right: Yokogawa measurements in the borehole of filled 2K Dual Cure RadP-ROMP and Single Cure RadP Mon13- and reference (HY 200-A) formulations.

Table 25. Gel times of Dual Cure RadP-ROMP Mon13- and Mon14-, Single Cure RadP Mon13- and reference (HY 150 and HY 200-A) formulations analysed with a Geltimer as well as a Yokogawa in the borehole (grey font) determined with thermal (GTT at +10 C and at 50 °C) and mechanical (GTM) sensors.

system	composition	Tempol wt%	GTT _{+10°C} min	GTT _{50°C} min	GTM min
Dual Cure RadP-ROMP Mon13	unfilled	0.35	5.83	6.65	6.35
	filled 1K		9.57	10.68	-
	filled 2K - batch 1	0.23	4.88	5.60	5.20
	filled 2K - batch 2		4.78	5.53	5.00
	filled 2K - batch 2	0.23	4.97	5.65	5.00
			6.08	6.68 ^a	-
			5.92	6.45	-
	filled 2K - batch 3	0.23	6.67	7.05 ^b	-
Single Cure RadP Mon13	filled 2K - batch 3	0.23	5.67	6.25	-
Dual Cure RadP-ROMP Mon14	unfilled	0.23	3.73	7.21	7.15
	filled 1K		11.37	12.15	-
reference (HY150)	unfilled	0.46	5.10	5.55	4.31
	filled 2K		5.12	5.35	5.20
reference (HY 200-A)	filled 2K	0.46	7.55	7.90 ^c	-
			7.55	7.95 ^d	-

maximum temperature: [a] 49.6 °C, [b] 43.8 °C; [c] 38.8 °C, [d] 42.6 °C.

PULL OFF TESTS

Pull off tests were performed to determine the adhesive properties of the filled formulations. New round-shaped metal moulds were used to reduce the additional stress induced by the sharp edges as seen with the old moulds. For this set of pull off tests the same Mon13 (batch 1)- and Mon14-formulations were used as in the pull out tests and geltimer measurements described above (Table 22, for more details see Experimental, Table 45). A new static mixer tip was needed and the first 20 g of mixed formulation were rejected. The formulations were filled directly into the moulds which were already fixed on the dry concrete with an adhesive tape. The adhesion strength was determined after 24 h curing and adhesive failure was observed predominantly (Figure 32 and Table 26). The pulled off samples were covered with a very thin layer of concrete. In the case of Mon13-formulations, a more pronounced layer of concrete was detected (Figure 32, red circles). Compared to the unfilled formulations, filled Mon13-formulations achieved better adhesion. In the case of filled Mon14-formulations, the values deviated strongly, but reached higher adhesion in one measurement.

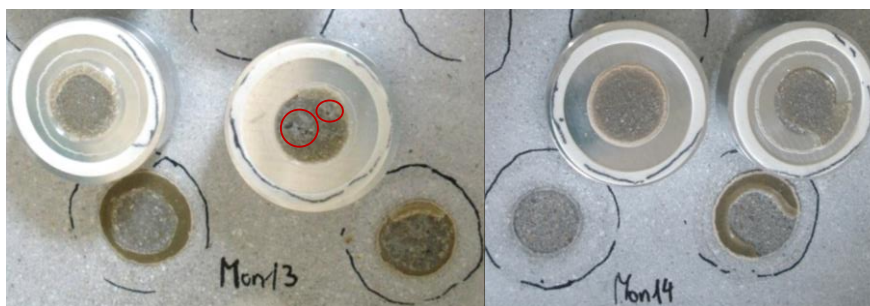


Figure 32. Filled 2K 10+1 Dual Cure RadP-ROMP Mon13- (left) and Mon14- (right) formulations on dry concrete after pull off tests, red circles: concrete adhered to the cured formulation.

Table 26. Adhesion strength of unfilled compared to filled 2K 10+1 Dual Cure RadP-ROMP Mon13- and Mon14- formulations.

monomer	sample	un/filled	strength at failure / MPa	type of failure
Mon13	1	unfilled	1.79	cohesive, incomplete filling
	2		2.23	
	3		3.27	
	4		2.94	
	5	filled	3.67	adhesive
	6		4.83	
Mon14	1	unfilled	1.78	adhesive
	2		0.79	
	3		1.20	
	4	filled	0.89	adhesive
	5		2.89	

THERMAL ANALYSIS

Thermal analysis of the Dual Cure RadP-ROMP and Single Cure RadP systems was performed to gain more information about the curing processes and the temperature dependence. For this purpose, we used the same formulations filled in 2K cartridges as for the pull out tests. The freshly mixed formulations were filled in crucibles which were put in plastic vials and snap-frozen in liquid nitrogen. The samples were stored in liquid nitrogen in order to avoid the curing of the samples prior to the measurements.

The curing process was investigated by means of differential scanning calorimetry (DSC). Dynamic DSC measurements were performed heating the formulations up to 250 °C with a heating rate of 8 °C·min⁻¹. A distinctive exothermic peak above 50 °C (A) and an endothermic one at around 170 °C (B) was observed in both samples (Figure 33). The first peak was associated to the exothermic polymerisation reaction. The Dual Cure system exhibited an additional exothermic process after the main peak, which was not observed in the Single Cure system. This process could be assigned to one of the two polymerisation reaction. The origin of the second peak was not clear at first. It might result from the evaporation or degradation of a compound. In this case, thermogravimetric analyses might give a better insight.

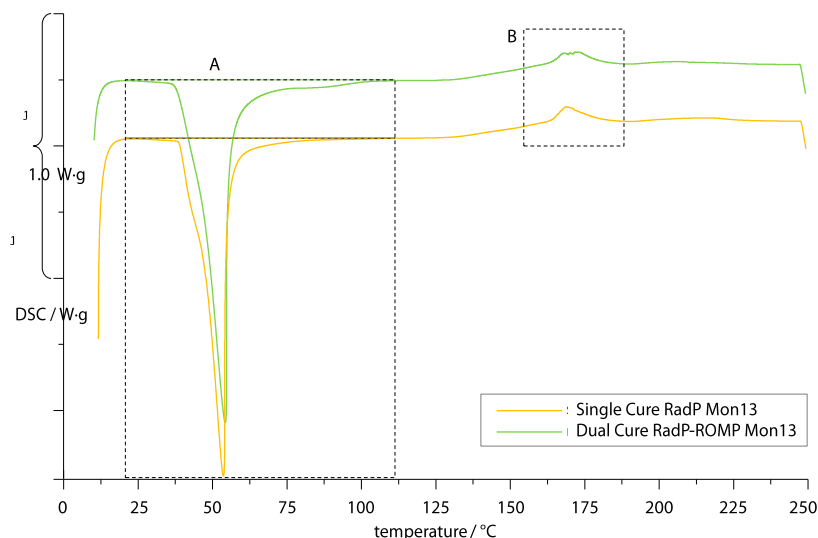


Figure 33. Dynamic DSC measurements of Single Cure RadP and Dual Cure RadP-ROMP Mon13-formulations at 8 °C·min⁻¹.

Thermogravimetric analysis of the formulations compared to the neat monomer Mon13 provided information on the curing efficiency and possible degradation processes. Heating of Mon13 led to complete evaporation starting at approximately 140 °C (A and C). Curing of the formulations was nearly complete (B). Only a small fraction of gas ($\approx 1\%$) was released at round 170 °C corresponding to monomer components (D). The overall mass loss of less than 12% at 350 °C suggested good thermal stability of the cured materials.

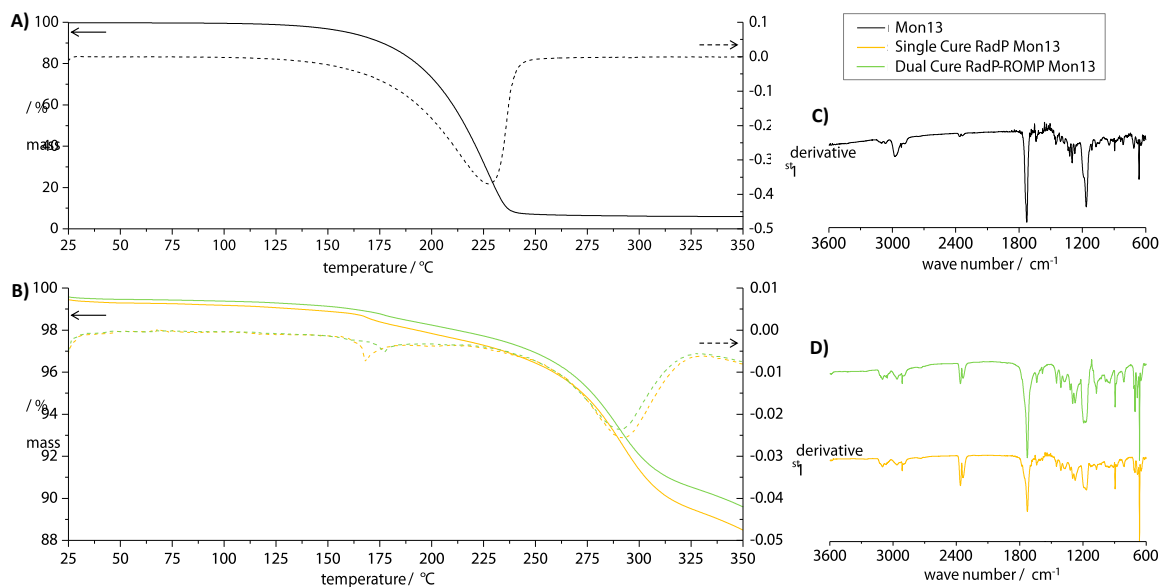


Figure 34. TGA measurement of the neat monomer Mon13 (A) and the Single Cure RadP and Dual Cure RadP-ROMP formulations (B) coupled with IR spectroscopy (IR spectra C and D of gases released at 170 °C).

Isothermal DSC measurements were performed to investigate the curing behaviour of the formulation at 5 °C and 25 °C (Figure 35 and Table 27). The onset time corresponds to the working time in the borehole at the respective temperature. It's important to note that

approximately 2 min required for the sample preparation– from dispensing from the cartridge to the start of the measurement – needs to be added. The time range might differ to some extent between the single samples. Generally, the results of both formulations were quite similar. At 25 °C, the onset of distinctive peaks associated to the curing process occurred within 4 min. Curing at 5 °C led to a delay of the curing start indicated by an onset after 10 and 18 min, respectively, and the exothermic peaks were less pronounced.

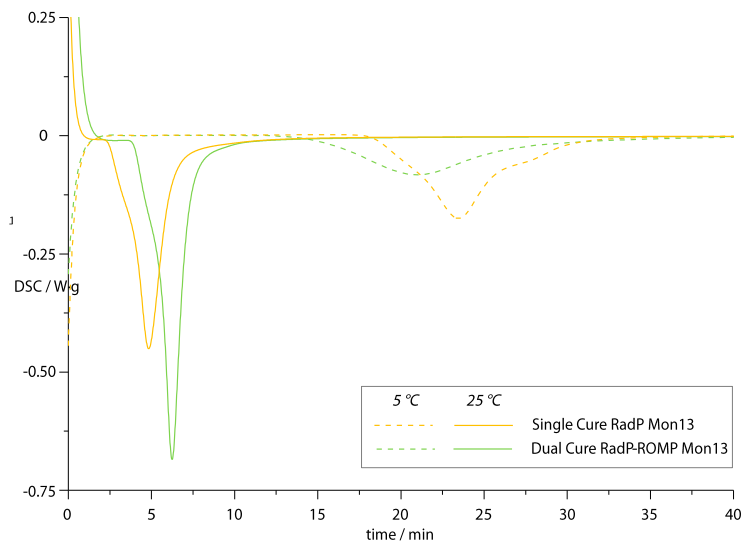


Figure 35. Isothermal DSC measurement to determine the temperature dependence of Single Cure and Dual Cure Mon13 formulations.

Table 27. Onset and peak maximum of the curing peak of Single Cure RadP and Dual Cure RadP-ROMP Mon13-formulations at 5 and 25 °C curing temperature.

formulation	temperature / °C	onset ^a / min	peak max. ^a / min
Single Cure RadP	5	18.2	23.4
	25	2.1	4.8
Dual Cure RadP-ROMP	5	10.0	20.8
	25	3.7	6.3

[a] sample preparation time needs to be added (approximately 2 min).

3.2.3 MON13 AND MON14 IN HY 200-A FORMULATIONS

The bifunctional monomers Mon13 and Mon14 are particularly interesting for the application as radically cured chemical anchor due to different favourable properties. As hypothesized before, the norbornene double bond contributes to the built-up of a cross-linked network with reduced polymerisation shrinkage compared to the radically polymerised methacrylates. This effect was already observed for shouldered test bars of Mon13 initiated thermally with BPO (*cf.* chapter 3.1). The pull out test results of the Single Cure RadP Mon13 formulation (*cf.* chapter 3.2.2) demonstrated the potential of the bifunctional monomers in radical polymerisation. It was therefore suggested to investigate the influence of Mon13 and Mon14 on the performance of the radically cured HY 200-A formulations.

Mon13 and Mon14 were implemented in a HY 200-A formulation by replacing the difunctional BDDMA making up $\frac{1}{3}$ of the mixed resin. The polymerisation shrinkage of the curing formulation was monitored via continuous distance measurement. Additionally, the shear strength, a parameter responsive to incomplete polymerisation, was determined. Both formulations with either Mon13 or Mon14 were shrinking less than the HY 200-A formulation (Table 28). But the shear strength was in the similar range for all formulations. The shear strength would be substantially decreased if the reduced shrinkage was caused by the unreacted norbornene double bond. Conclusively, these result again underline that the norbornene moiety is involved in the radical polymerisation.

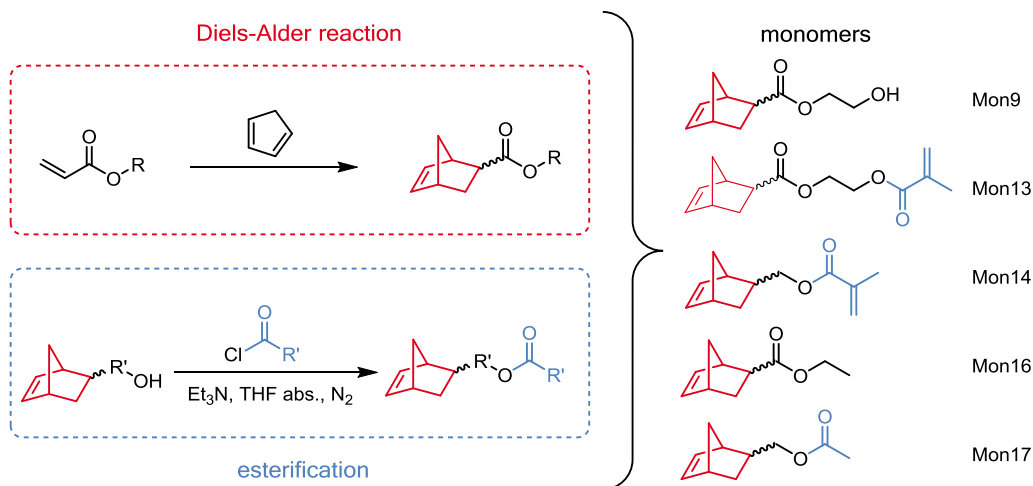
Table 28. Shrinkage and shear strength of HY 200-A and HY 200-A - Mon13 and HY 200-A - Mon14 formulations.

formulation	shrinkage / %	shear strength ^a / MPa
HY 200-A	3.32 ± 0.08	28.08 ± 2.21
HY 200-A - Mon13	2.85 ± 0.28	29.79 ± 1.5
HY 200-A - Mon14	2.85 ± 0.12	24.4 ± 0.9

[a] determined at room temperature

3.3 SYNTHESIS OF MONOMERS

The mono- and bifunctional monomers used in this contribution were synthesised in a one or two step procedure involving the Diels-Alder reaction with cyclopentadiene and the esterification with methacryloyl chloride (Scheme 27).



Scheme 27. Synthetic tool box for the preparation of mono- and bifunctional monomers.

The Diels-Alder reaction of various acrylates and an excess of cyclopentadiene (CP) was a well-established synthetic route to norbornenes. After full conversion in respect to the acrylic double bond, residual CP and the only by-product DCPD were removed via column chromatography (Cy/EtOAc 1:0, then 5:1) The *endo/exo*-ratio of $\approx 80:20$ was determined by means of $^1\text{H-NMR}$ spectroscopy (Figure 36).

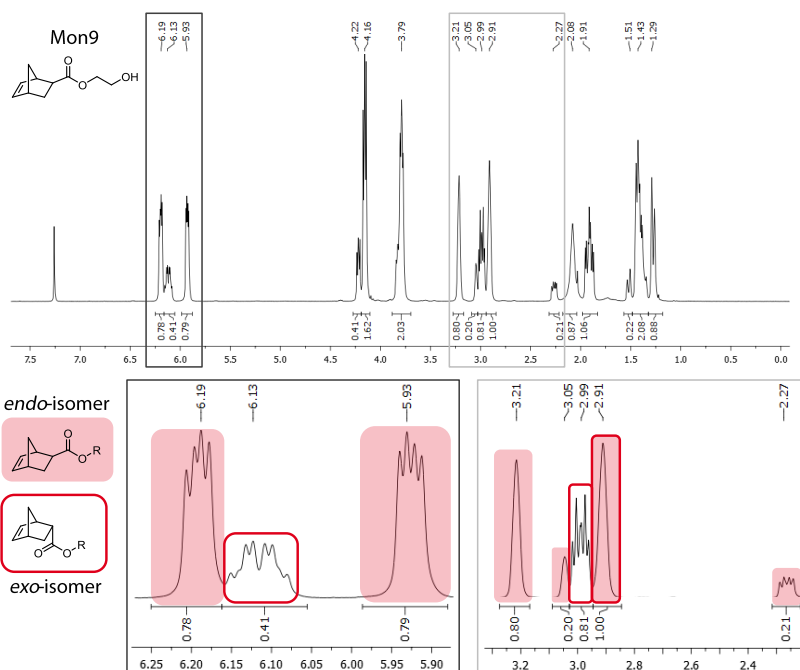


Figure 36. Determination of *endo/exo*-ratio from the $^1\text{H-NMR}$ spectrum (300 MHz, CDCl_3 , here: Mon9).

The esterification of hydroxy-functionalised norbornenes with acid chloride was performed under inert conditions using triethylamine as hydrogen chloride scavenger. Bifunctional monomers bearing both a norbornene and a methacrylate moiety were prepared using methacryloyl chloride (MA-Cl). The educts were degassed, diluted in absolute THF and inertly distilled Et₃N was added. The colourless solution was ice-cooled for 10 min. The acid chloride was added dropwise and immediately, the formation of a colourless precipitate (triethylammonium chloride, Et₃N·HCl) was observed. The reaction progress was monitored with TLC. The purification involved removal of the solvent under reduced pressure and aqueous work-up. Et₃N·HCl was removed using an aqueous solution of hydrochloric acid (5vol%). The organic phase was then washed with an aqueous solution of sodium hydroxide (0.5 M) in order to remove methacrylic acid which is formed from the excess of acid chloride. In the case of Mon13 and Mon14, this step was qualitatively followed via ¹H-NMR spectroscopy focusing on the area of 6.30 to 5.55 ppm (Figure 37). The proton signals of the methacrylic acid at 5.28 and 6.23 ppm disappeared upon the basic work-up (Figure 37, B, green bars). ¹H-spectra of the dried product showed that the formed esters are base-stable, at least up to pH 13. The monomers were stored at lower temperature and 200 ppm BHT was added to achieve long term stability.

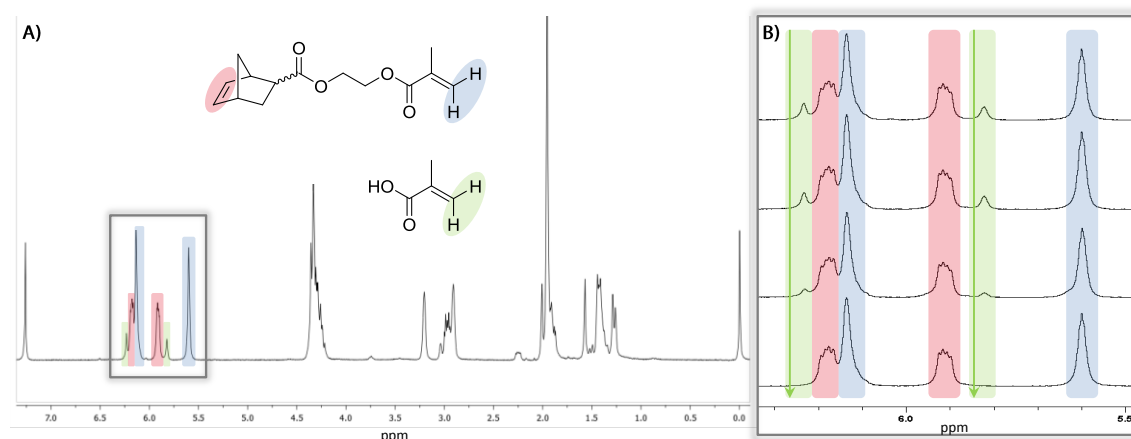


Figure 37. A) ¹H-NMR spectrum (300 MHz, CDCl₃) of Mon13 after acidic work-up contaminated with methacrylic acid; B) disappearing signals of methacrylic acid upon basic work-up.

The urgent need for a large amount of Mon13 and Mon14 for studies on unfilled and filled formulations (*cf.* chapter 3.1.6 and 3.2) called for up-scaling of respective syntheses. Several batches were run to yield the required amount giving the chance to test and improve the modifications of the preparative steps.

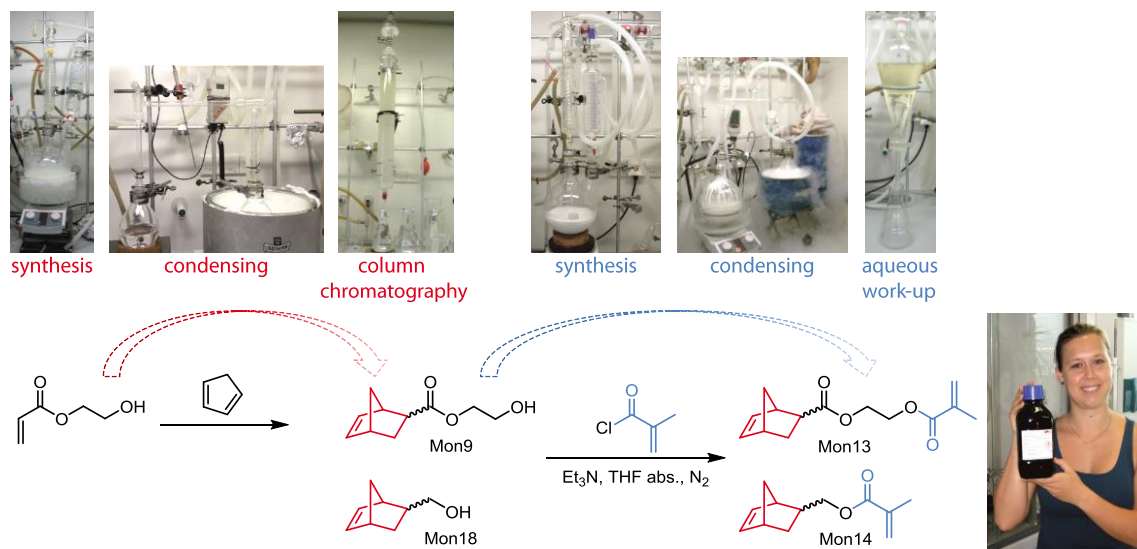


Figure 38. Operative steps in the up-scaled synthesis of Mon13 and Mon14.

The up-scaling of the Diels-Alder reaction yielding Mon9 was no issue as long as the autocatalytic self-heating was prevented with ice-cooling (up to 150 g HEA). Freshly cracked cyclopentadiene (CP) was used in excess in order to achieve full conversion of the acrylic double bonds. Residual CP was removed under reduced pressure using a condensing apparatus (Figure 38, left). However, DCPD which is formed as a by-product had to be removed with a column chromatography. A rather low ratio of silica to crude product (4:1, w/w) was chosen due to the large differences in the R_f -value in Cy of 0.99 and 0.0 for DCPD and the product, respectively. It is therefore comparable with a silica filtration. DCPD was eluted entirely with Cy and fractions were examined via TLC. Subsequently, a gradient (Cy/EtOAc 10:1, 5:1 1 L each, then 3:1, (v:v)) was chosen to eluate the product. The *exo*-product was eluted faster than its *endo*-isomer. After complete elution of the product the respective fractions were mixed (*endo/exo*-ratio of \approx 80:20, *cf.* Figure 36).

The esterification of the hydroxy-functionalised monomers (Mon9 and NB-MeOH) yielding Mon13 and Mon14, respectively, was performed in a 150 g-scale under inert conditions (Figure 38, right). After full conversion was detected with TLC, THF (500 mL) and some the residual MA-Cl was removed under reduced pressure with a condensing apparatus. This process was both faster than on a rotavapor and the release of the very bad smelling, partly toxic volatiles to the laboratory could be avoided. The residue was mixed with 200 mL aqueous hydrochloric acid (5vol%) and dichloromethane each and transferred into a separation funnel. The aqueous work proceeded similar to the small scale protocol. Again, the removal of methacrylic acid was examined by means of $^1\text{H-NMR}$ spectroscopy (*cf.* Figure 37).

4 CONCLUSION

The current work discloses the development of a Dual Cure System based on radical polymerisation of methacrylates and ring opening metathesis polymerisation of norbornenes for the application as chemical anchor in concrete. Excellent performance also at low curing temperature was anticipated as the new system combines the high reactivity of a radically initiated system with the reduced polymerisation shrinkage of ROMP. Bifunctional monomers bearing both functionalities allow for the built up of a cross-linked polymeric network with high glass transition temperature.

The feasibility of a Dual Cure system was studied in terms of the curing performance and the compatibility of the involved reactants. In order to elucidate the role of ROMP, exclusively radically initiated Single Cure systems were examined as a reference. Controlled radical initiation systems based on single electron transfer (SET) and atom transfer radical addition (ATRA) were tested as peroxide-free alternative to benzoyl peroxide/amine systems (RadP) used in commercially available products.

Fully cured polymers were obtained also at curing temperature below 0 °C except for SET. The radical polymerisation led to cross-linked polymers indicating the participation of the norbornene double bond. The performance of the ROMP initiator was impaired when stored with Cu compounds or the peroxide. Based on these results, two component (2K) formulations were developed. For further tests, the Single Cure RadP system prevailed over the other two radical systems because of easier handling and reduced complexity.

The curing characteristics of unfilled Single Cure RadP, Single Cure ROMP and Dual Cure RadP-ROMP formulations based mono- and bifunctional monomers as well as mixtures of those were analysed. The gel time depended on the monomer (monofunctional \approx mixtures < bifunctional), while the polymerisation shrinkage was influenced by the initiation system (Single Cure ROMP < Dual Cure RadP-ROMP < Single Cure RadP). The fully cured samples were analysed by means of dynamic mechanical analysis. The glass transition temperature (T_g) of Single Cure ROMP formulations was well below 0 °C, while the other systems reached T_g s between 66 and 114 °C (Dual Cure RadP-ROMP < Single Cure RadP).

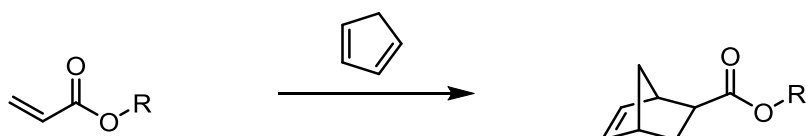
Filled 2K Dual Cure RadP-ROMP and Single Cure RadP formulations were tested as chemical anchors. The results revealed lower bond strength compared to commercially available products. However, both systems hold high promise to improve state of the art anchoring systems after optimisation of the formulation.

5 EXPERIMENTAL

5.1 SYNTHESSES

5.1.1 MONOMER SYNTHESIS

STANDARD OPERATING PROCEDURE FOR DIELS-ALDER REACTIONS



Freshly distilled cyclopentadiene (>1.3 eq) was added dropwise to the respective ice-cooled acrylate (1.0 eq). After 2.0 hours the ice cooling was removed and the mixture was stirred at room temperature. As the reaction exhibited exothermic behaviour, ice cooling was applied for 15 min. Afterwards no further exothermic behaviour was observed and reaction was stirred at 40 °C overnight. Full conversion was monitored via ¹H-NMR spectroscopy. Excessive cyclopentadiene was removed via flash column chromatography using cyclohexane as eluent. The pure product was eluted with Cy/EtOAc (3:1 (v:v)) as eluent and dried under reduced pressure.

Mon9	2-Hydroxyethyl-<i>endo,exo</i>-5-norbornene-carboxylate	
C ₁₀ H ₁₄ O ₃ [182.22]		

Cyclopentadiene (45.0 mL, 35.40 g, 0.535 mol, 1.3 eq), 2-hydroxyethyl acrylate (40.0 mL, 44.33 g, 0.382 mol, 1.0 eq).

Yield: 66.78 g (96%), yellowish liquid, *endo/exo*: 80/20

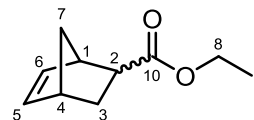
TLC: R_f = 0.62 (Cy/EtOAc, 1:1, (v:v), detection: KMnO₄)

¹H-NMR (300 Hz, CDCl₃): δ = 6.21 - 6.18 (m, 1H, 6_{endo}), 6.16 - 6.08 (m, 2H, 5_{exo}, 6_{exo}), 5.95 - 5.92 (m, 1H, 5_{endo}), 4.24 - 4.21 (t, 2H, 8_{exo}), 4.17 - 4.14 (t, 2H, 8_{endo}), 3.84 - 3.77 (m, 2H, 9_{endo/exo}), 3.22 (s, 1H, 1_{endo}), 3.05 (s, 1H, 1_{exo}), 3.02 - 2.96 (m, 1H, 2_{endo}), 2.91 (s, 1H, 4_{endo/exo}), 2.29 - 2.24 (m, 1H, 2_{exo}), 2.08 (s, b, OH), 1.96 - 1.87 (m, 1H, 3_{aendo/exo}), 1.54 - 1.51 (d, 1H, 3_{bexo}), 1.45 - 1.35 (m, 2H, 7_{endo/exo}), 1.29 - 1.26 (d, 1H, 3_{bendo}) ppm.

^{13}C -NMR (75 Hz, CDCl_3): $\delta = 176.7$ (1C, C_q , 10_{exo}), 175.2 (1C, C_q , 10_{endo}), 138.2 (1C, 6_{exo}), 137.9 (1C, 6_{endo}), 135.7 (1C, 5b_{exo}), 132.2 (1C, 5b_{endo}), 66.1 (1C, 8_{exo}), 65.9 (1C, 8_{endo}), 61.4 (2C, 9_{endo/exo}), 49.7 (1C, 7_{endo}), 46.7 (1C, 7_{exo}), 46.4 (1C, 1_{exo}), 45.8 (1C, 1_{endo}), 43.3 (1C, 2_{endo}), 43.1 (1C, 2_{exo}), 42.6 (1C, 4_{endo}), 41.7 (1C, 4_{exo}), 30.3 (1C, 3_{exo}), 29.3 (1C, 3_{endo}) ppm.

Mon16 2-Ethyl-*endo,exo*-5-norbornene-carboxylate

$\text{C}_{10}\text{H}_{14}\text{O}_2$ [166.22]



Cyclopentadiene (8.20 mL, 6.45 g, 97.5 mmol, 1.4 eq), 2-ethyl acrylate (7.50 mL, 6.89 g, 68.8 mmol, 1.0 eq).

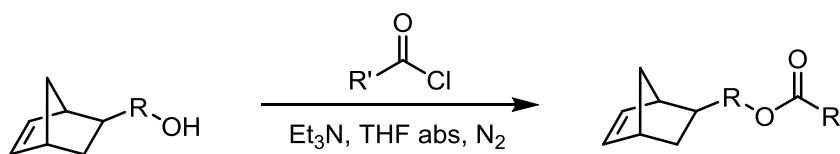
Yield: 10.67 g (93%), clear, colourless liquid, *endo/exo*: 74/26

TLC: $R_f = 0.75/0.68$ (Cy/EtOAc, 5:1, (v:v), detection: KMnO_4)

^1H -NMR (300 Hz, CDCl_3): $\delta = 6.23 - 6.15$ (m, 1H, 6_{endo}), 6.15 - 6.06 (m, 2H, 5_{exo}, 6_{exo}), 5.97 - 5.88 (m, 1H, 5_{endo}), 4.21 - 3.99 (q, 2H, $^3J_{\text{HH}} = 7.0$ Hz, 8_{exo}; dq, 2H, $^3J_{\text{HH}} = 8.3$ Hz, 8_{endo}), 3.20 (s, 1H, 1_{endo}), 3.04 (s, 1H, 1_{exo}), 2.97 - 2.93 (m, 1H, 2_{endo}), 2.93 - 2.85 (m, 1H, 4_{endo/exo}), 2.24 - 2.17 (m, 1H, 2_{exo}), 1.96 - 1.81 (m, 1H, 3a_{endo,exo}), 1.56 - 1.48 (m, 1H, 7a_{exo}), 1.47 - 1.37 (m, 2H, 3b_{endo}, 7a_{endo}), 1.37 - 1.30 (m, 2H, 3b_{exo}, 7b_{exo}), 1.30 - 1.16 (m, 4H, 7b_{endo}, 9_{endo/exo}) ppm.

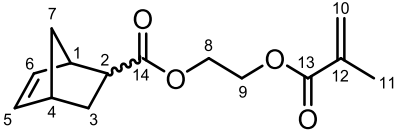
^{13}C -NMR (75 Hz, CDCl_3): $\delta = 176.4$ (1C, C_q , 10_{exo}), 174.9 (1C, C_q , 14_{endo}), 138.2 (1C, 6_{exo}), 137.8 (1C, 6_{endo}), 135.9 (1C, 5a_{exo}), 132.5 (1C, 5b_{endo}), 60.5 (1C, 8_{exo}), 60.2 (1C, 8_{endo}), 49.7 (1C, 7_{endo}), 46.7 (1C, 7_{exo}), 46.5 (1C, 1_{exo}), 45.8 (1C, 1_{endo}), 43.5 (1C, 4_{endo}), 43.3 (1C, 2_{exo}), 42.7 (1C, 2_{endo}), 41.8 (1C, 4_{exo}), 30.4 (1C, 3_{exo}), 29.4 (1C, 3_{endo}), 14.4 (1C, 9) ppm.

STANDARD OPERATING PROCEDURE FOR ESTERIFICATION REACTIONS



Hydroxy-functionalised norbornene (1.0 eq), absolute triethylamine (1.5 eq) and absolute tetrahydrofuran were mixed under inert conditions and ice cooling. A pre-cooled, colourless solution of acid chloride (1.5 eq) in tetrahydrofuran abs. was added dropwise over 45 minutes and the formation of a colourless precipitate (triethylamine-hydrochloride) was observed. The reaction proceeded in an ice bath for one hour and then at room temperature overnight. Full conversion to the respective ester was monitored with TLC. The solvent was removed under reduced pressure and the residue was taken up in diethyl ether and an aqueous solution of

hydrochloric acid (5 vol%). The phases were separated and the organic phase was washed again with the HCl-solution to remove the colourless precipitate. The organic phase was further washed with an aqueous solution of sodium hydroxide (0.5 M) to remove residual acid which is formed from the excess of acid chloride during work-up. The amount of residual acid can be determined via ¹H-NMR spectroscopy. The solution was dried over anhydrous sodium sulfate and the solvent was removed under reduced pressure.

Mon13	2-(Methacryloyloxy)ethyl-<i>endo,exo</i>-5-norbornene-carboxylate	
	C ₁₄ H ₁₈ O ₄ [250.29]	

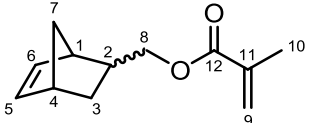
Mon9 (97.50 g, 0.535 mol, 1.0 eq), methacryloyl chloride (78.4 ml, 83.90 g, 0.803 mol, 1.5 eq), triethylamine (111.25 mL, 81.22 g, 0.803 mol, 1.5 eq), tetrahydrofuran (ca. 500 mL).

Yield: 124.56 g (93%), clear, yellowish liquid, *endo/exo*: 80/20

TLC: R_f = 0.71/0.79 (Cy/EtOAc, 3:1, (v:v), detection: KMnO₄)

¹H-NMR (300 Hz, CDCl₃): δ = 6.22 – 6.15 (m, 1H, 6_{endo}), 6.15 – 6.06 (m, 1H, 5_{exo}, 6_{exo}; s, 1H, 10_{trans}), 5.94 – 5.86 (m, 1H, 5_{endo}), 5.59 (s, 1H, 10_{cis}), 4.40 – 4.17 (m, 4H, 8_{endo,exo}, 9_{endo,exo}), 3.19 (s, 1H, 1_{endo}), 3.03 (s, 1H, 1_{exo}), 3.00 – 2.93 (m, 1H, 2_{endo}), 2.90 (s, 1H, 4_{endo/exo}), 2.28 – 2.21 (m, 1H, 2_{exo}), 1.95 (s, 3H, 11), 1.92 – 1.83 (m, 1H, 3_{aendo}) 1.55 – 1.46 (d, 1H, 3_{aexo}), 1.46 – 1.31 (m, 2H, 7_{endo/exo}, 1H, 3_{bexo}), 1.31 – 1.18 (d, 1H, 3_{bendo}) ppm.

¹³C-NMR (75 Hz, CDCl₃): δ = 176.1 (1C, C_q, 14_{exo}), 174.6 (1C, C_q, 10_{endo}), 167.2 (1C, C_q, 13), 138.2 (1C, 6_{exo}), 138.0 (1C, 6_{endo}), 136.1 (1C, C_q, 12), 135.8 (1C, 5_{exo}), 132.4 (1C, 5_{endo}), 126.10 (1C, 10), 62.6 (1C, 8_{endo}), 62.2 (1C, 8_{exo}), 62.0 (1C, 9_{endo,exo}), 49.7 (1C, 7_{endo}), 46.8 (1C, 7_{exo}), 46.5 (1C, 1_{exo}), 45.8 (1C, 1_{endo}), 43.4 (1C, 2_{endo}), 43.2 (1C, 2_{exo}), 42.7 (1C, 4_{endo}), 41.8 (1C, 4_{exo}), 30.4 (1C, 3_{exo}), 29.4 (1C, 3_{endo}), 18.4 (1C, 11) ppm.

Mon14	<i>endo,exo</i>-5-Norbornene-2-methyl methacrylate	
	C ₁₂ H ₁₆ O ₂ [192.26]	

Mon18/ *endo,exo*-5-norbornene-2-methanol (97.37 mL, 100.0 g, 0.805 mol, 1.0 eq), methacryloyl chloride (118.0 ml, 126.26 g, 1.208 mol, 1.5 eq), triethylamine (167.44 mL, 122.23 g, 1.208 mol, 1.5 eq), tetrahydrofuran (ca. 500 mL).

Yield: 121.42 g (78%), clear, yellowish liquid, *endo/exo*: 76/24

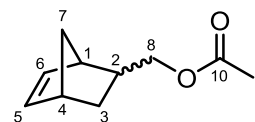
TLC: R_f = 0.76 (Cy/EtOAc, 5:1, (v:v), detection: KMnO₄)

$^1\text{H-NMR}$ (300 Hz, CDCl_3): δ = 6.22 – 6.13 (m, 1H, 5_{endo}), 6.13 – 6.02 (m, 1H, 5_{exo} , 6_{exo} ; s, 1H, 10_{trans}), 6.03 – 5.87 (m, 1H, 5_{endo}), 5.54 (s, 1H, 10_{cis}), 4.23 – 3.99 (m, 2H, 8_{exo}), 3.99 – 3.64 (m, 2H, 8_{endo}), 2.90 (s, 1H, 1_{endo}), 2.82 (s, 1H, $4_{\text{endo/exo}}$), 2.72 (s, 1H, 1_{exo}), 2.53 – 2.36 (m, 1H, 2_{endo}), 1.95 (s, 3H, 11), 1.91 – 1.80 (m, 1H, $3a_{\text{endo}}$), 1.80 – 1.70 (m, 1H, 2_{exo}), 1.51 – 1.41 (m, 1H, $7a_{\text{endo}}$), 1.41 – 1.31 (m, 1H, $7a,b_{\text{exo}}$), 1.31 – 1.24 (m, 1H, $7b_{\text{endo}}$), 1.24 – 1.11 (m, 1H, $3a,b_{\text{exo}}$), 0.65 – 0.52 (m, 1H, $3b_{\text{endo}}$).

$^{13}\text{C-NMR}$ (75 Hz, CDCl_3): δ = 167.7 (1C, C_q , 12_{exo}), 167.6 (1C, C_q , 12_{endo}), 137.7 (1C, 5_{endo}), 137.1 (1C, 5_{exo}), 136.7 (1C, C_q , 11_{endo}), 136.6 (1C, C_q , 11_{exo}), 136.4 (1C, 6_{exo}), 132.3 (1C, 6_{endo}), 125.4 (1C, 10_{exo}), 125.2 (1C, 10_{endo}), 68.9 (1C, 8_{exo}), 68.2 (1C, 8_{endo}), 49.5 (1C, 7_{endo}), 45.1 (1C, 7_{exo}), 44.1 (1C, 1_{endo}), 43.8 (1C, 1_{exo}), 42.3 (1C, 4_{endo}), 41.7 (1C, 4_{exo}), 38.1 (1C, 2_{exo}), 38.0 (1C, 2_{endo}), 29.7 (1C, 3_{exo}), 29.1 (1C, 3_{endo}), 18.5 (1C, 9) ppm.

Mon17 *endo,exo*-5-Norbornene-2-methyl acetate

$\text{C}_{10}\text{H}_{14}\text{O}_2$ [166.22]



Mon18/ *endo,exo*-5-norbornene-2-methanol (14.50 mL, 14.89 g, 0.120 mol, 1.0 eq), acetyl chloride (12.80 mL, 14.12 g, 0.180 mol, 1.5 eq), triethylamine (25.0 mL, 18.20 g, 0.180 mol, 1.5 eq), tetrahydrofuran (ca. 200 mL).

Yield: 13.08 g (66%), clear, dark yellow liquid, *endo/exo*: 77/23

TLC: R_f = 0.68 (Cy/EtOAc, 3:1, (v:v), detection: KMnO_4)

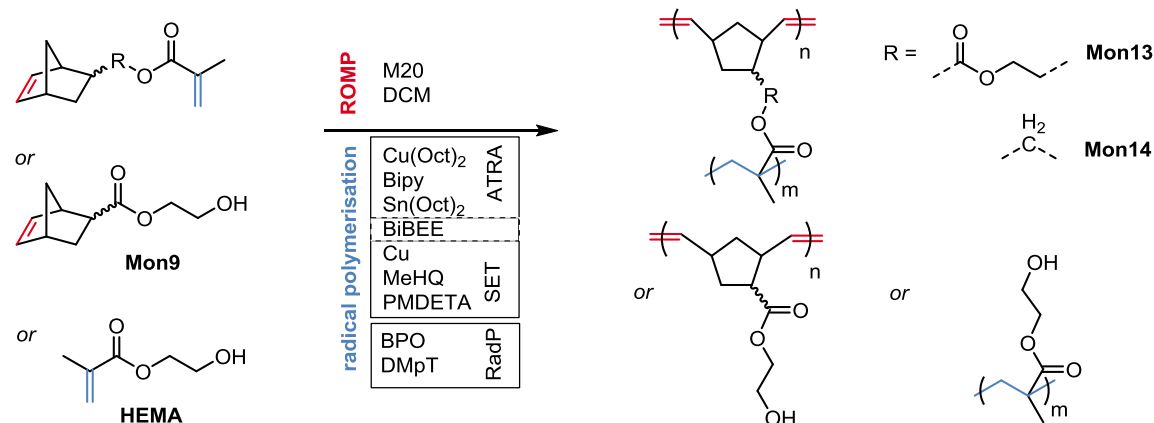
$^1\text{H-NMR}$ (300 Hz, CDCl_3): δ = 6.24 – 6.11 (m, 1H, 5_{endo}), 6.11 – 6.03 (m, 1H, 5_{exo} , 6_{exo}), 5.99 – 5.83 (m, 1H, 6_{endo}), 4.21 – 3.90 (m, 1H, 8_{exo}), 3.90 – 3.56 (m, 1H, 8_{endo}), 2.88 (s, 1H, 1_{endo}), 2.81 (s, 1H, 4), 2.70 (s, 1H, 1_{endo}), 2.45 – 2.29 (m, 1H, 2_{endo}), 2.07 (s, 3H, 9_{exo}), 2.05 (s, 3H, 9_{endo}), 1.90 – 1.77 (m, 1H, $3a_{\text{endo}}$), 1.77 – 1.63 (m, 1H, 2_{exo}), 1.49 – 1.39 (m, 1H, $7a_{\text{endo}}$), 1.39 – 1.30 (m, 1H, $7a,b_{\text{exo}}$), 1.30 – 1.20 (m, 2H, $7b_{\text{endo}}$, $3a_{\text{exo}}$), 1.20 – 1.10 (m, 1H, $3b_{\text{exo}}$), 0.61 – 0.49 (m, 1H, $3b_{\text{endo}}$) ppm.

$^{13}\text{C-NMR}$ (75 Hz, CDCl_3): δ = 171.3 (1C, C_q , 10_{exo}), 171.2 (1C, C_q , 10_{endo}), 137.7 (1C, 5_{endo}), 137.0 (1C, 5_{exo}), 136.3 (1C, 6_{exo}), 132.3 (1C, 6_{endo}), 68.7 (1C, 8_{exo}), 68.1 (1C, 8_{endo}), 49.5 (1C, 7_{endo}), 45.0 (1C, 7_{exo}), 44.0 (1C, 1_{endo}), 43.8 (1C, 1_{exo}), 42.3 (1C, 4_{endo}), 41.7 (1C, 4_{exo}), 38.0 (1C, 2_{exo}), 37.9 (1C, 2_{endo}), 29.7 (1C, 3_{exo}), 29.1 (1C, 3_{endo}), 21.1 (1C, $9_{\text{endo/exo}}$) ppm.

5.1.2 POLYMERISATION IN BULK

SINGLE CURE SET, ATRA AND RADP AND DUAL CURE ATRA-ROMP - PRELIMINARY CURING TESTS

Preliminary tests were performed to evaluate the feasibility of the Dual Cure System combining ROMP with radical polymerisation techniques. Several monomers were tested as shown in Scheme 28, namely Mon13, Mon14, Mon9 and HEMA.



Scheme 28. Combined polymerisation methods (ROMP, ATRA, SET, RadP) of Mon13, Mon14, Mon9, HEMA and monomer mixtures.

The formulations were prepared freshly as described in the following. The change in colour and condition of the formulation referring to an index for 0 to 100 (Table 29) was recorded frequently in the beginning and in larger intervals within 24 h.

Table 29. Change in condition of the formulation upon curing.

Category	Consistency of curing formulation
0	no apparent change in viscosity
5	slightly viscous
10	viscous
15	more viscous
20	highly viscous
25	stacked, highly viscous, sticky
30	gelation, soft & sticky
35	solid, gel-like, slightly sticky
40	solid, gel-like, not sticky
50	solid, very elastic
60	solid, rather elastic
70	solid, elastic
80	solid, slightly elastic
90	solid, hardly elastic
95	solid, barely elastic
100	solid, fully cured

Single Cure SET polymerisation

Tempol, MeHQ and Cu were filled into a 2.5 mL glass vial and mixed with the respective monomer or monomer mixture. BiBEE and PMDETA were added and the formulation was subjected to ultrasonication. The weighted portions are stated in Table 30.

Table 30. Composition of Single Cure SET formulations for preliminary curing tests.

	materials	mass / g	proportion
1	monomer	1.00	100 wt%
2	Cu	0.0063	0.63 wt%
3	MeHQ	0.0037	0.37 wt%
4	Tempol	0.0005	0.05 wt%
5	BiBEE	0.0110	1.10 wt%
6	PMDETA	0.0110	1.10 wt%

Single Cure ATRA polymerisation

Cu(Oct)₂ and Bipy were mixed in a 2.5 mL glass vial and dissolved in the respective monomer or monomer mixture forming component A. Sn(Oct)₂ and BiBEE were mixed in another 2.5 mL glass vial and mixed in the respective monomer or monomer mixture forming component B. Component A was transferred to component B with a glass pipette and the components were mixed homogeneously by shaking by hand. The weighted portions are stated in Table 31 and the curing progress for HEMA-Mon9, HEMA-Mon13 and HEMA-Mon14 formulations are summarised in Table 32, Table 33 and Table 34.

Table 31. Composition of Single Cure ATRA formulations for preliminary curing tests.

comp. A	materials	mass / g	proportion ^a
1	monomer	0.75	75 wt%
2	Cu(Oct) ₂	0.0064	0.64 wt%
3	Bipy	0.0024	0.24 wt%
comp. B	materials	mass / g	proportion ^a
1	monomer	0.25	25 wt%
2	Sn(Oct) ₂	0.0098	0.98 wt%
3	BiBEE	0.0060	0.60 wt%

[a] monomer = 100 wt%.

Table 32. Curing progress of Single Cure ATRA HEMA-Mon9 formulations at various curing temperatures.

curing temp.	HEMA:Mon9	100:0	75:25	50:50	25:75	10:90	0:100
room temperature	after 24 h	-	solid (100)	solid, hardly elastic (90)	solid, rather elastic (60)	highly viscous (20)	no apparent change (0)
5 °C	after 24 h	-	solid (100)	solid, slightly elastic (80)	solid, rather elastic (60)	gelation, soft & sticky (30)	no apparent change (0)
-20 °C	after 24 h	solid (100)	solid, barely elastic (95)	solid, hardly elastic (90)	-	-	-

Table 33. Curing progress of Single Cure ATRA HEMA-Mon13 formulations at various curing temperatures.

curing temp.	HEMA:Mon13	100:0	75:25	50:50	25:75	0:100
room temperature	after 1 min	solid (100), hot	warm	warm	-	-
	after 10 min	solid (100)	solid (100)	solid (100)	solid (100)	solid, slightly elastic (80)
	after 24h	solid (100)	solid (100)	solid (100)	solid (100)	solid (100)
5 °C	after 15 min	solid (100)	solid (100)	highly viscous (20)	viscous (15)	unchanged (0)
	after 24 h	solid (100)	solid (100)	solid (100)	solid (100)	solid (100)
-20 °C	after 24 h	solid (100)	solid (100)	solid, elastic (70)	solid, elastic (70)	solid, elastic (70)
	after 48 h	solid (100)	solid (100)	solid (100)	solid (100)	solid (100)

Table 34. Curing progress of Single Cure ATRA HEMA-Mon14 formulations at various curing temperatures.

curing temp.	HEMA:Mon14	100:0	75:25	50:50	25:75	0:100
room temperature	after 1 min	solid (100), hot	warm	warm	-	-
	after 10 min	solid (100)	solid (100)	solid (100)	solid (100)	solid, slightly elastic (80)
	after 24h	solid (100)	solid (100)	solid (100)	solid (100)	solid (100)
5 °C	after 15 min	solid (100)	solid (100)	solid (100)	solid (100)	solid (100)
-20 °C	after 24h	solid (100)	solid (100)	solid (100)	solid, hardly elastic (95)	solid, hardly elastic (90)

Dual Cure ATRA-ROMP polymerisation

Cu(Oct)₂ and Bipy were mixed in a 2.5 mL glass vial and dissolved in the respective monomer or monomer mixture forming component A. Sn(Oct)₂ and BiBEE were mixed in another 2.5 mL glass vial and mixed in the respective monomer or monomer mixture forming component B. A M20-stock solution was prepared in dichloromethane (50 ppm/30 µL). Component A and an aliquot of the M20 stock solution was transferred simultaneously to component B and the components were mixed homogeneously by shaking by hand. The weighted portions are stated in Table 35, the curing progress for HEMA-Mon13 and HEMA-Mon14 formulations are summarised in Table 36 and Table 37.

Table 35. Composition of Dual Cure ATRA-ROMP formulations for preliminary curing tests.

comp. A	materials	mass / g	proportion ^a
1	monomer	0.75	75 wt%
2	Cu(Oct) ₂	0.0063	0.64 wt%
3	Bipy	0.0024	0.24 wt%
comp. B	materials	mass / g	proportion ^a
1	monomer	0.25	25 wt%
2	Sn(Oct) ₂	0.0098	0.98 wt%
3	BiBEE	0.0060	0.60 wt%
comp. C	materials	amount	proportion
1	M20	relative to monomer	50 ppm
2	DCM	30 µL	-

[a] monomer = 100 wt%.

Table 36. Curing progress of Dual Cure ATRA-ROMP HEMA-Mon13 formulations at various curing temperatures.

curing temp.	HEMA:Mon13	75:25	50:50	25:75	0:100
room temperature	after 7 min	solid (100)	gel-like (40), hot	highly viscous (20)	slightly warmer
	after 10 min	solid (100)	solid (100)	solid, very elastic (50)	solid, very elastic (50)
	after 24 h	solid (100)	solid (100)	solid (100)	solid (100)

Table 37. Curing progress of Dual Cure ATRA-ROMP HEMA-Mon14 formulations at various curing temperatures.

curing temp.	HEMA:Mon14	75:25	50:50	25:75	0:100
room temperature	after 10 min	solid (100)	solid, elastic (70)	solid, elastic (70)	solid (100)
	after 24 h	solid (100)	solid (100)	solid (100)	solid (100)
5 °C	after 24 h	solid (100)	solid (100)	solid (100)	solid (100)
-20 °C	after 24 h	solid (100)	solid (100)	solid (100)	solid (100)

SINGLE CURE RADP AND DUAL CURE RADP-ROMP - RHEOKINETICS

Rheokinetic measurements were performed to evaluate the curing behaviour of Single Cure RadP and Dual Cure RadP-ROMP. The formulations were prepared freshly before each measurement (Table 38) and an aliquot was poured on the lower plate of the plate-plate rheometer apparatus. Subsequently, the upper plate was moved to the measuring position and the measurement could be started. The time between the mixing of the components and the first measured data point (15 s after the start of the measurement) was taken into account for the determination of the gel time.

Single Cure RadP polymerisation

Component A was prepared by mixing 75% of the respective monomer or monomer mixture with Perkadox 20S in a 10 mL glass vial and placed in an ultrasonic bath for 3 min. DMpT was dissolved in the residual amount of monomer or monomer mixture forming component B. Component B was transferred to component A with a plastic pipette and the components were mixed homogeneously by shaking by hand.

Dual Cure RadP-ROMP polymerisation

Component A was prepared by mixing 75% of the respective monomer or monomer mixture with Perkadox 20S in a 10 mL glass vial and placed in an ultrasonic bath for 3 min. DMpT was dissolved in the residual amount of monomer or monomer mixture forming component B. A M20-stock solution was prepared in dichloromethane (50 ppm/100 μ L). Component B and an aliquot of the M20 stock solution was transferred simultaneously to component A and the components were mixed homogeneously by shaking by hand.

Table 38. Composition of Single Cure RadP and Dual Cure RadP-ROMP formulations for rheokinetic measurements.

comp. A	materials	mass / g	proportion ^a
1	monomer	1.50	75 wt%
2	Perkadox 20S ^b	0.10	5 wt%
comp. B	materials	mass / g	proportion ^a
1	monomer	0.50	25 wt%
2	DMpT	0.01	0.5 wt%
comp. C	materials	amount	proportion
1	M20	relative to monomer	50 ppm
2	DCM	100 μ L	-

[a] monomer = 100 wt% [b] 20 wt% BPO in Perkadox 20S.

SINGLE CURE RADP AND DUAL CURE RADP-ROMP - SHRINKAGE TESTS

The formulations were prepared as described in the following section. Exactly 1.0 mL of the formulation was transferred with a syringe (1.0 mL/0.01 mL) into the hand-scaled shrinkage test vial and cured for 24 h at room temperature. The volumetric shrinkage was determined by adding as much water as needed to fill up to the 2.0 mL mark.

Single Cure RadP polymerisation

An ultrasonic bath was used to dissolve BPO in the aliquot portion in a 2.5 mL glass vial forming component A. The residual amount of monomer was mixed with DMpT in another 2.5 mL glass vial forming component B. Component A was transferred to component B with a glass pipette and the components were mixed homogeneously by shaking by hand. The weighted portions are summarised in Table 39.

Table 39. Composition of Single Cure RadP formulations for shrinkage tests.

comp. A	materials	mass / g	proportion ^a
1	monomer	1.00	67 wt%
2	BPO	0.015	1.0 wt%
comp. B	materials	mass / g	proportion ^a
1	monomer	0.50	33 wt%
2	DMpT	0.0075	0.5 wt%

[a] monomer = 100 wt%

Dual Cure RadP-ROMP polymerisation

An ultrasonic bath was used to dissolve BPO in the aliquot portion in a 2.5 mL glass vial forming component A. The residual amount of monomer was mixed with DMpT in another 2.5 mL glass vial forming component B. A M20-stock solution was prepared in dichloromethane (50 ppm/100 μ L). Component A and an aliquot of the M20 stock solution was transferred simultaneously to component B and the components were mixed homogeneously by shaking by hand. The weighted portions are stated in Table 40.

Table 40. Composition of Dual Cure ATRA-ROMP formulations for preliminary curing tests.

comp. A	materials	mass / g	proportion ^a
1	monomer	1.00	67 wt%
2	BPO	0.015	1.0 wt%
comp. B	materials	mass / g	proportion ^a
1	monomer	0.50	33 wt%
2	DMpT	0.0075	0.5 wt%
comp. C	materials	amount	proportion
1	M20	relative to monomer	50 ppm
2	DCM	100 μ L	-

[a] monomer = 100 wt%

SINGLE CURE RADP AND ROMP AND DUAL CURE RADP-ROMP - DYNAMIC MECHANICAL ANALYSIS

The Single Cure RadP and Dual Cure RadP-ROMP formulations were prepared as described above (*cf.* shrinkage tests). The preparation of Single Cure ROMP formulations is described below. For specimen preparation, several closed Teflon® moulds were filled completely with the formulations. The moulds were stored for 24 h at room temperature in an upright position directing possibly occurring air bubbles to the one end of the specimen. Afterwards, the cured samples are removed cautiously from the moulds.

Single Cure ROMP polymerisation

A M20-stock solution was prepared in dichloromethane (50 ppm/100µL). An aliquot of the M20 stock solution was mixed homogeneously with the monomer by shaking by hand (Table 41).

Table 41. Composition of Single Cure ROMP formulations for preliminary curing tests.

	materials	mass / g	proportion
1	monomer	1.00	
2	M20	relative to monomer	50 ppm
3	DCM	100 µL	-

DUAL CURE RADP-ROMP - CURING TESTS

Preliminary curing tests were performed to adopt the composition of a radically cured reference system (Table 16) for the novel Dual Cure RadP-ROMP systems. The formulations were prepared freshly as described in the following. The change of the viscosity and heat was followed and the gel time determined by manual evaluation.

Mon13 and Mon14 were mixed with Perkadox 20S in a 40 mL glass vial and hand stirred for a homogeneous distribution forming component A. A stock solution of Tempol in BDDMA was prepared by mixing the two compounds in a 40 mL glass vial equipped with a magnetic stir bar. The mixture was stirred at 50 °C for 15 min. The exact amount of M20 needed was dissolved in an aliquot of the Tempol/BDDMA-stock solution in a 20 ml glass vial. DMpT was added volumetrically to this solution now forming component B. This component was taken up in a syringe and added quickly to component A. The two components were mixed homogeneously by shaking by hand. The weighed portions are stated in Table 42; the gelation progress is stated in Table 43.

Table 42. Composition of Dual Cure RadP-ROMP formulations for preliminary curing tests.

comp. A	materials	mass	proportion
1	Mon13/Mon14	10 g	100 wt%
2	Perkadox 20S ^a	3 g	30 wt%
comp. B	materials	amount	proportion
1	M20	relative to Mon13/Mon14	0-200 ppm
2	BDDMA	0.5 mL	5 wt%
3	Tempol	23-35 mg	0.23 - 0.35 wt%
4	DMpT	111 µL	1.05 wt%

[a] 20 wt% BPO in Perkadox 20S.

Table 43. Influence of Tempol- and M20-content on the curing behaviour of Mon13- and Mon14-formulations (entry 1 – 9 and 10 – 14, respectively).

entry	Tempol / mg	M20 / ppm (mg)	curing behaviour
1	23	-	4 min gelation
			5.5 min harder, hot
2	23	25 (0.93)	3.5 min gelation
			4 min solid
3	23	50 (1.86)	3.5 min gelation
			4 min solid
4	23	75 (2.79)	3.5 min gelation
			4 min solid
			4.5 min hot
5	23	100 (3.72)	3.5 min gelation
			4 min solid
6	23	150 (5.58)	2.5 min gelation, rt
			3 min solid, 40 °C
			3.5 min solid, hot
7	23	200 (7.44)	2.5 min gelation
			3 min solid, hot
8	30	-	6.5 min gelation
			8 min solid, hot
9	35	-	9.3 min gelation
			12 min solid, very elastic
10	23	-	16 min gel
11	23	50 (2.42)	20 min solid
			1 min increased viscosity
			4 min high viscosity
			9 min gelation
12	23	60 (2.91)	10.5 min solid, hot
			0.5 min increased viscosity
			2 min high viscosity
			7 min gelation
			10.5 min solid, 40 °C
13	23	75 (3.63)	11 min hot
			2 min high viscosity
			7 min gelation
14	23	100 (4.84)	8.5 min solid, hot
			0.5 min partially polymerised (ROMP)
			3 min high viscosity
			7 min solid, hot

DUAL CURE RADP-ROMP - GELTIMER MEASUREMENTS AND PULL OFF TESTS

Geltimer measurements and pull off tests were performed to determine the gel time and adhesive properties of various unfilled and filled formulations.

The unfilled and filled formulations (Table 44) were prepared analogously to those for preliminary curing tests. For the preparation of filled formulations, the whole amount of fillers was added to component A. The compounds were mixed homogeneously in a speed mixer and component A was stored at constant 25 °C. Then, component B was added and again, homogeneous mixing was achieved with a speed mixer.

Table 44. Composition of (un)filled Dual Cure RadP-ROMP formulations for preliminary Geltimer measurements and pull off tests.

comp. A	materials	mass / g	proportion	% (w/w)
1	Mon13/Mon14	50.0	100 wt%	20
2	Perkadox 20S ^a	15.0	30 wt%	
comp. B	materials	mass / g	proportion	% (w/w)
1	M20	0.0093/ 0.0121	50 ppm	20
2	BDDMA	1.023	2 wt%	
3	Tempol	0.175/ 0.115	0.35/0.23 wt%	
4	DMpT	0.522	1.05 wt%	
fillers	materials	mass / g	proportion	% (w/w)
5	Cab-O-Sil TS-720	3.90	7.8 wt%	3
6	Quarzsand F32	48.35	96.7 wt%	37
7	Millisil W12	26.65	53.3 wt%	20

[a] 20 wt% BPO in Perkadox 20S.

DUAL CURE RADP-ROMP AND SINGLE CURE RADP - 2K 10+1 FORMULATIONS - PULL OUT AND PULL OFF TESTS, GELTIMER AND YOKOGAWA MEASUREMENTS AND THERMAL ANALYSIS

Pull out (Table 46) and pull off tests as well as Geltimer and Yokogawa measurements were carried out to characterise the curing performance of filled 2K Dual Cure RadP-ROMP formulations (Table 45). The respective monomer was mixed with Perkadox 20S in a speed mixer for 30 s. The fillers were added and the speed mixer was used again to get a homogeneously mixed component A. Component B was prepared analogously to the protocol for preliminary curing tests using speed mixer boxes instead of glass vials. The finished components were then filled in the respective chamber of 2K 10+1 cartridges. These were stored at ambient temperature except for Geltimer measurement for which they were stored at constant 25 °C for at least one hour. The formulations were mixed and applied at the respective test area with a dispensing gun equipped with a static mixer tip. The first 20 g of mixed formulation were rejected for each new static mixer tip needed. The boreholes were filled with the formulation and a metal threaded rod was inserted subsequently. The pull out tests were performed after 48 h, except for boreholes at -5 °C which were tested after 6 days. For thermal analysis, the formulations were dispensed into a paper cut and filled manually into the respective crucibles (aluminium for DSC measurements and aluminium oxide for TGA/IR-measurements). The crucibles were placed into plastic vial and snap-frozen in liquid nitrogen until used for the measurements.

Table 45. Composition of filled 2K Dual Cure RadP-ROMP formulations for 10+1 cartridges.

comp. A	materials	mass / g	proportion	% (w/w)	
1	Mon13/Mon14	184.65	100 wt%	31	40
2	Perkadox 20S ^a	55.40	30 wt%	9	
3	Cab-O-Sil TS-720	18.20		3	60
4	Quarzsand F32	221.10		37	
5	Millisil W12	120.80		20	
sum		600.20	≈ 300.10 mL		
comp. B	materials	mass / g	proportion	% (w/w)	
1	BDDMA	21.69	11.7 wt%	36	40
2	Tempol	0.4247	0.23 wt%	0.7	
3	DMpT	1.92	1.05 wt%	3.2	
4	M20	0.04471	50 ppm	0.1	60
5	Cab-O-Sil TS-720	1.80		3	
6	Quarzsand F32	22.10		37	
7	Millisil W12	12.10		20	
sum		60.10	≈ 30.05 mL		

[a] 20 wt% BPO in Perkadox 20S.

Table 46. Force, bond strength and type of failure of RE 500 V1- (epoxy-amine), HY 200-A (RadP) and filled Dual Cure RadP-ROMP Mon13- and Mon14- and Single Cure RadP Mon13-formulations determined in pull out tests.

system	borehole condition	force kN	bond strength N-mm ²	cause of failure ^a	average	
					kN	N-mm ²
RE 500 V1 (epoxy-amine) ^b	F1Ref					33.0
	F1b					28.0
	oversized					25.0
	+5 °C					23.0
HY 200-A (RadP)	F1Ref	90.17	33.69	Be	90.48 ± 0.96	34.13 ± 0.52
		91.56	34.70	Be		
		89.71	33.99	Be		
	F1b	70.74	26.06	Be	65.93 ± 6.94	24.49 ± 2.21
		69.07	25.45	Be		
		57.97	21.97	Be		
	oversized	76.72	28.26	Be	74.61 ± 5.88	27.88 ± 2.32
		79.15	29.99	Be		
		67.97	25.39	Be		
		66.35	25.14	Be		
+5 °C	60.98	22.47	Be	65.29 ± 3.89	24.53 ± 1.83	
	68.53	25.97	Be			
Dual Cure RadP-ROMP Mon13 (batch 1)	F1Ref	25.16	09.27	Bb	25.0 ± 4.8	9.22 ± 1.77
		29.77	10.97	Bb		
		20.18	7.43	Bb		
	F1b	49.48	18.23	Be	48.6 ± 6.1	17.9 ± 2.2
		42.11	15.51	Bbe		
		54.19	19.96	Be		
	oversized ^{c,d}	40.67	14.98	Bbe	52.1 ± 6.6	19.2 ± 2.4
		52.15	19.21	Bbe		
		52.13	19.21	Be		
-5 °C ^e	0.07	0.03	Be	0.07	0.03	
Dual Cure RadP-ROMP Mon13 (batch 2)	F1Ref	46.51	17.13	Bb	41.7 ± 4.5	15.3 ± 1.7
		37.59	13.85	Bbe		
		40.87	14.85	Bbe		
	F1b	50.22	18.5	Be	46.5 ± 3.6	17.1 ± 1.3
		46.42	17.10	Be		
		42.95	15.82	Bbe		
	oversized ^c	26.03	9.33	Bbe	30.3 ± 4.3	10.9 ± 1.5
		34.58	12.40	Bbe		
		30.31	11.01	Bbe		
		23.00	8.36	Be		
+5 °C	29.50	10.72	Be	28.3 ± 4.9	10.3 ± 1.8	
	32.50	11.81	Bb			

[a] Bb: failure at borehole wall. Be: failure at rod. Bbe: failure at both borehole wall and rod; [b] averaged reference values (5% SD); [c] borehole diameter = 16 mm; [d] 1st value rejected; [e] one measurement only.

(Table 46- to be continued)

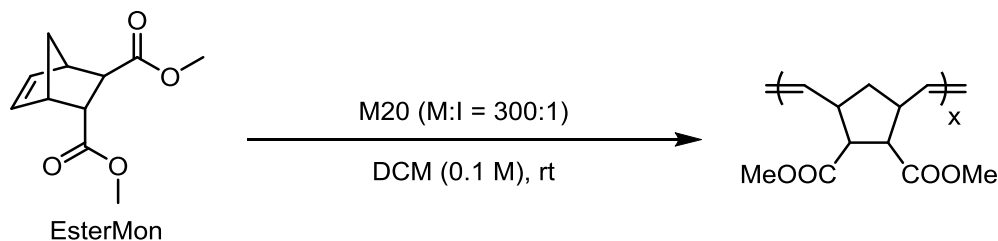
system	borehole condition	force kN	bond strength N-mm ²	cause of failure ^a	average kN	average N-mm ²
Dual Cure RadP-ROMP Mon13 (batch 3) ^f	F1Ref	29	10.99	Bb	35.67 ± 7.02	13.38 ± 2.55
		35	13.07	Bb		
		43	16.06	Bb		
	F1b	30	13.07	Bbe	29.33 ± 5.03	10.94 ± 1.89
		24	9.46	Bb		
		34	10.28	Bbe		
	oversized	20	7.47	Bb	17.67 ± 2.52	6.65 ± 0.85
		15	5.77	Bb		
		18	6.73	Bb		
	+5 °C	34	12.70	Bbe	24.67 ± 8.14	9.25 ± 3.01
		21	7.85	Bb		
		19	7.20	Bb		
Single Cure RadP Mon13 (batch 3) ^f	F1Ref	34	12.52	Be	38.21 ± 4.02	14.14 ± 1.50
		38.63	14.43	Be		
		42	15.47	Bbe		
	F1b	27	10.23	Bbe	25.33 ± 2.08	9.56 ± 0.86
		26	9.85	Bb		
		23	8.59	Bb		
	oversized	28	10.61	Bb	28.33 ± 1.53	10.54 ± 0.56
		27	9.95	Bbe		
		30	11.05	Bbe		
	+5 °C	20	7.47	Bbe	18.00 ± 2.00	6.73 ± 0.75
		18	6.73	Bb		
		16	5.98	Bbe		
Dual Cure RadP-ROMP Mon14	F1Ref	5.76	2.12	Bb	6.43 ± 1.19	2.37 ± 0.44
		7.81	2.88	Bb		
		5.73	2.11	Bb		
	F1b ^f	5.00	1.84	Bbe/Bb	5.00	1.84
	oversized ^{c,d}	2.21	0.81	Bb	4.05 ± 1.28	1.49 ± 0.47
		4.76	1.75	Bb		
	-5 °C ^e	3.34	1.23	Bb	0.09	0.03

[a] Bb: failure at borehole wall. Be: failure at rod. Bbe: failure at both borehole wall and rod; [c] borehole diameter = 16 mm; [d] 1st value rejected; [e] one measurement only; [f] maximum value of force and bond strength before failure, expanding anchor after failure.

5.1.3 POLYMERISATION IN SOLUTION

STANDARD BENCHMARK ROMP REACTION

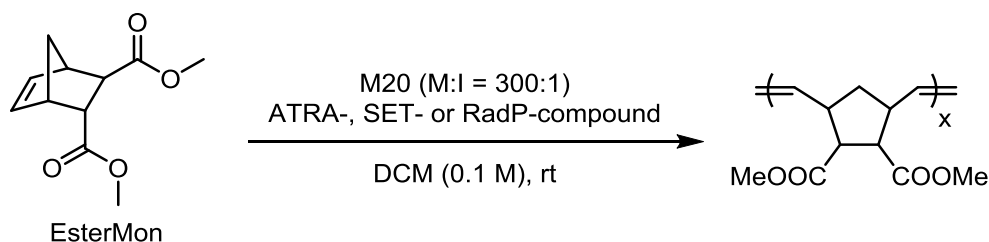
ROMP of EsterMon:



This protocol is referred to as blank reaction (Table 47, entry 1): 400 mg (1.9 mmol, 1. eq) EsterMon was dissolved in 18 mL dichloromethane. A stock solution of initiator (5.9 mg/mL, 50 ppm) was prepared in dichloromethane. The polymerisation reactions were started subsequently and 15 h after the preparation of the stock solutions. The reaction mixture was stirred at room temperature and the progress was monitored via TLC ($R_f(\text{EsterMon})=0.62$ (Cy/EtOAc, 3:1, (v:v), detection: KMnO_4)). In case of full conversion, the reaction was quenched with 400 μL ethyl vinyl ether and stirred for additional 20 min. The solution was concentrated under reduced pressure. The residual solution was added dropwise to rigorously stirred, cooled methanol. The precipitated, colourless polymer was dried under reduced pressure.

If the conversion is incomplete within 24 h, the monomer:polymer ratio was determined via $^1\text{H-NMR}$ before quenching and work-up of the reaction mixture.

ROMP of EsterMon in presence of single compounds of the radical initiation systems:



These polymerisations (Table 47, entry 2-10) were performed analogously to the protocol for the blank reaction. Two approaches were used for the addition of the single compounds:

- mixing of EsterMon with the single radical initiation compounds in DCM, addition of the M20-stock solution to start the polymerisation (=0 h).
- addition of the single radical initiation compounds to a freshly prepared M20-stock solution, storage for 15 h follow by the addition of the respective M20-stock solution to an Ester-Mon solution in DCM (=15 h)

Table 47. ROMP of EsterMon with M20 (M:I = 300 : 1) in DCM (0.1M) in presence of ATRA-, SET- or RadP-compounds.

#	entry	compound		M20-solution h	yield _{Mon} = 100 % ^b		conversion ^c Mon : Poly	polymer ^d	
		name	amount (prop. ^a)		h	h		M _n (GPC) / g·mol ⁻¹	PDI
134					1		-	79 000	2.11
135				0	0.66		-	101 000	1.66
165	1	M20	5.9 mg (50 ppm)		0.66		-	148 000	1.86
139Ref				15	n.r. (24)		1 : 300	370 000	1.61
166					n.r. (24)		1 : 300	235 000	1.67
136a				0	n.r. (17)		1 : 1.5	30 000	1.82
162	2	+ Cu(Oct) ₂	2.54 mg (0.64 wt%)		24		-	37 000	2.27
139a				15	n.c. (24)		1 : 0	-	-
164a					n.c. (72)		1 : 0	-	-
136b				0	0.66		-	100 000	1.68
162b	3	+ Bipy	0.94 mg (0.24 wt%)		0.66		-	139 000	1.64
139b				15	n.r. (24)		1 : 45	310 000	1.93
164b					1.33		-	273 000	2.08
136c				0	n.r. (17)		1 : 116	71 000	1.96
160a	4	+ Sn(Oct) ₂	3.12 μL (0.98 wt%)		4		-	79 000	2.14
139c				15	0.66		-	125 000	1.76
163a					1		-	119 000	2.31
136d				0	0.66		-	102 000	1.63
160b	5	+ BiBEE	1.80 μL (0.60 wt%)		0.5		-	112 000	2.06
139d				15	n.r. (24)		1 : 47	360 000	1.91
163b					n.r. (24)		1 : 3.5	456 000	1.96
140a				0	17		-	126 000	1.51
162c	6	+ Cu	2.48 mg (0.63 wt%)		0.66		-	142 000	1.81
141a				15	n.c. (24)		1 : 2	-	-
164c					n.c. (72)		1 : 0	-	-
140b				0	17		-	124 000	1.51
162d	7	+ MeHQ	1.56 mg (0.37 wt%)		0.66		-	162 000	1.66
141b				15	1.66		-	152 000	1.56
164d					1.66		-	165 000	1.93
140c				0	n.r. (17)		1 : 6	58 000	2.21
160c	8	+ PMDETA	5.68 μL (1.18 wt%)		n.r. (17)		1 : 6	57 000	1.91
141c				15	n.r. (24)		1 : 6	68 000	1.91
163c					n.r. (24)		1 : 4.2	61 000	1.97
146				0	0.66		-	109 000	1.77
159	9	+ BPO	4.0 mg (1.0 wt%)		0.66		-	101 000	1.93
158				15	n.c. (24)		1 : 0	-	-
179				0	0.66		-	108 000	1.60
185	10	+ DMpT	2.77 μL (0.5 wt%)		0.66		-	90 000	1.67
182				15	1.33		-	142 000	1.68

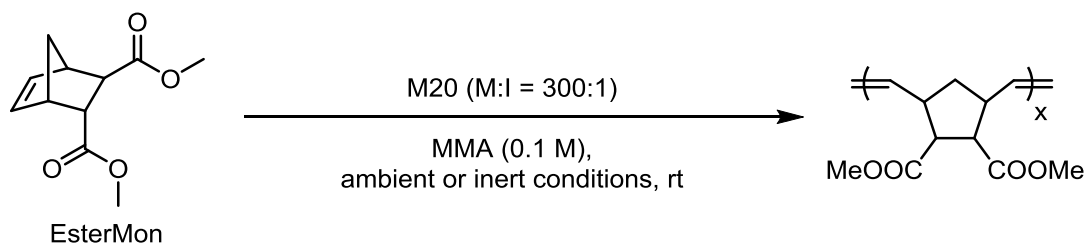
[a] with respect to monomer; [b] determined by TLC, *n.r.* = full conversion not reached (reaction time); *n.c.* = no conversion (reaction time); [c] if yield_{Mon} ≠ 100% (TLC), determined by NMR; [d] determined by GPC in chloroform and reported relative to polystyrene standards.

(Table 47 - to be continued)

#	entry	compound		M20-solution		yield _{Mon} = 100 % ^b	conversion ^c	polymer ^d	
		name	amount (prop. ^a)	h	h			Mon : Poly	M _n (GPC) / g·mol ⁻¹
378	11	Tempol	0.32 mg (0.08 wt%)	0		0.66	-		
379				15		n.r. (24)	1 : 0.06		

[a] with respect to monomer; [b] determined by TLC, n.r. = full conversion not reached (reaction time); n.c. = no conversion (reaction time); [c] if yield_{Mon} ≠ 100% (TLC), determined by NMR; [d] determined by GPC in chloroform and reported relative to polystyrene standards.

ROMP of EsterMon in MMA



These polymerisation reactions (Table 48) were performed analogously to the protocol for the blank reaction. Two approaches were used:

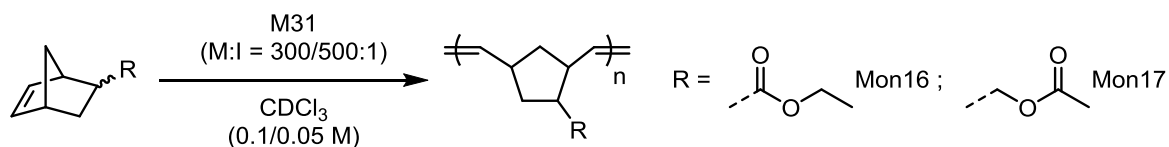
- polymerisation MMA (= 0 h)
- preparation of a M20-stock solution in MMA; storage for 17 h; addition of an aliquot of the M20-stock solution to an Ester-Mon solution (in the respective solvent (=17 h))
- both steps were conducted under ambient and inert conditions.

Table 48. ROMP of EsterMon with M20 (M:I = 300 : 1) in MMA and MMA- inert (0.1 M).

#	entry	solvent	M20-solution		yield _{Mon} = 100 % ^a	polymer ^b	
			h	h		M _n (GPC) / g·mol ⁻¹	PDI
332	1	MMA	0		0.33	18 000	1.97
333			17		23	26 000	2.63
356	2	MMA - inert	0		0.33	16 000	1.87
357			17		0.25	16 000	2.12

[a] determined by TLC, n.r. = full conversion not reached (reaction time); [b] determined by GPC in chloroform and reported relative to polystyrene standards.

KINETIC STUDIES – NMR SPECTROSCOPY



The ring opening metathesis polymerisations of Mon16 and Mon17 using M31 as initiator (M:I = 300:1, 500:1) were monitored via kinetic ¹H NMR experiments. The polymerisations were performed in CDCl₃ (0.1/0.05 M) at room temperature in presence of pyridine (5 eq based on M31 loading).

At first, the respective amount of monomer (11.64 mg) was dissolved in 0.6 mL CDCl₃ and a ¹H-NMR spectrum was recorded to determine the actual *endo/exo*-ratio. Second, an M31 (0.1745/0.1047 mg) + pyridine (0.0923/0.055 mg)-stock solution was prepared in CDCl₃. 0.1 mL of the stock solution was added to start the polymerisation and spectra were accumulated every minute for the first quarter hour, then every two minutes until one hour and subsequently with increasing intervals. For GPC analysis, the solution was concentrated and added dropwise to rigorously stirred, cold methanol. The precipitating polymer was dried under reduced pressure. The molecular weight and PDIs were determined with GPC in chloroform and reported relative to polystyrene standards.

5.2 DEGRADATION STUDIES

UV/VIS SPECTROSCOPY

M20-stock solutions with and without Sn(Oct)₂ (0.53 μL) in dichloromethane were prepared (1 mg/mL). For UV/Vis measurement, 200 μL of the stock solution was transferred into a sealed quartz cuvette and diluted with 2 mL dichloromethane. UV/Vis spectra in the range of 300 - 800 nm were recorded every 10 min within the first hour and afterwards in larger intervals.

NMR SPECTROSCOPY

The samples for NMR spectroscopic studies were prepared by dissolving 10 mg M20 in 700 μL deuterated chloroform with and without Sn(Oct)₂ (5.3 μL). ¹H- and ³¹P-NMR spectra were recorded subsequently after mixing and after 24, 48 and 72 hours.

6.1 CHEMICALS AND INSTRUMENTS

All **chemicals and substances** for the syntheses in this contribution were purchased from commercial sources (Sigma Aldrich, ABCR, Alfa Aesar, Thermo Scientific, TCI Chemicals) and used without further purification unless specified otherwise. Complexes M20 [1,3-bis(2,4,6-trimethylphenyl)-2-imidazolidinylidene] dichloro (3-phenyl-1H-inden-1-ylidene) (triphenylphosphine) ruthenium(II) and M31 [1,3-Bis(2,4,6-trimethylphenyl)-2-imidazolidinylidene]dichloro(3-phenyl-1H-inden-1-ylidene)(pyridyl)ruthenium(II) for ring opening metathesis polymerisation (ROMP) was obtained from UMICORE AG & Co. KG. Reactions were carried out either under atmospheric conditions or applying Schlenk technique under inert atmosphere of N₂ gas. Unless specified otherwise, solvents and auxiliary materials were used as purchased.

For TLC silica gel 60 F254 on aluminium sheets (Merck) was used. Visualization was done by exposure with UV light (254 nm) and / or dipping into an aqueous solution of KMnO₄ (0.1wt%) or sulphuric solution of cerium sulphate /ammonium molybdate (CAM).

Silica gel 60 (220-440 mesh ASTM) was used for column chromatography.

¹H- and ¹³C-NMR measurements were performed on a Bruker Avance 300 MHz spectrometer (¹H 300.36 MHz, ¹³C 75.53 MHz) at 25 °C. Chemical shifts are given in ppm relative to a tetramethylsilan (TMS) standard. Deuterated solvents were obtained from Cambridge Isotope laboratories Inc. and spectra were referenced against the residual proton signals according to literature.^{81,82} Peak shapes are specified as follows: *s* (*singlet*), *bs* (*broad singlet*), *d* (*doublet*), *dd* (*doublet of doublets*), *t* (*triplet*), *q* (*quadruplet*), *m* (*multiplet*). Kinetic NMR studies were performed on a Varian Unity INOVA 500 MHz (¹H 499.894 MHz, ¹³C 125.687 MHz) FT NMR instrument with a ¹H {¹⁵N-³¹P} 5 mm PFG Indirect Detection Probe.

³¹P NMR experiments were carried out with a 200 MHz Bruker Avance DPX spectrometer (¹H 200.0 MHz, ³¹P 80.96 MHz) at 25 °C.

Infrared spectra were recorded on a Bruker ALPHA-P FT-IR spectrometer equipped with ALPHA's Platinum single reflection diamond attenuated total reflection (ATR) module. Spectra were obtained in a scan range between 4000 to 400 cm⁻¹ with 48 scans and a resolution of 4 cm⁻¹. Fourier transformation (FT), processing and evaluation were done using an OPUS 6.5 software package.

UV/Vis-absorption spectra were recorded on a Shimadzu spectrophotometer UV-1800. The emission was measured on a Hitachi F-7000 fluorescence spectrometer equipped with a red-

sensitive photomultiplier R928 from Hamamatsu. The absorbance was determined using a TIDAS UV-VIS spectrometer (J&M, Germany).

Rheokinetic studies were performed on a Malvern Kinexus Ultra rheometer at Hilti Entwicklungsgesellschaft mbH, Kaufering, Germany. The monomer/initiator-formulations were applied between two disposable aluminium plates (diameters: 25 mm (upper), 56 mm (lower), 1 mm gap). The measurements were performed at 23 °C with a deformation of 0.5% at a frequency of 1 Hz. If the measured storage modulus exceeds 1.0 MPa, the deformation was reduced to 0.05% automatically in order to ensure contact between the curing sample and the plates. Data was accumulated every 15 s.

Two set-ups of **dynamic mechanical analyses** (DMA) were used in this contribution, one from TA Instruments Waters GmbH situated at ICTM, Graz University of Technology, and one from Malvern at Hilti Entwicklungsgesellschaft mbH, Kaufering, Germany. The DMA Q 800 from TA Instruments Waters GmbH was used in the 3-point bending mode with a frequency of 1 Hz and amplitude of 25 µm. The cuboidal samples (3 x 5 x 22 mm) were heated in a temperature range from -90 to maximum 180 °C (3 °C / min) depending on the sample properties. For DMA measurements with Bohlin C-VOR 120 from Malvern cylindrical samples (Ø 5 mm, 32 mm length) were used. A shear stress of 10⁵ Pa was applied with a frequency of 1 Hz in the temperature range from -20 °C up to 180 °C (10 °C/min).

Gel permeation chromatographic (GPC) measurements were conducted on LC-20 AD system from Shimadzu operated with chloroform. The instrument is equipped with two MZ-Gel Sdplus Linear 5 µm separation columns from MZ Analysentechnik in line and a refractive index (RD-20A) as well as a UV/VIS detector (SPD-20A). Polystyrene standards purchased from Polymer Standard Service were used for calibration and data was evaluated applying LabSolutions GPC software.

The bond strength of the chemical anchors was determined with a **pull-out** device F-100-4 from Kindsmüller equipped with a Hoko 100 B cylinder.

The adhesion strength of unfilled and filled formulations on dry and wet concrete was analysed with the **pull-off** device DY-216 from Proceq SA.

The **gel time** of unfilled and filled formulations was tested with two set-ups. First, the GELNORM®-Geltimer PS-1 from H. Saur Laborbedarf (referred to as “Geltimer”) equipped with a mechanical sensor MK-B-10 was used. The formulations were filled in glass tubes which were placed in a thermostat (Eco RE2025 from Lauda Dr. R. Wobser GmbH & Co. KG) set at constant 25 °C. The temperature profile was measured with the thermal sensor PT 100 from Pico Technology. Second, the temperature profile upon curing of filled formulations in concrete boreholes was determined with quartz glass fibre disturbed temperature sensors connected to the

data acquisition system DAQstation D1006-3-4-2 from Yokogawa Electric Corporation at ambient 23 °C (referred to as “Yokogawa”).

Differential scanning calorimetry (DSC) analyses were measured on DSC 1, 821 and 822 instruments from Mettler Toledo with FRS 5+ and HSS7 120 TC thermal sensors and nitrogen as purge gas (70 mL·min⁻¹). Dynamic DSC measurements were run at 8 °C·min⁻¹ in a temperature range from 10 °C to either 110, 180 or 250 °C in the 1st run, followed by a cooling run at 10 °C·min⁻¹ down to 10 °C and a 2nd run at the same heating rate up to 250 °C. T_g values were retrieved from the 2nd heating run. Isothermal measurements were performed at either 5 or 25 °C.

Thermogravimetric analyses were conducted on a TGA/DSC 1 instrument from Mettler Toledo purged with nitrogen (70 mL·min⁻¹). The measurements were run in a temperature range from 25 to 350 °C and a heating rate of 10 °C·min⁻¹. The instrument was coupled with a Nicolet iS10 FTIR spectrometer from Thermo Scientific.

The **inner stress** of filled formulations was determined with a Z050 instrument from Zwick Roell.

The **polymerisation shrinkage** of filled formulations was tested with a distance measuring device Schwindkegel from Scheibinger Geräte coupled with a deltaEL Laser controller for data acquisition.

6.2 ABBREVIATIONS

abs.	absolute	GPC	gel permeation chromatography
AIBN	azobisisobutyronitrile		
ARGET	activators regenerated by electron transfer	GTM	Geltimer - mechanical sensor
ATRA	atom transfer radical addition	GTT	Geltimer - thermal sensor
ATR-FTIR	attenuated total reflection Fourier transformation infrared spectroscopy	G1	Grubbs 1 st generation catalyst
ATRP	atom transfer radical polymerisation	G3	Grubbs 3 rd generation catalyst
BA	<i>n</i> -butyl acrylate	h	hours
BDDMA	butane-1,4-diol dimethacrylate	HEA	2-hydroxyethyl acrylate
BHT	2,6-Di- <i>tert</i> -butyl-4-methylphenol (butylated hydroxytoluene)	HEMA	2-hydroxyethyl methacrylate
BiBEE	ethyl α -bromoisobutyrate	Ip	isoprene
Bipy	2,2'-bipyridine	LC	liquid crystalline
BPO	dibenzoyl peroxide	M	molar, mol·L ⁻¹
CM	cross metathesis	MA	methacrylate
COD	1,5-cyclooctadiene	MA-Cl	methacryloyl chloride
Cp	cyclopentadiene	MA-CO	5-methacryloyl-1-cyclooctene
CRP	controlled free radical polymerisation	Me-A	methyl acrylate
CTA	chain-transfer agent	MeHQ	2-methyl-hydroquinone
Cy	cyclohexane	M:I	monomer:initiator-ratio
DCM	dichloromethane	min	minutes
DCPD	dicyclopentadiene	MMA	methyl methacrylate
Dippt	<i>N,N</i> -diisopropyl- <i>para</i> -toluidine	M _n	number average molecular weight
DMA	dynamic mechanical analysis	mol%	mol percent
DMAEMA	2-(dimethylamino)ethyl methacrylate	M:P	monomer:polymer-ratio
DMpT	<i>N,N</i> -dimethyl- <i>para</i> -toluidine	MWD	molecular weight distribution
DSC	differential scanning calorimetry	NB	norbornene
E', G'	storage modulus	NHC	N-heterocyclic carbene
E'', G''	loss modulus	NMP	nitroxide mediated polymerisation
eq	equivalents	NMR	nuclear magnetic resonance
EtOAc	ethyl acetate	Oct	octoate, 2-ethylhexanoate
		PAA	poly(acrylic acid)
		PBA	poly(<i>n</i> -butyl acrylate)
		PBD	polybutadiene
		PCL	poly(ϵ -caprolactone)
		PDI	polydispersity index
		PEG	poly(ethylene glycol)
		PIp	polyisoprene
		PMDETA	pentamethyldiethylene triamine

PMMA	poly(methyl methacrylate)
PNB	polynorbornene
PO	polyoctene
PONB	poly(oxanorbornene dicarboximide)
PS	polystyrene
PtBA	poly(<i>tert</i> -butyl acrylate)
ppm	parts per million
py	pyridine
RadP	(free) radical polymerisation
RAFT	reversible addition fragmentation chain transfer
R_f	retardation factor
ROMP	ring opening metathesis polymerisation
rt	room temperature
SEC	size exclusion chromatography
SET LRP	single-electron transfer living radical polymerisation
SD	standard deviation
St	styrene
tBA	<i>tert</i> -butyl acrylate
tBMA	<i>tert</i> -butyl methacrylate
TEMPO	2,2,6,6-tetramethylpiperidinyloxy
Tempol	4-hydroxy-2,2,6,6-tetramethylpiperidinyloxy
TFA	trifluoroacetic acid
T_g	glass transition temperature
TGA	thermogravimetric analysis
THF	tetrahydrofuran
TLC	thin layer chromatography
vol%	volume percent
v/v	volume fraction
wt%	weight percent
w/w	mass fraction
1K	one component
2K	two components

6.3 FURTHER CONTRIBUTION

In this section, the investigation on bulk effects, heat dissipation and oxygen inhibition with a thermal camera published in a reviewed journal is presented:

- R. Geier, C. Wappl, H. Freißmuth, C. Slugovc, G. Gescheidt-Demner
Thermal Effects in Polymerizations - A Live View Differentiating between Bulk Effects, Thermal Diffusion, and Oxygen Inhibition
Polymer Chemistry **2015**, *6*, 2488-2492.



Cite this: *Polym. Chem.*, 2015, **6**, 2488

Thermal effects in polymerisations – a live view differentiating between bulk effects, thermal diffusion, and oxygen inhibition

Roman Geier,^a Christina Wappl,^a Hilde Freiszmuth,^a Christian Slugovc^b and Georg Gescheidt^{*a}

Received 15th December 2014,
Accepted 23rd January 2015

DOI: 10.1039/c4py01739k

www.rsc.org/polymers

Thermography has been shown to be an efficient tool for the screening of the efficiency of exothermic reactions. Here we show that the use of a thermal IR camera reveals effects of heat transfer in polymerising mixtures if appropriately designed reaction vessels are used. We report on case studies illustrated by photo-induced radical polymerisation of butyl acrylate and thermally triggered ring-opening metathesis polymerisation of dicyclopentadiene.

Introduction

Generally, polymerisation reactions are exothermic. It is well established that bulk effects lead to rather high temperatures in polymerising mixtures. These thermal effects have been investigated by a variety of methods, in particular DSC or *in situ* with thermal sensors. Another important aspect in real systems is that heat is dissipated at the interfaces between the reaction mixture and its environment, *i.e.*, the vessel and the atmosphere. This obviously causes a rather inhomogeneous heat distribution, which may substantially alter the homogeneity and the properties of the final polymeric product. This feature is well established and has been addressed particularly using simulations.^{1–4} A related aspect is the inhibition of radical polymerisations by oxygen, which also appears at the interface between the polymerising formulation and air.⁵ A detailed analysis of these above-mentioned phenomena requires a corresponding technique, which provides information offering spatial and time resolution appropriate for polymerisation reactions.

It has been shown that the use of a thermal sensor⁶ and, particularly, a thermal camera provides valuable insights for assessing the efficiency of (preferably) exothermic events.^{7–9} Although thermal images exclusively display the temperature at the surface of the sample and disturbing reflections may occur, an image representing a two-dimensional spatial heat distribution offers useful insights into environmental effects of chemical reactions.¹⁰

We have, therefore, evaluated the use of a high-resolution thermal camera for simultaneously following the temperature and its dissipation depending on various reaction conditions. Moreover we have developed and tested reaction vessels for this type of study. Here we report our initial results, which indicate the scope (and caveats) of this experimental approach.

Results and discussion

As a first example, we have chosen a photo-initiated radical polymerisation for our investigations.^{11–14} Such a procedure provides a clearly defined trigger for starting the polymerisation. In a thin-walled NMR tube, a mixture of the phosphine oxide based photoinitiator Irgacure 819 and butyl acrylate (Fig. 1A) in benzene was irradiated using a Hg/Xe high-pressure lamp for 10 s (shutter). The corresponding setup is shown in Fig. 1B. The Hg/Xe lamp is oriented perpendicular toward the NMR tube. This allows following the development of heat in a cross section below and above the centre of the irradiating light. The dissipation of heat together with the corresponding thermographic curves is displayed in Fig. 1C and D. Fig. 1C shows that a hot spot is immediately created at the position where the sample is irradiated. The temperature gradually decreases at larger distances. Upon stopping irradiation after 10 s, the temperature rises to its maximum, then gradually cools down but still being above room temperature after 140 s. In Fig. 1D, the influence of oxygen is illustrated. The three samples shown contain identical mixtures of the initiator and butyl acrylate. The sample on the left side is degassed on a vacuum line and sealed under N₂ (identical to the sample in the middle of Fig. 1C), the one in the middle reflects atmospheric conditions, whereas that on the right is saturated with O₂. All three images are obtained immediately

^aInstitute of Physical and Theoretical Chemistry, Graz University of Technology, NAWI Graz, Stremayrgasse 9, 8010 Graz, Austria

^bInstitute for Chemistry and Technology of Materials, Graz University of Technology, NAWI Graz, Stremayrgasse 9, 8010 Graz, Austria.

E-mail: g.gescheidt-demner@tugraz.at



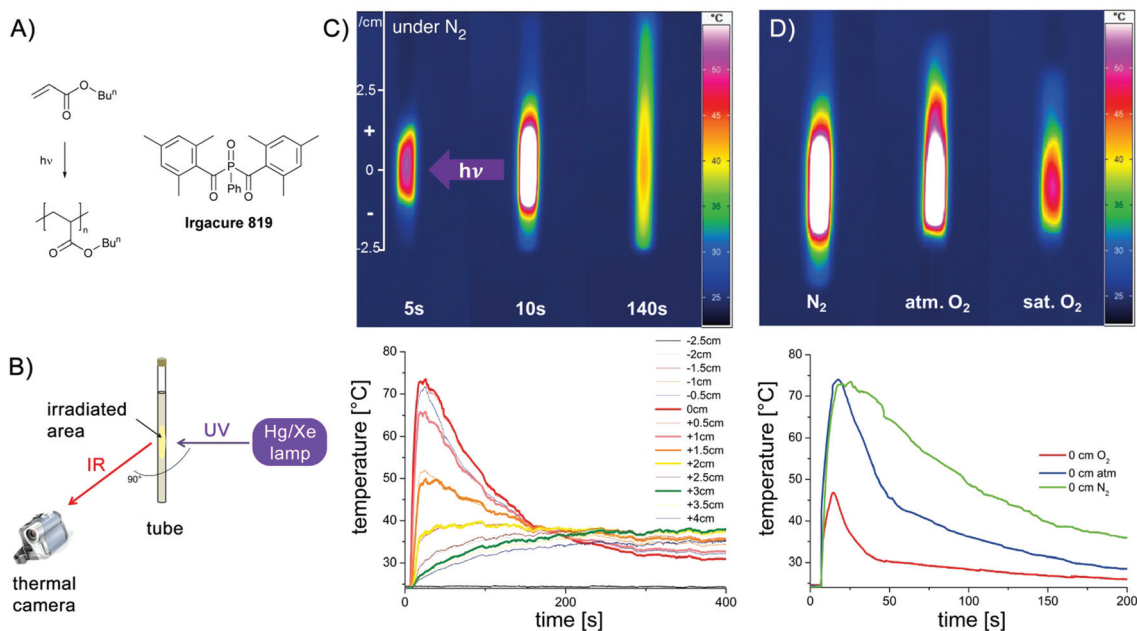


Fig. 1 Polymerisation under investigation (A), experimental setup for the recording of thermal images (B), thermal images of formulations irradiated for 10 s at 5, 10, and 140 s after irradiation was stopped (under N_2) (C, above) and time/temperature profiles for the same experiment at selected distances from the position of irradiation (C, below) as well as thermal images of samples at different oxygen concentrations recorded 10 s after irradiation was stopped (D, above) and time/temperature profiles at the centre of irradiation of these samples (D, below).

after the irradiation ended. In the sample under an inert atmosphere, the heat is evenly distributed above and below the centre of irradiation. Although the highest temperature is essentially identical in the image in the middle, the heat distribution becomes inhomogeneous. The substantial inhibiting effect of oxygen can be clearly distinguished in the right sample: the temperature is much lower (less than half compared to the degassed case), clearly showing a substantially hampered polymerisation. This is shown in Fig. 1D (lower part) comparing the rise and decrease of the temperature in these three samples over 200 s at the centre of the irradiation. Whereas the green curve recorded under inert conditions (N_2 saturated sample) reaches the highest temperature (T_{max}) and decreases only slowly indicating a rather long period of polymerisation, the blue curve recorded under atmospheric atmosphere has an identical T_{max} but a substantially faster decay. When the solution is saturated with oxygen, T_{max} is markedly lower and the decay is even more pronounced. Fig. 1C reveals that particularly at later stages of the polymerisation, the dissipation of heat is not uniform, but systematically depends on convection and, possibly on the thermal properties of the environment. This is mirrored by the fact that the temperature above the centre of irradiation (positive values in Fig. 1C) is higher than that at the corresponding distance below.

The spatially-resolved images shown in Fig. 1C reveal that under an inert atmosphere, a maximum number of active initiating radicals is produced. Accordingly many polymer chains start to grow. Moreover, since chain growth is not quenched by oxygen, recombination and disproportionation reactions appear as side reactions of the radical-chain reaction. A sub-

stantial portion of the heat is produced by the formation of novel C–C bonds. As soon as oxygen is present, the formation of active initiating radicals is hindered by the deactivation of the initiating radicals by oxygen. Since the photo-induced α cleavage is rather fast and the quenching of the initiating radicals by O_2 is a second-order diffusion-controlled reaction, this reaction is not dominating in the very first phase of polymerisation under atmospheric conditions. However, this becomes much more pronounced in the O_2 saturated sample where the initiating radicals are attacked by oxygen at a higher rate. The oxygen quenching of the C-centred radicals of the growing chain is evident in both oxygen-containing samples showing a much faster decrease of the temperature relative to the degassed one.

Not all effects discussed above are exclusively caused by the role of oxygen. Heat transfer to the interfaces between the sample and the glass walls and the atmosphere definitely contribute to the efficacy of the polymerisation reaction. We have therefore specifically addressed the influence of the bulk and the interface area in a second series of experiments. To this end, we have chosen ROMP (ring-opening metathesis polymerisation, Fig. 2) since the progress of ROMP (initiated with the particular class of ruthenium compounds used) is hardly affected by the presence of oxygen and starts after an induction period of a few minutes allowing a proper mixing of the solutions and placing them in appropriate vessels.¹⁵

In a first set of measurements, four vials were filled with differing volumes of the same polymerising mixture (0.5–3.7 mL) and immediately, the thermal development of the samples was monitored with the thermal camera (Fig. 2). After an induction period of *ca.* 4 min, the sample with the highest



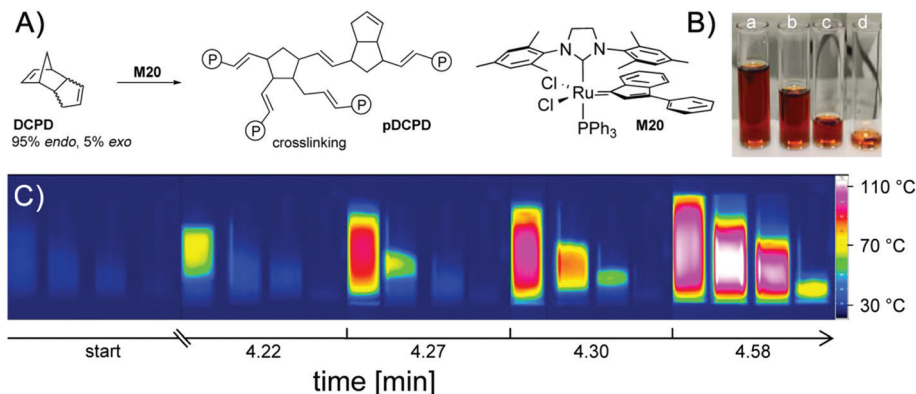


Fig. 2 ROMP of dicyclopentadiene initiated with M20 (A), photographs of reaction vessels ((a) 3.7, (b) 2.6, (c) 1.2 and (d) 0.5 mL) containing the formulation for ROMP (B) and thermal images showing the heat evolution during polymerisation depending on the volume (C).

volume starts to polymerise, consecutively followed by the samples with decreasing volumes of the formulation. The starting area of the reaction is always the (*a priori*) warmest region of the samples. This can be additionally perceived by the fact that even a slight heat transfer from one sample to another (if they are in close vicinity) creates a “hot spot” becoming the starting area for the polymerisation in the adjacent vessel. The lower the volume of the sample, the longer it takes for the start of the polymerisation and the lower the highest temperature achieved. Clearly these effects can be traced back to bulk effects counterbalanced by heat transfer across interfaces. To assess the influence of the overall volume and the interface area in a systematic way (walls of the sample

vessel and atmosphere), we have constructed reaction chambers (Teflon) providing specific volume/interface area ratios. To avoid heat transfer between the samples, the reaction chambers were positioned well apart from each other (Fig. 3A and B). The measurement of the reaction temperature at the surface of the samples was achieved by positioning the camera above the reaction chambers. Selected results are displayed in Fig. 3C. In analogy with the measurements shown in Fig. 2, an induction period of *ca.* 3 min was observed. Polymerisation started first in the sample with the highest volume. This can be seen in Fig. 3C and D, where column a, corresponding to the reaction chamber with the highest volume (Table 1), reveals the first detection of heat after 211 s.

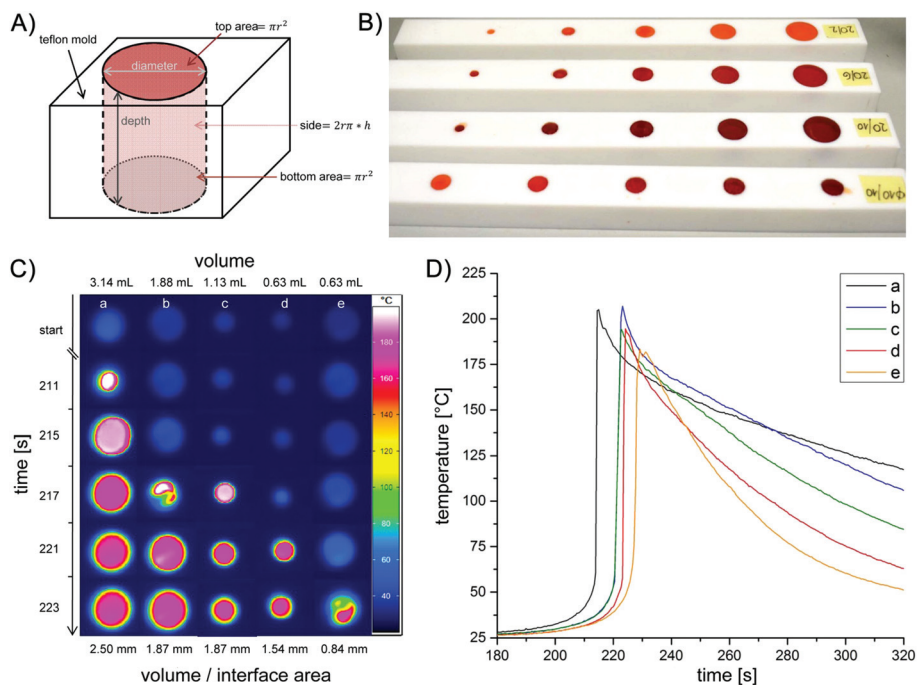


Fig. 3 General shape of the reaction chambers (A), photograph of the reaction chambers made of Teflon (B), thermal image showing the heat evolution during ROMP in dependence of the dimensions of the reaction chambers (*cf.* Table 1) (C) and time/temperature profiles of the reaction chambers a–e (D).



Table 1 Dimensions of reaction chambers

Reaction chamber	a	b	c	d	e
Diameter [mm]	20	20	12	10	20
Depth [mm]	10	6	10	8	2
Volume [mL]	3.14	1.88	1.13	0.63	0.63
Volume–interface area ratio [mm]	2.50	1.87	1.87	1.54	0.84

Columns b–d in Fig. 3C then follow in the order of their gradually smaller volumes.

In addition to this ‘volume effect’, also the volume/interface ratio appears to play a major role. The polymerisation in chambers b and c starts almost simultaneously (see 4th line in Fig. 3C) although the volume of chamber c is only 60% of that of b. Remarkably, b and c have the same volume/interface area ratio. This implies that the heat is evenly dissipated across the interfaces between the sample and Teflon/atmosphere. Comparing the reaction in chambers d and e underpins the influence of the volume/interface area ratio. These chambers have identical volumes (0.63 mL) but different interface areas (volume/interface area ratio 1.54 and 0.84 mm, respectively). Significantly, in sample e with a lower volume/interface area ratio, the polymerisation starts later and reaches a lower maximum temperature (Fig. 3D). Here, a larger amount of the reaction heat is transferred from the bulk to the surrounding. Generally Fig. 3D indicates that the samples with higher volume and bigger volume/interface ratio polymerise earlier and reach higher temperatures. Moreover the observation that the decay of the maximum temperature is substantially less pronounced in a, b than in d, e (Fig. 3D) is in line with the higher volume/surface ratio of the former samples.

Experimental section

For the temperature measurements, we have used an InfraTec VarioCam hr M83072 thermography system providing a 640 × 480 dpi resolution at a frequency of 60 Hz. We used 10 Hz and 2 Hz for photoinitiated and ring opening metathesis polymerisation reactions, respectively.

Since thermal camera images exclusively present surface temperatures, our measurements were either performed in thin-walled glass tubes (NMR) or in specifically produced reaction vessels (Teflon). The specific shapes of the latter were designed to account for the effects of the overall reaction volume and the ratio of volume *vs.* the interfacing area with the atmosphere and the contact area of the polymerising mixture with the Teflon surface.

For the photoinitiated reactions benzene solutions of butyl acrylate and Irgacure 819 (phenylbisacylphosphine oxide, BASF, Germany) were used. For the measurements 0.8 mL of a prepared stock solution consisting of 9.8 wt% benzene, 0.1 wt% Irgacure 819 and 90.1 wt% of butyl acrylate was filled in thin-walled 5 mm NMR tubes. The NMR tubes were sealed with septa and either degassed (N₂ bubbling for 3 min) or enriched with oxygen under light exclusion (wrapped in aluminium

foil). Samples representing atmospheric oxygen levels were kept untreated. Every sample was freshly prepared before the experiment. A Hg/Xe lamp (Hamamatsu LC4, L8252 lamp, max at 365 nm) equipped with a light guide (diameter 5 mm) was used. This setup yielded 2200 ± 300 mW cm⁻². A cross section of 15 mm was irradiated for 10 s (shutter). The recording of the thermal response was started 7 s before irradiation.

For the ring opening metathesis polymerisation in bulk, dicyclopentadiene (97%, a mixture of *endo* and *exo* isomer (95 : 5), ABCR; 7.84 g and 14.7 g for measurements in glass vials and Teflon moulds, respectively) was molten and mixed with dichloromethane (30 μL per mL DCPD) to keep it in the liquid state. A stock solution of the initiator M20 (Umicore)¹⁶ in dichloromethane (34.5 mg mL⁻¹) was prepared. For the thermal measurements, the polymerisation was initiated by the addition of initiator-solution (240 and 450 μL; equal to 150 ppm M20 in respect of DCPD) to the monomer. Subsequently, the formulation was filled in the respective moulds and the heat evolution was measured.

Conclusions

Although thermal measurements were reported for several cases as a (semi)quantitative tool for describing the efficiency of chemical reactions,¹⁷ our results illustrate pretty well the power of thermography to visualize, study and quantify the polymerisation progress under different conditions. The aim of our investigation was testing whether the use of a thermal camera provides new and useful insights into polymerisation phenomena. The images and the curves shown in Fig. 1 and 3 illustrate that we have been capable of systematically establishing and distinguishing bulk effects, heat transfer, the influence of interfaces, and the impact of oxygen. Although the recorded images provide only information on the temperature of the surface of the investigated samples, the non-isotopic heat flow can be followed rather precisely and reproducibly.

In these terms, the use of a high-resolution thermal camera is very useful for investigating the efficiency of the formation of polymers on a convenient time scale (1/60 s) and an appropriate resolution (sub mm), which is likely to be useful for studying rather subtle details during the curing of photo-polymerisable coatings in addition to standard IR procedures monitoring the conversion of double bonds.¹⁸ Such investigations require custom-made reaction chambers that allow following the desired phenomena, always bearing in mind that the surface temperature is monitored exclusively. It is also crucial to control the environmental conditions very precisely to achieve a perfect reproducibility of the results.

We are currently expanding our studies toward frontal polymerisation, non-homogeneous systems, *etc.* and developing specific vials for enhancing the scope of this approach. A detailed look on thermographic images seems to be valuable and should also enhance the development of theoretical models.¹⁹



Acknowledgements

We are indebted to Herbert Lang (Workshop Physical and Theoretical Chemistry TU Graz) for preparing the Teflon-based reaction vessels.

Notes and references

- 1 G. L. Batch and C. W. Macosko, *J. Appl. Polym. Sci.*, 1992, **44**, 1711–1729.
- 2 A. Boddapati, S. B. Rahane, R. P. Slopek, V. Breedveld, C. L. Henderson and M. A. Grover, *Polymer*, 2011, **52**, 866–873.
- 3 C. E. Corcione, A. Greco and A. Maffezzoli, *Polym. Eng. Sci.*, 2006, **46**, 493–502.
- 4 P. M. Johnson, J. W. Stansbury and C. N. Bowman, *Macromolecules*, 2008, **41**, 230–237.
- 5 S. C. Ligon, B. Husar, H. Wutzel, R. Holman and R. Liska, *Chem. Rev.*, 2014, **114**, 557–589.
- 6 B. J. Falk, S. M. Vallinas and J. V. Crivello, *J. Polym. Sci., Part A: Polym. Chem.*, 2003, **41**, 579–596.
- 7 A. Holzwarth, H.-W. Schmidt and W. F. Maier, *Angew. Chem., Int. Ed.*, 1998, **37**, 2644–2647.
- 8 M. T. Reetz, M. H. Becker, K. M. Kühling and A. Holzwarth, *Angew. Chem., Int. Ed.*, 1998, **37**, 2647–2649.
- 9 Y. M. Kim, L. K. Kostanski, J. F. MacGregor and A. E. Hamielec, *J. Therm. Anal. Calorim.*, 2004, **78**, 153–164.
- 10 T. Nagasawa, B. Ochiai and T. Endo, *J. Polym. Sci., Part A: Polym. Chem.*, 2006, **44**, 5519–5524.
- 11 K. Dietliker, T. Jung, J. Benkhoff, H. Kura, A. Matsumoto, H. Oka, D. Hristova, G. Gescheidt and G. Rist, *Macromol. Symp.*, 2004, **217**, 77–97.
- 12 I. Gatlik, P. Rzadek, G. Gescheidt, G. Rist, B. Hellrung, J. Wirz, K. Dietliker, G. Hug, M. Kunz and J.-P. Wolf, *J. Am. Chem. Soc.*, 1999, **121**, 8332–8336.
- 13 S. Jockusch and N. J. Turro, *J. Am. Chem. Soc.*, 1998, **120**, 11773–11777.
- 14 Y. Yagci, S. Jockusch and N. J. Turro, *Macromolecules*, 2010, **43**, 6245–6260.
- 15 A. Leitgeb, J. Wappel, C. A. Urbina-Blanco, S. Strasser, C. Wappl, C. S. J. Cazin and C. Slugovc, *Monatsh. Chem.*, 2014, **145**, 1513–1517.
- 16 J. Broggi, C. A. Urbina-Blanco, H. Clavier, A. Leitgeb, C. Slugovc, A. M. Z. Slawin and S. P. Nolan, *Chem. – Eur. J.*, 2010, **16**, 9215–9225.
- 17 J. Loskyll, K. Stoewe and W. F. Maier, *ACS Comb. Sci.*, 2012, **14**, 295–303.
- 18 K. Taki, Y. Watanabe, H. Ito and M. Ohshima, *Macromolecules*, 2014, **47**, 1906–1913.
- 19 M. D. Goodner and C. N. Bowman, *Chem. Eng. Sci.*, 2002, **57**, 887–900.



6.4 REFERENCES

- ¹ R. Eligehausen, J. J. Appl, B. Lehr, J. Meszaros, W. Fuchs, *Beton- und Stahlbetonbau* **2004**, *99*(7), 561.
- ² R. A. Cook, R. Eligehausen, J. J. Appl, *Beton- und Stahlbetonbau* **2007**, *102*, 16.
- ³ L. Li, J. Nam, W.H. Hartt, *Cement Concrete Res.* **2005**, *35*, 277-283.
- ⁴ A. Pfeil, Presentation in the series of lectures of "Doctoral School Chemistry TU Graz, "Molecules-Products-Patents; Application of Polymer Chemistry in the Field of Chemical Anchors", Graz, **2010**.
- ⁵ Hilti Product Data Sheet, "HIT-HY 150 MAX with HIT-V / HAS", **2011**.
- ⁶ Hilti information brochure, "Hilti Lösungen für nachträgliche Bewehrungsanschlüsse", **2009**.
- ⁷ R.A. Cook, J. Kunz, W. Fuchs, R. C. Konz, *ACI Structural Journal* **1998**, *95*(1), 9.
- ⁸ Hilti information brochure, "Hilti HIT Injektionstechnik", **2007**.
- ⁹ T.M. Trnka, R.H. Grubbs, *Acc. Chem. Res.* **2001**, *34*, 18-29.
- ¹⁰ J.L. Hérisson, Y. Chauvin, *Makromol. Chem.* **1971**, *141*, 161.
- ¹¹ C. W. Bielawski, R. H. Grubbs, *Prog. Polym. Sci.* **2007**, *32*, 1.
- ¹² A.-C. Knall, C. Slugovc, in: "*Olefin Metathesis: Theory and Practice*", K. Grela, Ed., John Wiley & Sons, Inc., Hoboken, N. J., **2014**, Chapter 7.
- ¹³ A. Goto, T. Fukuda, *Prog. Polym. Sci.* **2004**, *29*, 329.
- ¹⁴ H. Ito, D. Miller, N. Sveum, M. Sherwood, *J. Polym. Sci. Part A: Polym. Chem.* **2000**, *38*, 3521.
- ¹⁵ S. Elyashiv-Barad, N. Greinert, A. Sen, *Macromolecules* **2002**, *35*, 7521.
- ¹⁶ K. Tanaka, K. Matyjaszewski, *Macromol. Symp.* **2008**, *261*, 1.
- ¹⁷ E. Ihara, S. Honjyo, K. Kobayashi, S. Ishii, T. Itoh, K. Inoue, H. Momose, M. Nodono, *Polymer* **2010**, *51*, 397.
- ¹⁸ http://www.jofamericanscience.org/journals/am-sci/0401/13_0401_yeh_am.pdf [14.11.2014].
- ¹⁹ R. M. Kriegel, W. S. Ress Jr., M. Weck, *Macromolecules* **2004**, *37*, 6644.
- ²⁰ D.-J. Liaw, C.-C. Huang, S.-M. Hong, *J. Polym. Sci. Part A: Polym. Chem.* **2006**, *44*, 6287.
- ²¹ D.-J. Liaw, C.-C. Huang, S.-M. Hong, W.-H. Chen, K.-R. Lee, J.-Y. Lai, *Polymer* **2006**, *47*, 4613.
- ²² A. Li, J. Ma, K. L. Wooley, *Macromolecules* **2009**, *42*, 5433.
- ²³ C. Cheng, E. Khoshdel, K. L. Wooley, *Macromolecules* **2005**, *38*, 9455.
- ²⁴ G. Morandi, V. Montembault, S. Pascual, S. Legoupy, N. Delorme, L. Fontaine, *Macromolecules* **2006**, *39*, 2732.
- ²⁵ Y. Xia, J. A: Kornfield, R. H. Grubbs, *Macromolecules* **2009**, *42*, 3761.
- ²⁶ A. K. Chatterjee, T.-L. Choi, D. P. Sanders, R. H. Grubbs, *J. Am. Chem. Soc.* **2003**, *125*, 11360.
- ²⁷ C. Lexer, R. Saf, C. Slugovc, *J. Polym Sci. Part A: Polym Chem.* **2009**, *47*, 299.

-
- ²⁸ Z. Li, K. Zhang, J. Ma, C. Cheng, K. L. Wooley, *J. Polym. Sci. Part A: Polym. Chem.* **2009**, *47*, 5557.
- ²⁹ C. Cheng, E. Khoshdel, K. L. Wooley, *Nano Lett.* **2006**, *6*, 1741.
- ³⁰ B. R. Maughon, R. H. Grubbs, *Macromolecules* **1996**, *29*(18), 5765.
- ³¹ M. Kato, M. Kamigaito, M. Sawamoto, T. Higashimura, *Macromolecules* **1995**, *28*, 1721.
- ³² M. Kato, M. Kamigaito, M. Sawamoto, T. Higashimura, *Macromolecules* **1995**, *28*(5), 1721.
- ³³ J. Ueda, M. Matsuyama, M. Kamigaito, M. Sawamoto, *Macromolecules* **1998**, *31*, 557.
- ³⁴ F. Simal, A. Demonceau, A. F. Noels, *Angew. Chem. Int. Ed.* **1999**, *38*(4), 538.
- ³⁵ F. Simal, S. Delfosse, A. Demonceau, A. F. Noels, K. Denk, F. J. Kohl, T. Weskamp, W. A. Herrmann, *Chem. Eur. J.* **2002**, *8*(13), 3047.
- ³⁶ T. Opstal, F. Verpoort, *Angew. Chem. Int. Ed.* **2003**, *42*, 2876.
- ³⁷ J. Lee, J. M. Grandner, K. M. Engle, K.N. Houk, R. H. Grubbs, *J. Am. Chem. Soc.* **2016**, *138*, 7171.
- ³⁸ S. Banerjee, T. K. Paira, T. K. Mandal, *Polym. Chem.* **2014**, *5*, 4135.
- ³⁹ S. Coca, H. Paik, K. Matyjaszewski, *Macromolecules* **1997**, *30*, 6513.
- ⁴⁰ M. Li, P. Keller, P.-A. Albouy, *Macromolecules* **2003**, *36*, 2284.
- ⁴¹ C. W. Bielawski, T. Morita, R. H. Grubbs, *Macromolecules* **2000**, *33*, 678.
- ⁴² H. Katayama, F. Yonezawa, M. Nagao, F. Ozawa, *Macromolecules* **2002**, *35*, 1133.
- ⁴³ N. Cerit, N. Cakir, A. Dag, O. Sirkecioglu, H. Durmaz, C. Hizal, U. Tunca, *J. Polym. Sci. Part A: Polym. Chem.* **2011**, *49*, 2850.
- ⁴⁴ R. Charvet, B. M. Novak, *Macromolecules* **2004**, *37*, 8808.
- ⁴⁵ G. Morandi, S. Pascual, V. Montembault, S. Legoupy, N. Delorme, L. Fontaine, *Macromolecules* **2009**, *42*, 6927.
- ⁴⁶ C. Cheng, K. Qi, E. Khoshdel, K. L. Wooley, *J. Am. Chem. Soc.* **2006**, *128*, 6808.
- ⁴⁷ C. Cheng, K. Qi, D. S. Germack, E. Khoshdel, K. L. Wooley, *Adv. Mater.* **2007**, *19*, 2830.
- ⁴⁸ C. Cheng, E. Khoshdel, K. L. Wooley, *Macromolecules* **2007**, *40*, 2289.
- ⁴⁹ J. Zhang, P. J. Pellechia, J. Hayat, C. G. Hardy, C. Tang, *Macromolecules* **2013**, *46*, 1618.
- ⁵⁰ P.R. Schleyer, J. E. Williams, K. R. Blanchard, *J. Am. Chem. Soc.* **1970**, *92*, 2377.
- ⁵¹ G. Morandi, S. Piogé, S. Pascual, V. Montembault, S. Legoupy, L. Fontaine, *Mater. Sci. Eng.* **2009**, *29*, 367.
- ⁵² A. Li, J. Ma, G. Sun, Z. Li, S. Cho, C. Clark, K. L. Wooley, *J. Polym. Sci. Part A: Polym. Chem.* **2012**, *50*, 1681.
- ⁵³ M. Xie, J. Dang, H. Han, W. Wang, J. Liu, X. He, Y. Zhang, *Macromolecules* **2008**, *41*, 9004.
- ⁵⁴ C. W. Bielawski, J. Louie, R. H. Grubbs, *J. Am. Chem. Soc.* **2000**, *122*, 12872.
- ⁵⁵ D. Quémener, A. Bousquet, V. Héroguez, Y. Gnanou, *Macromolecules* **2006**, *39*, 5589.
- ⁵⁶ C. Airaud, V. Héroguez, Y. Gnanou, *Macromolecules* **2008**, *41*, 3015.
- ⁵⁷ L. Ding, J. Qiu, J. Wei, Z. Zhu, *Macromol. Rapid Commun.* **2014**, *35*, 1509.

-
- ⁵⁸ M. P. Patel, M. Braden, K. W. M. Davy, *Biomaterials* **1987**, *8*, 53.
- ⁵⁹ Y. Gnanou, G. Hizal, *J. Polym. Sci. Part A: Polym. Chem.* **2004**, *42*, 351.
- ⁶⁰ B. M. Rosen, V. Percec, *Chem. Rev.* **2009**, *109*, 5069.
- ⁶¹ P. M. Wright, G. Mantovani, D. M. Haddleton, *J. Polym. Sci. Part A: Polym. Chem.* **2008**, *46*, 7376.
- ⁶² W. Jakubowski, K. Matyjaszewski, *Macromolecules* **2005**, *38*, 4139.
- ⁶³ J. K. Oh, K. Matyjaszewski, *J. Polym. Sci. Part A: Polym. Chem.* **2006**, *44*, 3787.
- ⁶⁴ K. L. Beers, S. Boo, S. G. Gaynor, K. Matyjaszewski, *Macromolecules* **1999**, *32*, 5772.
- ⁶⁵ M. Buback, C. H. Kurz, *Macromol. Chem. Phys.* **1998**, *199*, 2301.
- ⁶⁶ S. Beuermann, M. Buback, T.P. David, R. G. Gilbert, R.A. Hutchinson, O. F. Olaj, G. T. Russel, J. Schweer, A. M. van Herk, *Macromol. Chem. Phys.* **1997**, *198*, 1545.
- ⁶⁷ X.-D. Feng, *Makromol. Chem. Macromol. Symp.* **1992**, *63*, 1.
- ⁶⁸ M. Buback, H. Frauendorf, F. Gunzler, P. Vana, *Polymer* **2007**, *48*, 5590.
- ⁶⁹ A. Zoller, D. Gimes, Y. Guillaneuf, *Polym. Chem.* **2015**, *6*, 5719.
- ⁷⁰ C. Slugovc, S. Demel, Silvia Riegler, J. Hobisch, F. Stelzer, *J. Mol. Catal. A-Chem.* **2004**, *213*, 107.
- ⁷¹ K. Matyjaszewski, H. Dong, W. Jakubowski, J. Pietrasik, A. Kusumo, *Langmuir* **2007**, *23*, 4528.
- ⁷² S. H. Hong, A. G. Wenzel, T. T. Salguero, M. W. Day, R. H. Grubbs, *J. Am. Chem. Soc.* **2007**, *129*, 7961.
- ⁷³ C. Slugovc, S. Demel, S. Riegler, J. Hobisch, F. Stelzer, *Macromol. Rapid Commun.* **2004**, *25*, 475.
- ⁷⁴ J. D. Rule, J.S. Moore, *Macromolecules* **2002**, *35*, 7878.
- ⁷⁵ J. M. Pollino, L. P. Stubbs, M. Weck, *Macromolecules* **2003**, *36*, 2230.
- ⁷⁶ N. Seehof, S. Grutke, W. Risse, *Macromolecules* **1993**, *26*, 695.
- ⁷⁷ S. Loshaek, T.G. Fox, *J. Am. Chem. Soc.* **1953**, *75*, 3544.
- ⁷⁸ C.L. Davidson, A.J. Feilzer, *J. Dent.* **1997**, *25* (6), 435.
- ⁷⁹ S.R. White, N.R. Sottos, P.H. Geubelle, J.S. Moore, M.R. Kessler, S.R. Sriram, E.N. Brown, S. Viswanathan, *Nature* **2001**, *409*, 794.
- ⁸⁰ E.A. Turi, *Thermal Characterization of Polymeric Materials*, 2nd Ed., Vol. I., Academic Press, Brooklyn, New York, 1997.
- ⁸¹ R. K. Harris, E. D. Becker, S. M. Cabral de Menezes, P. Granger, R. E. Hoffman, K. W. Zilm, *Pure Appl. Chem.* **2008**, *80*, 59-84.
- ⁸² H.E. Gottlieb, A. Kotlyar, A. Nudelman, *J. Org. Chem.* **1997**, *62*, 7512.